CONTENTS

Establishment of an Anti-HIV/AIDS Agents Screening Technique Based on Human CXCR4 Promoter

Yunyun Ma[1, 2], Long Feng[1], Ming Li[1], Yanping Wei[1, 3], Tingyu He[1], Wentao Guo[1], Jing Jin[1, 2], Ziming Dong[1], and Guoqiang Zhao[*1]

[1]DEPARTMENT OF IMMUNOLOGY & MICROBIOLOGY, BASIC MEDICAL COLLEGE OF ZHENGZHOU UNIVERSITY, ZHENGZHOU, HENAN 450001, CHINA ; [2]DEPARTMENT OF IMMUNOLOGY & MICROBIOLOGY, HENAN MEDICAL COLLEGE FOR STUFF AND WORKERS, ZHENGZHOU 451191, CHINA ; [3]JIAOZUO PEOPLE'S HOSPITAL, JIAOZUO, HENAN 454002, CHINA

zhaogq@zzu.edu.cn

Abstract — Objective: To construct an anti-HIV/AIDS agents screening system by handling human CXCR4 promoter with medicated serum. Medthods: Human CXCR4 (CXC Chemokine Receptor 4) promoter gene was inserted into the reporter vector pGL4. Recombinant plasmid pGL4-CXCR4 was transfected into Jurkat cells (the cell line of acute T lymphocyte leukemia). The stable transfected cell were screened by G418. Thirteen kinds of traditional Chinese medicine were given to rats intragastrically and the medicated serum were collected. After the stable transfected cells were handling separately by medicated serum, CXCR4 promoter expression in the cells was detected. CXCR4 protein expression in change groups cells were tested by Western blotting analysis. Result: Cortex phellodendri chinensis and Herba houttuyniae can depress the activity of the transfected CXCR4 promoter in Jurkat cell, the luciferase activity of which is lower remarkably than of control group ($p<0.05$). Herba lobeliae chinensis can enhance the activity of the transfected CXCR4 promoter in Jurkat cells, the luciferase activity of which is higher remarkably than that of the control group ($p<0.05$). Conclusion: An anti-HIV/AIDS agents screening system based on Human CXCR4 promoter was constructed. Cortex phellodendri chinensis and Herba houttuynia were presumed to have the potential anti-AIDS effect. [Life Science Journal 7(2): 1 – 7] (ISSN: 1097 – 8135).

Key Words: Promoter of CXCR4, medicine screening, anti-AIDS agents.

I. Introduction

The entry of human immunodeficiency virus type 1 (HIV-1) into target cell critically depends on two cell surface components, CD4 and a chemokine coreceptor. Usually the chemokine coreceptor refers to CXCR4 or CCR5 (CC Chemokine Receptor 5) **[1-3]**. The chemokine receptor CXCR4, a member of the superfamily of G-protein-coupled receptors (GPCRs) like CXCR1-CXCR6 、 CCR1-CCR11 、 XCR1 and XCR2 etc., is the first to be discovered HIV coreceptor **[4]**, and mainly found on the surface of immune cells **[5, 6]**. The HIV-1 envelope (Env) consists of gp120 and gp41. gp120 contains the CD4 binding site and a hydrophobic fusion peptide directly involved in membrane fusion respectively. During the infection, CD4 binding induces conformational changes in gp120 that exposes the coreceptor binding determinants. The gp120 interaction with the coreceptor then induces a further conformational change in Env which results in insertion of the fusion peptide into the target cell membrane **[3, 7, 8]**. Then HIV-1 RNA integrates into the infected cell genome **[9]**. The study of anti-AIDS drugs targeting on HIV-1 membrane fusion and virus entry becomes a hotspot of research interests nowadays.

The coreceptors are important determinants of viral tropism and pathogenesis and are obvious targets for antiviral drug development. CCR5 mediates the entry of R5 viruses, previously called M-tropic, or non-syncytium-inducing viruses **[2, 10-13]**, that is mainly isolated from patients in the early (asymptomatic) stage of HIV-infection. CXCR4 mediates entry of X4 viruses, previously called T-tropic, or syncytium-inducing viruses **[1, 4],** often emerge in HIV-infected persons in a later stage of disease progression towards AIDS **[5, 14]**. The drugs target of interfering the CXCR4 expression is one of the main study in anti-AIDS/HIV drugs **[15-20]**. Thus, it may be possible to delay or prevent the progression of AIDS through decreasing the expression of CXCR4 by interaction of the activity of CXCR4 promoter. Traditional Chinese medicines are the peculiar drugs in China. Their pharmacology has a wide variety of different functions. Some of these traditional Chinese medicines, whether they could interact the CXCR4 promoter and cause CXCR4 expression decline, are worthy of further research.

The pGL4 Luciferase Reporter Vector is the next generation of reporter gene vectors optimized for expression in mammalian cells. It includes the synthetic firefly luc2 (Photinus pyralis) and Renilla hRluc (Renilla reniformis) genes, which have been codon optimized for more efficient expression in mammalian cells. We cloned the DNA fragment of CXCR4 promoter into pGL4 vector, then transfected the recombinant into Jurkat cells, and then select the transfected cell by G418. Thirteen kinds of traditional Chinese medicines were given to rats by gastric gavage once a day. 7 days later, the serum samples were separated. After being stimulated by the thirteen medicated serums, the luciferase activity inside the transfected Jurkat cells were analyzed in order to know the activity of CXCR4 promoter. Through analyzing the effects on the CXCR4 promoter transcriptions by the thirteen traditional Chinese medicines, we established an anti-HIV/AIDS drugs screening technique targeting on CXCR4 promoter.

TABLE I
DOSE OF TRADITIONAL CHINESE MEDICINE

Traditional Chinese Medicine	Crude Herbal Dose (g/ml)
Radix scutellariae (Huangqin)	0.63
Rhizoma coptidis (Huanglian)	0.35
Cortex phellodendri chinensis (Huangbo)	0.84
Flos lonicerae japonicae (Jinyinhua)	1.05
Fructus forsythiae (Lianqiao)	1.05
Herba lobeliae chinensis (Banbianlian)	1.05
Herba houttuyniae (Yuxingcao)	1.75
Folium isatidis (Daqingye)	1.05
Radix isatidis (Banlangen)	1.05
Ganoderma (Lingzhi)	0.84
Herba andrographis (Chuanxinlian)	0.63
Polyporus (Zhuling)	0.84
Radix et rhizoma glycyrrhizae (Gancao)	0.63

II. Materials and Methods

A. Materials

Traditional Chinese medicine of Radix scutellariae (Huangqin), Rhizoma coptidis (Huanglian), Cortex phellodendri chinensis (Huangbo), Flos lonicerae japonicae (Jinyinhua), Fructus forsythiae (Lianqiao), Herba lobeliae chinensis (Banbianlian), Herba houttuyniae (Yuxingcao), Folium isatidis (Daqingye), Radix isatidis (Banlangen), Ganoderma (Lingzhi), Herba andrographis (Chuanxinlian), Polyporus (Zhuling) and Radix et rhizoma glycyrrhizae (Gancao) were purchased form Zhangzhongjing Medicamentarius (Henan). All of them are recorded in the Chinese Pharmacopoeia. Active principles of Chinese herbs were extracted by decocting **[21, 22]**. Dose of traditional Chinese medicines (crude herbal dose in the decoction) are shown in Table I.

B. pGL4-CXCR4 Vector Construction

Primers with restriction enzyme sites of Kpn I and Nhe I (TaKaRa) were designed according to the DNA sequence of CXCR4 promoter: M1: 5'-CGG TAC CAA GCA CTA TTC GCG AAT TGG TTA C-3', M2: 5'-TGC TAG CGG TAA CCG CTG GTT CTC CAG A-3'. CXCR4 promoter fragment was obtained by PCR amplification from plasmid pUC-CXCR4. After digested by Kpn I and Nhe I, it was connected with pGL4 vector (Promega) using T4 ligase (QIAGEN). Positive recombinant vector pGL4-CXCR4 was identified through DNA sequencing and restriction enzyme digestion with Kpn I and Nhe I.

C. Cells Transfection and Selection

Jurkat cells were cultured in RPMI-1640 medium containing 100g/L fetal bovine serum at 37℃ and 5% CO_2. The vector pGL4-CXCR4 and pGL4-CMV (contain the CMV promoter fragment) were transfected into Jurkat cells by Lipofectamine^{TM}2000 (Invitrogen) respectively. Then transfected cells were screened by G418 (Invitrogen) for 4 weeks. The concentration of G418 is 600μg/ml during the cell selection and 200μg/ml during the amplification culture of stable transfected cells.

D. Preparation Medicated Serum

Forty-four adult Wistar rats (180-220g), purchased from laboratory animal center of Zhengzhou University and used in the following experiments according to the guiding principles for the care and use of laboratory animals. Rats were randomly divided into fourteen groups. The rats of thirteen experimental groups were administered intragastrically with thirteen kinds of traditional Chinese medicines decoction respectively, for 3ml/rat (equivalent to 10 times of clinical equivalent dose for adult person of 60kg), once a day at 4pm-5pm for 7 days **[23]**. Blood was obtained by abdominal aorta puncture 24h after the last administration and the separated serum were termed as medicated serum. In one control group, rats were orally administrated normal saline in the same protocol; Their serum were used as control serum **[24]**. Both the medicated and control serum were inactivated by heating at 56℃ for 30 min **[25, 26]**, then filtered through 0.22 μm filter, and stored at -80℃ until use. (The serum of same group were mixed for storage **[27]**)

E. Stimulating Cells by Serum

The Jurkat cells stably expressing pGL4-CXCR4 were randomly distributed into fourteen groups: one is control serum group stimulated by control serum; the other thirteen experimental serum groups stimulated by thirteen medicated serum respectively. 2ml cell suspension at a density of 5×10^5/ml was inoculated into 6-well plates and cultured in RPMI-1640 with thirteen 10% medicated serum and one 10% control serum respectively. There were 5 sub-wells in each group and incubated at 37℃ in a humidified incubator with 5% CO_2. 24h later, the same culture medium was changed once again. Meanwhile, the untransfected Jurkat cell was served as blank control group.

F. Luciferase Activity Assay

After a further culture for 16h, the cells were collected (3×10^5/well) and the luciferase activities of the reporter gene were measured by using E1500 luciferase assay kit (Promega) according to the manufacturer's protocol. Fluorescent value was detected by using Glomex^{TM}20/20 luminometer (Promega). Each well was performed three times.

TABLE II
DETECTION OF LUCIFERASE ACTIVITY

Group	n	Fluorescent Value	*P*
Radix scutellariae (Huangqin) Group	15	899839.6 ± 20855.6	.389
Rhizoma coptidis (Huanglian) Group	15	865065 ± 46150.0	.908
Cortex phellodendri chinensis (Huangbo) Group	15	406175.2 ± 35146.2*	.000
Flos lonicerae japonicae (Jinyinhua) Group	15	804546.4 ± 19439.3	.073
Fructus forsythiae (Lianqiao) Group	15	930277.2 ± 25787.3	.089
Herba lobeliae chinensis (Banbianlian) Group	15	1146839 ± 106138.3*	.000
Herba houttuyniae (Yuxingcao) Group	15	612186.8 ± 38890.9*	.000
Folium isatidis (Daqingye) Group	15	927398.6 ± 106458.0	.105
Radix isatidis (Banlangen) Group	15	850857.4 ± 81690.6	.607
Ganoderma (Lingzhi) Group	15	921582.0 ± 113271.1	.144
Herba andrographis (Chuanxinlian) Group	15	867962.6 ±62413.1	.973
Polyporus (Zhuling) Group	15	843579.0 ± 87317.3	.473
Radix et rhizoma glycyrrhizae (Gancao) Group	15	832654.2 ± 92261.2	.306
Control Group	15	869159.0 ± 62618.8	
Blank control Group	15	39088.4 ± 3867.9	

*There are significant difference between the control group and experimental group（*P*<0.05）

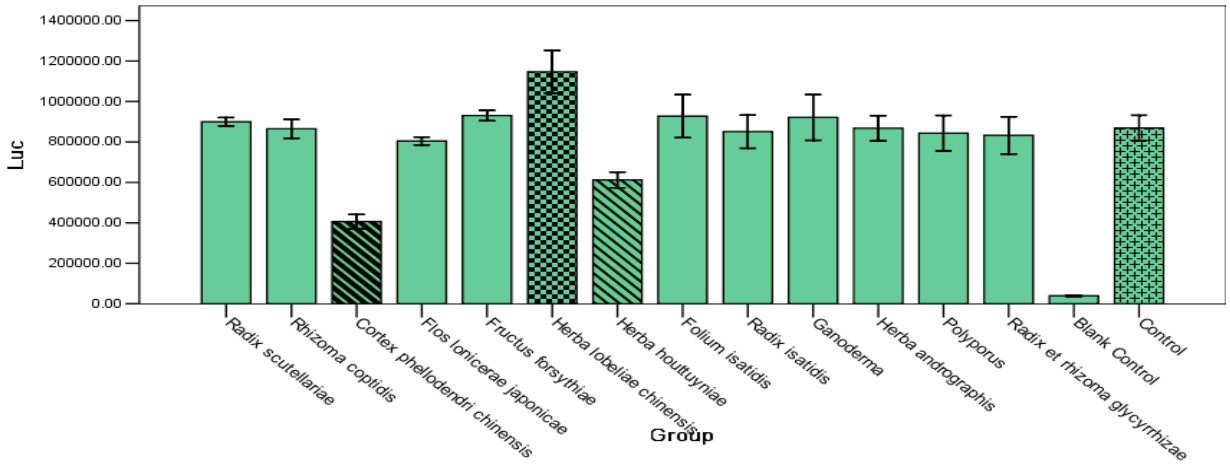

Fig. 3. Detection of the luciferase activity. There are significant difference between the control group and experimental group (Cortex phellodendri chinensis group, Herba lobeliae chinensis group and Herba houttuyniae group). （*P*<0.05）

G. Statistical Analysis

All data were analyzed with SPSS 13.0 Software and the results were expressed with means ± standard deviation. Data in groups were compared with single factor variance analysis (ANOVA). P ＜ 0.05 showed significant difference.

H. Western Blot Analysis

Four groups of cells (Cortex phellodendri chinensis group, Herba lobeliae chinensis group, Herba houttuyniae group and control group) were sonicated and purifed protein were separated on 12% SDS-PAGE, transferred to a nitrocellulose membrane, and subjected to Western blot analysis, using a polyclonal antibody to CXCR4 as a primary antibody. Sheep anti-rabbit horseradish peroxidase-conjugated antibody was used as a secondary antibody. The bands were coloured with electrochemiluminescence method.

I. Analysis of Independent Control Group

Using the same method, the Jurkat cells stably expressing pGL4-CMV were distributed into four groups and stimulated by four kinds of medicated serum: Cortex phellodendri chinensis serum, Herba lobeliae chinensis serum, Herba houttuyniae serum and control serum. Then the fluorescent value was detected and the data were analyzed.

III. Result

A. PCR Amplification Results of CXCR4 Promoter

CXCR4 promoter gene fragment was amplified by PCR from pUC-CXCR4. PCR products were detected by agarose gel electrophoresis. The detected outcome is that typical electrophoretic band is close to DNA marker 770bp. The outcome is consistent with the theory (777bp). See the captions for Fig. 1.

B. Identification of Recombinant Vector

The positive pGL4-CXCR4 plasmid was digested by Kpn I / Nhe I and then confirmed by their digestion. The result of agarose gel electrophoresis showed that the band is

TABLE III
THE LUCIFERASE ACTIVITY DETECTION (PGL4-CMV)

Group	n	Fluorescent Value	*P*
Cortex phellodendri chinensis (Huangbo) Group	15	899839.6 ± 20855.6	.843
Herba lobeliae chinensis (Banbianlian) Group	15	85166.5 ± 82304.6	.193
Herba houttuyniae (Yuxingcao) Group	15	841427.8 ± 58223.1	.110
Control Group	15	893616.6 ± 64088.2	

more or less around 770bp (Fig. 2). At the same time, insertion sequence in pGL4-CXCR4 was confirmed identical with the designed sequence of CXCR4 promoter by sequencing.

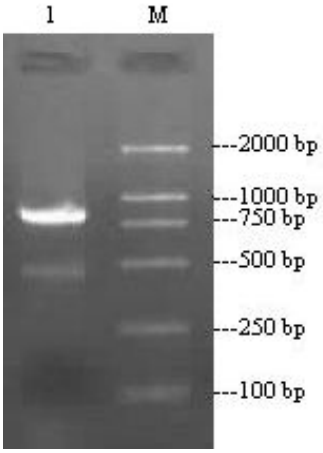

Fig. 1. Agarose gel electrophoresis of PCR products. 1: PCR products of CXCR4 promoter; M: DNA Marker DL2000

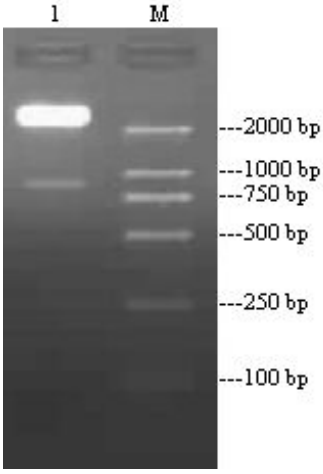

Fig. 2. Agarose gel electrophoresis of the recombinant plasmid after digestion with Kpn I / Nhe I. 1: digestion result of pGL4-CXCR4; M: DNA Marker DL2000

C. Result of Luciferase Activity Assay

Fluorescent value of each group cells is detected by Glomex^{TM}20/20 luminometer after these cells were stimulated by the medicated serum. All data of the detection were analyzed with SPSS 13.0 Software, and conducted with single factor variance analysis (ANOVA). Variance of any a totality is equal to another, $P<0.05$ was considered significant. The results of detections are shown in Table II and Fig. 3. The test data shown that the fluorescent value of Herba lobeliae chinensis group was significantly increased when compared with the control group ($P<0.05$); the fluorescent value of Cortex phellodendri chinensis group and Herba houttuyniae group were significantly decreased when compared with that of the control group ($P<0.05$). These show that the luciferase activity in the Jurkat cells of Herba lobeliae chinensis group was significantly higher than those in the control, while the luciferase activity in the Jurkat cells of Cortex phellodendri chinensis group and Herba houttuyniae group were greatly decreased. Because the segment of CXCR4 promoter was inserted into pGL4 vector, we can know that the CXCR4 promoter activity should increase in Herba lobeliae chinensis group than that in the control; the CXCR4 promoter activity should decrease in Cortex phellodendri chinensis group and Herba houttuyniae group. All data were analyzed statistically and shown with bar chart (Fig. 3). From this bar chart, the fluorescent values of each group could be compared directly, and there were obvious difference from the control group between the Herba lobeliae chinensis group, Cortex phellodendri chinensis group and Herba houttuyniae group. In addition, according to Table II and Fig. 3, we can find that the fluorescent value of the control group was 20+ times than those in the blank control group, which suggests that the Jurkat cell was transfected stably with pGL4-CXCR4 and expressed the luciferase activity.

D. Western Blot for CXCR4 Protein

CXCR4 Western-blotting (Fig. 4) showed that protein level in Cortex phellodendri chinensis group and Herba houttuyniae group were higher than that in control group; protein level in Herba lobeliae chinensis group were lower than control group.

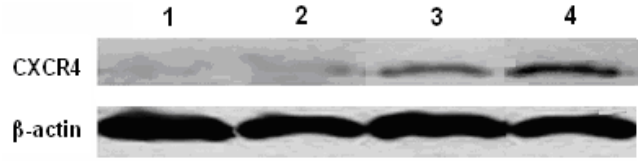

Fig. 4. The comparison of CXCR4 protein expression 1-4: Cortex phellodendri chinensis group, Herba houttuyniae group, Control group, Herba lobeliae chinensis group.

E. Result of Independent Control Group

The Jurkat cells stably expressing pGL4-CMV were stimulated by four kinds of serum, the luciferase activity in the cells showed no difference between control group and medicated serum group.($P>0.05$) (Table III, Fig. 5)

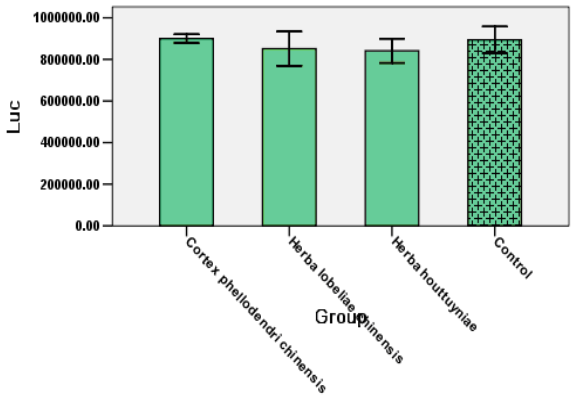

Fig. 5 The luciferase activity detection (pGL4-CMV)

IV. Discussion

Chemokines are small soluble proteins of about 70 amino acid residues and its molecular mass is 8 to 10 kD. They are natural ligands of the most known HIV coreceptor. CXCR4, a member of CXC chemokine receptor, is the principal coreceptor and mediates entry of the T-cell-line-tropic HIV-1 isolate which is involved in the onset of AIDS-defining symptoms **[3, 28, 29]**. Study in vivo and in vitro show that antagonism or function interference of CXCR4/CCR5 can have a marked effect on HIV (super-) infection at the entry step, thus inhibit HIV-1 replication. The purpose of this experiment was to establish a medicine screening system to investigate the effect of some medicines acting on CXCR4 promoter. These medicines have the efficacy of down-regulation CXCR4 expression, then play its roles of anti-AIDS.

Chinese herbs serum pharmacology method was proposed by Japanese scholar in 1984. It is an in vitro method of using medicated serum which was collected after the animal was given single Chinese herb or compound traditional Chinese medicine oral administration. It has become an important method on traditional Chinese medicine pharmacology research recently. This method avoids the interference of herb physicochemical properties in vitro study when the herb is used directly. It also reflects the pharmacologic actions of herb and its metabolites, and better fit the actual process in the living body environment **[30]**. If the crude preparation of traditional Chinese medicine adds directly into reaction system (e.g. cultured cells) the nonspecific physical and chemical factors (such as pH values, osmotic pressure, tannins and inorganic salts etc.) in the crude preparation will effects on cell growth, thus produce false positive results or false negative results. These false positive results & false negative results will affect the results' reliability and scientificity. But, the serum can add directly into reaction system and be a single & controllable influencing factor to evaluate the experimental results, if using serum pharmacology method. This serum contained the effective components of drugs after the body absorbs and metabolize these drugs. This kind of method can reflect drug effect and mechanism objectively and directly. Moreover, some drugs could affect the CXCR4 promoter not by their original form but by metabolic form, or some drugs could affect the CXCR4 promoter directly but lose this ability after these drugs were absorbed. Metabolism and factors in the serum can influence these drugs effect. My above descriptions could be reflected accurately by the serum pharmacology method. So, the experimental results can be considered more reliability by this method **[31]**. Animals currently employed for the study are rats **[27]**. But, there are differences in absorption and metabolism of drugs between animals and human body. So, the proper drug dose is important to ensure the success of the experiment. Firstly, should consider that because serum amount should not be bigger and diluted many times the plasma concentration should be as big as possible. And secondly, should consider how the drugs could achieve their proper concentration of the best effectiveness. Some scholars reported that cytotoxicity of the serum will inhibit cell growth when using higher concentration drug serum. So they think that concentration of the drug serum should be 10% in vitro **[32]**. Other scholars think that the amount of added serum should not be over 20% by considering the serum tolerance of the cultured cells **[32]**. Therefore, the establishment of the amount of adding drug serum in vitro study should refer the reported literatures and we should select a proper amount according to the preliminary experiment results: avoiding the cytotoxicity of higher concentration of drug serum, and making the drug serum concentration close to the blood concentration in order to reflect the drugs holistic effect objectively. In this experiment, drug serum addition amount is 10% each well. To make drug concentration in vitro identical with those in vivo, dosage given to rats by oral administration is: commonly used clinical amount ×equivalent area coefficient of animal ×sera diluted of culture medium **[33]**. Drug feeding times was in accordance with routine usage of 7-10 days **[23]**. In addition, traditional Chinese medicine preparation has larger granules and easy interfered with food, therefore most of animals can absorb medicine effectively and quickly in the fasting state. The rat is a nocturnal animal and food intake at night. Giving drugs in the afternoon is also to obey this law **[34]**. For the treatment of experimental serum, we tend to inactivate the serum by heating at 56℃ for 30 min **[25, 26]**. Inactivation not only can help to eliminate the interference of complement component activity, but also accord with the aseptic requirements of conventional cell culture **[35]**. Meanwhile, in order to control the authenticity and reliability of experimental result, when the experiments are arranged on the base of serum pharmacology method, we not only study the relationship between the serum adding amount and the effective drug concentration, but also set up control serum group to eliminate the interfering substances effect of serum itself on the study system **[24, 35]**. In this experiment, each group include three rats and the serum in the same group were collected for mixing use, which can also reduce individual difference in drug absorption among experimental animals **[27]**.

There are two stages in the regulating of gene expression: transcriptional regulation and post-transcriptional

regulation. In this experiment we used reporter gene research method to investigate the transcriptional regulation of traditional Chinese medicine on CXCR4 promoter. If the screened medicines can up-regulated CXCR4 promoter activity they could induce the increase of CXCR4 gene transcription. CXCR4 gene transcription's increase will induce the CXCR4 protein expression level to increase, no change or decrease because of the existence of post-transcriptional regulation. Contrarily, if the screened medicines can down-regulate CXCR4 promoter activity and reduce the CXCR4 gene transcription, the diminution of CXCR4 protein expression will be finally affirmed. This is because the post-transcriptional can only down-regulate the gene transcription. Thus, the medicines' down-regulated effect on CXCR4 promoter is more reliable in our experiment. The western blot for CXCR4 protein coincide with the above-mentioned experiments.

At the same time, these three kinds of traditional Chinese medicines (Cortex phellodendri chinensis, Herba lobeliae chinensis， Herba houttuyniae) could not affect the activity of CMV promoter. These showed that the effects of these medicines for CXCR4 promoter were specific.

The experimental results show that Cortex phellodendri chinensis and Herba houttuyniae can down-regulate the activity of CXCR4 promoter. We speculate that Cortex phellodendri chinensis and Herba houttuyniae have potential anti-AIDS effect. Certainly, in order to confirm the preventative and therapeutical effect of these medicines on AIDS, we should also detect the expression of CXCR4 on the surface of $CD4^+$ T cells, the absolute value of $CD4^+$ T cells and the variation of viral loads in AIDS patients, etc. Also, because of (a) the serum were collected from the different individuals with the different physiological and pathological showing individual difference; (b) That serum containing drug stimulated cells by twice maybe cover up the drug's actual function; (c) The difference of absorption & metabolism between human and animal with the same drug and (d) the limit of some experimental conditions, this experimental method has some limitations. But, this experimental method is an effective screening system for anti-AIDS Chinese drugs, and is feasible for setup a rapid and high-throughput Chinese drugs screening program for CXCR4 promoter.

Acknowledgement

The authors gratefully acknowledge Guoqiang Zhao, for his thoughtful comments and critical review of the manuscript; the authors also thanks for the donation of plasmid pUC-CXCR4 by Mr. Phililp Ehrenberg.

References

1. Feng Y, Broder CC, Kennedy PE, Berger EA, "HIV-1 Entry Cofactor: Functional cDNA Cloning of a Seven-transmembrane, G Protein-coupled Receptor," Science., vol. 272, no. 5363, pp. 872-877, May 1996.
2. Dragic T, Litwin V, Allaway GP, Martin SR, Huang Y, Nagashima KA, Cayanan C, Maddon PJ, Koup RA, Moore JP, Paxton WA, "HIV-1 Entry into CD4+ Cells is Mediated by the Chemokine Receptor CC-CKR-5," Nature., vol. 381, no. 6584, pp. 667-673, Jun 1996.
3. Berger EA, Murphy PM, Farber JM, "Chemokine Receptors as HIV-1 Coreceptors: Roles in Viral Entry, Tropism, and Disease," Annu Rev Immunol., vol. 17, pp. 657-700, 1999.
4. Berson JF, Long D, Doranz BJ, Rucker J, Jirik FR, Doms RW, "A Seven Transmembrane Domain Receptor Involved in Fusion and Entry of T-cell-tropic Human Immunodeficiency Virus Type 1 Strins," J Virol., vol. 70, no. 9, pp. 6288-6295, Sep 1996.
5. Sallusto F, Baggiolini M, "Chemokines and Leukocyte Traffic," Nat Immunol., vol. 9, no. 9, pp. 949-952, Sep 2008.
6. Proost P, Wuyts A, van Damme J, "The Role of Chemokines in Inflammation," Int J Clin Lab Res., vol. 26, no. 4, pp. 211-223, 1996.
7. Wild C, Dubay JW, Greenwell T, Baird T Jr, Oas TG, McDanal C, Hunter E, Matthews T, "Propensity for a Leucine Zipper-like Domain of Human Immunodeficiency Virus Type 1 gp41 to form Oligomers Correlates with a Role in Virus-induced Fusion Rather than Assembly of the Glycoprotein Complex," Proc Natl Acad Sci U S A., vol. 91, no. 26, pp. 12676-12680, Dec 1994.
8. Wild CT, Shugars DC, Greenwell TK, McDanal CB, Matthews TJ, "Peptides Corresponding to a Predictive Alpha-helical Domain of Human Immunodeficiency Virus Type 1 gp41 are Potent Inhibitors of Virus Infection," Proc Natl Acad Sci U S A., vol. 91, no. 21, pp. 9770-9774, Oct 1994.
9. Doms RW， Trono D, "The Plasma Membrane as a Combat Zone in the HIV Battlefield," Gene Dev., vol. 14, no. 21, pp. 2677-2688, Nov 2000.
10. Alkhatib G, Combadiere C, Broder CC, Feng Y, Kennedy PE, Murphy PM, Berger EA, "CC CKR5: a RANTES, MIP-1alpha, MIP-1beta Receptor as a Fusion Cofactor for Macrophage-tropic HIV-1," Science., vol. 272, no. 5270, pp. 1955-1958, Jun 1996.
11. Choe H, Farzan M, Sun Y, Sullivan N, Rollins B, Ponath PD, Wu L, Mackay CR, LaRosa G, Newman W, Gerard N, Gerard C, Sodroski J, "The β-chemokine Receptors CCR3 and CCR5 Facilitate Infection by Primary HIV-1 Isolates," Cell., vol. 85, no. 7, pp. 1135-1148, Jun 1996.
12. Deng H, Liu R, Ellmeier W, Choe S, Unutmaz D, Burkhart M, Di Marzio P, Marmon S, Sutton RE, Hill CM, Davis CB, Peiper SC, Schall TJ, Littman DR, Landau NR, "Identification of a Major Co-receptor for Primary Isolates of HIV-1," Nature., vol. 381, no. 6584, pp. 661-666, Jun 1996.
13. Doranz BJ, Rucker J, Yi Y, Smyth RJ, Samson M, Peiper SC, Parmentier M, Collman RG, Doms RW, "A Dual-tropic Primary HIV-1 Isolate that uses Fusin and the Beta-chemokine Receptors CKR-5, CKR-3, and CKR-2b as Fusion Cofactors," Cell., vol. 85, no. 7, pp. 1149-1158, Jun 1996.
14. Schuitemaker H, Koot M, Kootstra NA, Dercksen MW, de Goede RE, van Steenwijk RP, Lange JM, Schattenkerk JK, Miedema F, Tersmette M, "Biological Phenotype of Human Immunodeficiency

Virus Type 1 Clones at Different Stages of Infection: Progression of Disease is Associated with a Shift from Monocytotropic to T-cell-tropic Virus Population," J Virol., vol. 66, no. 3, pp. 1354-1360, Mar 1992.
15. Hatse S, Princen K, Gerlach LO, Bridger G, Henson G, De Clercq E, Schwartz TW, Schols D, "Mutation of Asp(171) and Asp(262) of the Chemokine Receptor CXCR4 Impairs its Coreceptor Function for Human Immunodeficiency Virus-1 Entry and Abrogates the Antagonistic Activity of AMD3100," Mol Pharmacol., vol. 60, no. 1, pp. 164-173, Jul 2001.
16. Rosenkilde MM, Gerlach LO, Jakobsen JS, Skerlj RT, Bridger GJ, Schwartz TW, "Molecular Mechanism of AMD3100 Antagonism in the CXCR4 Receptor: Transfer of Binding Site to the CXCR3 Receptor," J Biol Chem., vol. 279, no. 4, pp. 3033-3041, Jan 2004.
17. Gerlach LO, Skerlj RT, Bridger GJ, Schwartz TW, "Molecular Interactions of Cyclam and Bicyclam Non-peptide Antagonists with the CXCR4 Chemokine Receptor," J Biol Chem., vol. 276, no. 17, pp. 14153-14160, Apr 2001.
18. Schols D, Struyf S, Van Damme J, Esté JA, Henson G, De Clercq E, "Inhibition of T-tropic HIV Strains by Selective Antagonization of the Chemokine Receptor CXCR4," J Exp Med., vol. 186, no. 8, pp. 1383-1388, Oct 1997.
19. Tamamura H, Hiramatsu K, Mizumoto M, Ueda S, Kusano S, Terakubo S, Akamatsu M, Yamamoto N, Trent JO, Wang Z, Peiper SC, Nakashima H, Otaka A, Fujii N, "Enhancement of the T140-based Pharmacophores leads to the Development of More Potent and Bio-stable CXCR4 Antagonists," Org Biomol Chem., vol. 1, no. 21, pp. 3663-3669, Nov 2003.
20. Xu Y, Zhang X, Matsuoka M, Hattori T, "The Possible Involvement of CXCR4 in the Inhibition of HIV-1 Infection Mediated by DP178/gp41, " FEBS Lett., vol. 487, no. 2, pp. 185-188, Dec 2000.
21. Gao H, "High Throughput Screening of Agonist for M1 Receptor from Traditional Chinese Medicine," Chongqing University (2003 graduation theses of master degree), pp. 23-24, 2003.
22. Cao Y, Xia QH, Meng H, Zhong Ap, "Antitumor and Synergistic Effect of Chinese Medicine 'Bushen Huayu Jiedu Recipe' and Chemotherapy on Transplanted Animal Hepatocarcinoma," World J Gastroenterol., vol. 11, no. 33, pp. 5218-5220, Sep 2005.
23. Umeda M, Amagaya S, Ogihara Y, "Effects of Certain Herbal Medicines on the Biotransformation of Arachidonic Acid: a New Pharmacological Testing Method Using Serum," J Ethnopharmacol., vol. 23, no. 1, pp. 91-98, May-Jun 1988.
24. Li YK, "Several of Questions about the Experimental Methods of Chinese Herb's Serum Pharmacology," Tradit Chin Drug Res Clin Pharmacol., vol. 10, no. 2, pp. 95-98, Mar 1999.
25. Liu C, Liu CH, Liu P, Xu LM, Hu YY, "Inhibitory Effect of Fuzhenghuayu Decoction on Ito Cell Proliferation in Rats," Chin J Trad., vol. 4, no. 2, pp. 97-99, 1996.
26. Liu CH, Liu P, Liu C, Ji G, Xu LM, "Study on a Seropharmacological Method for an Effective Antifibrotic Formula," Chin J Exp Tradit Med Form., vol. 2, no. 2, pp. 16-19, Apr 1998.
27. Liu P, "Some Thoughts on Serum Pharmacology," Chinese Journal of Integrated Traditional and Western Medicine., vol. 19, no. 5, pp. 263-266, May 1995.
28. Fauci AS, "Host Factors and the Pathogenesis of HIV-induced Disease," Nature., vol. 384, no. 6609, pp. 529-534, Dec 1996.
29. Moore JP, Trkola A, Dragic T, "Co-receptors for HIV-1 Entry," Curr Opin Immunol., vol. 9, no. 4, pp. 551-562, Aug 1997.
30. Sun YH, Fang XY, Liu HY, "Research Status of the Method in Herbal Serologic Pharmacological," Lishizhen Medicine and Materia Medica Research., vol. 13, no. 2, pp. 114-5, 2002.
31. Wang LQ, Yu SC, Li YK, Li Y, "Study on Antitumor Activity of the Sophora Flavescens Ait and Agrimonia Prlosa Ledeb by Method of Serum Phamaclolgy," Chinese Journal of Traditional Medical Science and Technology., vol. 2, no. 5, pp. 19-21, 1995.
32. Pan WS, Liu MF, Shi Y, Xing DM, Du LJ, He XH, Zhang HY, "Plasma Pharmacology and Plasma Chemistry and Pharmacokinetics of Traditional Chinese Medicines," World Science and Technology-Modernization of Traditional Chinese Medicine., vol. 4, no. 3, pp. 53-56, 2002.
33. Wang LQ, Li YK, Fu SG, Fu HD, "Discussion of Serum Pharmacological Method," Pharmacology and Clinics of Chinese Materia Medica., vol. 13, no. 3, pp. 92-93, 1997.
34. Zhao WH, Cao YX, Yuan ZF, "Discussion of the Method in Herbal Serologic Pharmacological," Traditional Chinese Drugs Research and Clinical Pharmacology., vol.13, no. 2, pp. 122-124, Mar 2002.
35. Zhang L, Xu L, Yuan DP, Fang TH, "Development of Study on Chinese Herbal Medicine Serum Pharmacology," Journal of Nanjing University of Traditional Chinese Medicine., vol. 18, no. 4, pp. 254-256, Jul 2002.

3/1/2010

Taxonomic Diversity of Understorey Vegetation in Kumaun Himalayan Forests

Geeta Kharkwal *[1], Poonam Mehrotra [2], Yaswant Singh Rawat [1]

[1] DEPARTMENT OF BOTANY, DSB CAMPUS, KUMAUN UNIVERSITY, NAINITAL, UTTARAKHAND 263002, INDIA ;
[2] DEPARTMENT OF BOTANY, BUNDELKHAND UNIVERSITY, JHASI, UTTARAKHAND 263002, INDIA
geetakh@gmail.com

Abstract: Taxonomic diversity of understorey vegetation (herb species) was studied in two evergreen forests, viz. oak and pine in the Kumaun Himalaya. In terms of taxonomic diversity, Asteraceae and Lamiaceae were the two dominant families in the sampling forest types. Maximum number of species was found at hill base and minimum at hill top in both the forests. The number of families, genera and species ratio observed for pine forest was of course higher with compared to the oak forest showed about the higher taxonomic diversity. Perennials form had higher contribution as compared to annuals forms indicated better ability to store up soil. Very few species (9 species) were found to be common indicates higher dissimilarity in both type of forests. Species richness (per m2) was higher in the pine forest than the oak forest. A high value of beta-diversity in the oak forest point out that the species composition varied from one stand to another. However, low concentration of dominance value in the pine forest with compare to the oak forest point towards the dominance, which is shared by many species. [Life Science Journal. 2010; 7(2): 8 – 12] (ISSN: 1097 – 8135).

Keywords: Species richness; beta-diversity; taxonomic diversity; forest

1. Introduction

The pattern and relationships between species diversity and ecosystem functioning are the current areas of great ecological interest throughout the world. Species diversity incorporates two components (Stirling and Wilsey, 2001); evenness (how evenly abundance or biomass is distributed among species) and richness (number of species per unit area). High evenness can increase invasion resistance, below-ground productivity and reduce total extinction rates (Smith et al., 2004). The spatial variations in biodiversity generally include species diversity in relation to size of the area, relationship between local and regional species diversity and diversity along gradients across space, and environmental factors such as latitude, altitude, depth, isolation, moisture and productivity (Gaston, 2000). In addition, species richness of a taxon is not only sufficient to express diversity but the equitability is also a important factor because communities however vary in properties of the total importance of the species and share their functional contribution (Tilman, 2000).

A fundamental characteristic of mountain ecosystems is to the drastic change in vegetation as well as in climatic conditions from the base to the summit of the mountain. Elevation gradients create varied climates, along with resultant soil differentiation; promote the diversification of plant species (Brown, 2001). Many studies have investigated on species richness along elevation gradient across habit and taxa (Sanders et al., 2003), as part efforts to understand ecosystem effects on biodiversity and maintenance of biodiversity (Gytnes and Vetaas, 2002). Furthermore, the observation relations between species distribution and elevation bands may also help to understand the possible effects of climate change, e.g. by providing baseline information to measure the effect of climate change and anthropogenic changes on vegetation.

The forest herbs, which play important role for rural communities for example, the livestock totally dependent on them for fodder and as traditional medicines, have been hardly studied from diversity standpoint (Singh and Singh 1987). Quantitative information on the forest floor species of the Central Himalaya region is generally lacking except for studies done by Rawat and Singh (1989), and Singh and Singh (1992). Interestingly, most of the recent major field experiments addressed questions relating to species diversity which has been carried out in grasslands. But forest herbs of the Himalayan region remain poorly studied.

In the present study we investigate herb species richness (spermatophyte) in terms of taxonomical diversity and species composition in relation to oak and pine forests in Central Himalayan forests.

2. Material and Methods

The study area is located between 29°21′ and 29°24′ N latitudes, and between 79°25′ and 79°29′E longitudes, in the elevational belt of 1600-1950 m asl around Nainital town in Kumaun region of Central Himalaya. The two major forest types, viz., Quercus leucotrichophora (oak) and Pinus roxburghii (pine) were selected for this study. The climate is monsoon temperate. The mean monthly temperature ranged from 11.5ºC (January) to 18.4ºC (June). The rocks of study area belongs to krol series which is a sequence of limestone, grey and greenish grey and purple slates, siltstones (Valdia, 1980). Soil texture is

sandy clay and it is acidic in nature. The sites having minimal biotic disturbances in terms of grazing or herbage removal were selected. The site variations due to the canopy changes are presented in Table 1. For detailed studies of plant biodiversity and other vegetational parameters, selected sites were divided into three stands, viz., hill base, hill slop and hill top (HB, HS and HT, respectively).

Table 1. Certain characteristic of study sites

Characters	Forest	
	Close	Open
Elevation (m)	1950	1600
Mean annual temperature (°C)	16	15.8
Total rainfall (cm)	216	200
pH	6.8	5.6
Nitrogen (%)	33	26
Organic carbon (%)	3.5	3.7
C: N ratio	10.6	14.2
Moisture content (%)	42	35

Phytosociological analysis of the herb species in each forest site was carried out by randomly placed 20, 1×1 m^2 quadrats during the peak growth month (September). Diversity was calculated by using Shannon-Wiener index (1963) as:

$$H' = -\sum_{n=1}^{i} Ni/N \quad \log 2 \quad Ni/N$$

where, Ni is the total number of species i and N is the number of individuals of all species in that site. Concentration of dominance was measured by Simpson's Index (1949) as: $C = \Sigma (Ni/N)2$ where Ni and N are the same as for the Shannon-Weiner information function. Beta-diversity was calculated following Whittaker (1975) as: $\beta = Sc/s$ where, Sc is the total number of species encountered in all quadrats and s is the average number of species per quadrat. Equitability or Evenness was calculated to represent the distribution of individuals among the species (Whittaker, 1972) as: E = S / (log Ni - log Ns) where, S is the total number of species, Ni is the number of individuals of most important species, Ns is the number of individuals of least important species and E is the evenness index.

3. Results

The forest herbs species in the oak and pine forests belongs to 21 families. The total number of species present in the oak forest and pine forest was 32 and 41, respectively.

Table 2. Taxonomic distribution of species
(G, Genus; S, Species)

Family	Oak		Pine	
	G	S	G	S
Asteraceae	4	4	9	9
Acanthaceae	1	1	1	1
Apiaceae	2	2	2	2
Amaranthaceae	1	1	-	-
Borngnaceae	-	-	1	1
Brassicaceae	-	-	1	1
Commelinaceae	1	1	1	1
Companulaceae	-	-	1	1
Cyperaceae	1	1	2	2
Fabaceae	2	2	2	2
Geraniaceae	1	2	-	-
Gentiaceae	1	1	1	1
Liliaceae	1	1	-	-
Lamiaceae	3	3	7	7
Orchidaceae	2	2	1	1
Oxalidaceae	1	1	-	-
Poaceae	1	1	2	2
Polygonaceae	1	1	1	1
Ranunculaceae	1	1	1	1
Rosaceae	1	1	1	1
Rubiaceae	1	1	2	3
Violaceae	1	1	-	-
Utricaceae	2	2	1	1
Zingiberaceae	2	2	1	1
Caryophyllaceae	-	-	1	1
Crassulaceae	-	-	1	1

Table 2 depicts diversity of the Angiosperm family in both forest sites. In the oak forest, Asteraceae was represented by four species, followed by Lamiaceae (3 spp.), Fabaceae, Orchidaceae, Utricaceae, Zingiberaceae, Apiaceae and Geraniaceae (2 spp. each) and remaining 13 families were represented by one species each. Taxonomically, Asteraceae was the dominant family (with 4 genera), followed by Lamiaceae (with 3 genera), Apiaceae, Fabaceae, Orchidaceae, Utricaceae and Zingiberaceae (with 2 genera each) and remaining 14 families were represented by single genus only.

In the pine forest, Asteraceae was represented by nine species followed by Lamiaceae (7 spp.), Rubiaceae, (3 spp.), Fabaceae, Poaceae, Apiaceae, and Cyperaceae (2 spp. each) and remaining 14 families were represented by single species. Taxonomically, Asteraceae (with 9 genera) was the most diverse family followed by Lamiaceae, (with 7 genera), Apiaceae, Poaceae, Rubiaceae and Cyperaceae (with 2 genera each) and remaining 13 families were each represented by a single genus (Table 2).

The number of species varied spatially in both forests. In oak forest it varied from 15 (HT) to 30 (HB) and in pine forest from 12 (HT) to 23 (HB). Across the forests, maximum species were present in oak forest (at HB, 30) as compared to pine forest (at HB, 23). Species richness

was higher (7.4) at HB and lower at HT (5.0) in oak forest. Similar pattern was found in pine forest, i.e., maximum species richness was at HB (10.5) and minimum at HT (4.7).

Table 3. Comparison of diversity indices (Sp, species number; Sr, speceis richness; Bd, beta-diversity; H', diversity; Cd, concentration of dominance; E, evenness/equitability)

Indices	Oak forest			Pine forest		
	HB	HS	HT	HB	HS	HT
Sp	30	23	15	23	17	12
Sr	7.4	6.9	5.0	10.5	6.5	4.7
Bd	4.5	4.6	4.6	2.8	2.9	2.8
H'	4.2	4.2	3.5	4.4	4.0	3.4
Cd	1.4	0.1	0.1	0.1	0.2	0.1
E	31.7	27.1	17	27.3	27.4	31.4

Among the both forest site, species richness value was maximum in pine forest at HB (10.5) and minimum in oak forest at HB (7.4). Beta diversity showed pronounced effect at both sites. The value for oak forest varied marginally from 4.5 (HB) to 4.6 (HS), respectively. While for pine forest, it remained approximately same at all sub-sites. Between the forests, the value was higher in oak forest than pine forest. The lowest value of beta-diversity in oak forest was observed at HB (4.5) and for pine forest at HS (2.8). Equitability/evenness value ranged from 17.0 (HT) to 31.7 (HB) in the oak forest. A reverse pattern was observed in the pine forest (31.4 at HT and 27.3 at HB).

Table 4. Forest wise ratio of species, genera and family (F, Family; G, Genus; S, Species)

Forest	F:G	F: S	G: S
Oak	1.2	1.3	1.0
Pine	1.4	1.5	1.1

The concentration of dominance fluctuated from 0.1 to 1.4 in oak and from 0.1 to 0.2 in pine forest (Table 3). It was comparatively higher in the oak forest. The low value of concentration of dominance indicates that the dominance is shared by many species. The ratio of family to species, family to genera and genera to species for the both forests indicated higher taxonomic diversity in pine forest than that in the oak forest (Table 4). Percent contribution of perennial herbs is maximum in oak forest than the pine forest (Figure 1).

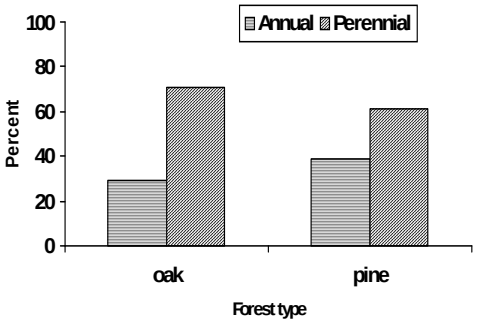

Fig. 1. Percent contribution by life forms in oak and pine forests

4. Discussions

The changes in topography, altitude, precipitation, temperature and soil conditions contribute to the diverse bioclimate that results in a mosaic of biotic communities at various spatial and organizational levels. Diversity represents the number of species, their relative abundance, composition, interaction among species and temporal and spatial variation in their properties. Where richness and evenness coincide, i.e., a high proportion of plant species in the vegetation are restricted, community of that area is supposed to have evolved through a long period of environmental stability.

The observation in the present study showed that the oak forest was typically moister than the pine forest which is consistent with the study of Saxena and Singh (1982). Pine forest was about 25% more diverse (40 spp.) in comparison to the oak forest (32 spp.).

Asteraceae was the dominant family in pine forest because most of the species of the family are primary successionals and have different types of growth forms. This family showed basal as well as erect forms in which basal forms emerged near the ground-level with well-developed petioles and formed a short-umbrella (Mehrotra, 1998). They can tolerate cool temperatures to high irradiances with low density of herb cover. However, erect forms are less able to capitalize on the spring window of light than any other form. This showed that the different growth forms reflect a mixed type of forest response (harsh dry to mesic). Moreover, basal forms of Violaceae showed affinity to mesic and cold conditions under the oak forest. Few species are able to tolerate the entire spectrum of environment and range throughout the gradient (Brown, 2001).

Our study showed that perennials gained dominance over annuals in oak forest as well as pine forest (Figure 1). Perennial have ability to conserve soil and with their extensive root systems of perennial grasses they also add more organic matter to the soil than annuals which can be

more favourable for plant growth. Singh and Singh (1987) observed that annuals colonize and dominate the early stages of succession. Annuals to perennials species ratio are higher at primary successional site than climax stage. Species richness generally increases during secondary succession when environmental and edaphic conditions are favourable with low fluctuations.

The above results indicate that the oak forest makes climax stage for succession. The evenness and β-diversity showed similar values in sub-sites of oak as well as pine forests. The high values of beta-diversity indicate that the species composition varied from one stand to another.

Equitability/evenness varied in pine forest with respect to sub-site from 27.3 (HB) to 31.4 (HT) (Table 3). This was because of the conditional presence or absence of functional relationship of species. Comparatively higher value of equitability in pine forest with respect to oak forest indicated that the individual herb species distribution is higher. This may perhaps due to intermediate level of disturbance.

The allocation of species in the Kumaun Central Himalaya is mainly governed by moisture and temperature gradients that incorporate the effect of many physical factors. Moustafa (1990) found that the association of community types is the result of the performance of the species in response to the environmental conditions that prevail in a particular forest type. Tewari (1982) assumed that the temperature gradient is the net product of elevation and aspect; while moisture gradient is a function of slope degree, soil texture and nature of soil surface.

In addition to that, hierarchical diversity concerns taxonomic differences at other than the species level. Pielou (1975) and Magurran (1998) suggested that hierarchical (taxonomic) diversity would be higher in an area in which the species are divided amongst many genera as opposed to one in which most species belong to the same genus, and still higher as these genera are divided amongst many families as opposed to few. The families, genera and species ratio was observed maximum in the pine forest as compared to the oak forest in the present study (Table 4), indicating diverse taxonomic vegetation in the pine forest.

Acknowledgements:
Authors are grateful to the Department of Science and Technology, Government of India for financial support to carry out this work.

Corresponding Author:
Dr. Geeta Kharkwal
Department of Botany
DSB Campus, Kumaun University
Nainital, Uttarakhand 263002, India
E-mail: geetakh@gmail.com

References

Stirilng G, Wilsey B. Emprical relationships between species richness, eveness and proporational diversity. Am Nat 2001;158(3):286-99.

Smith MD, Wilcox JC, Kelly T, Knapp AK. Dominance not richness determines invasibility of tallgrass prairie. Oikos 2004;106(2):253–62.

Gaston K J. Global pattern in biodiversity. Nature 2000;405(1):220-7.

Tilman D. Causes, consequences and ethics of biodiversity. Nature 2000;405(4):208-11.

Brown J. Mammals on mountainsides: elevational patterns of diversity. Global Ecology and Biogeography 2001;10(1):101-9.

Sanders NJ, Moss J, Wagner D. Pattern of ant species richness along elevational gradients in an arid ecosystem. Global Ecology and Biogeography 2003;10(2):77-100.

Grytnes JA, Vetaas OR. Species richness and altitude: A comparison between null models and interpolated plant species richness along the Himalayan altitudinal gradient, Nepal. The Am Nat 2002;159(3):294-304.

Singh JS, Singh SP. Forest vegetation of the Himalaya. Bot Rev 1987;52(2):80-192.

Rawat YS, Singh JS. Forest floor, litter falls, nutrient return in central Himalayan forests. Vegetatio, 1989;82(2):113-29.

Singh JS, Singh SP. Forest of Himalaya: Structure, Functioning and Impact of man. Gyanodaya Prakashan, Nainital, India, 1992.

Valida KS. Geology of Kumaun lesser Himalaya, Wadia Institute of Himalaya Geology, Dehradun, India, 1980;291.

Shannon CE, Wienner W. The mathematical theory of communication. Univ. Illinois Press, Urbana, 1963.

Simpson EH. Measurement of Diversity. Nature 1949;163(2):688-91.

Whittaker RH. Community and Ecosystems. IInd ed. McMillan, New York, 1975.

Whittaker RH. Evolution and measurement of species diversity. Taxon 1972;21:213-51.

Saxena AK, Pandey P, Singh JS. Biological Spectrum and other structural functional attributes of the vegetation of Kumaun Himalaya, Vegetatio 1982;49(1):111-9.

Mehrotra P. Adaptive significance of leaf in relation to other parts in oak forest herbs of Kumaun Himalaya, Ph. D. Thesis, Kumaun University, Nainital, India, 1988.

Moustafa AA. Environmental Gradient and Species Distribution on Sinai Mountains. Ph. D. Thesis, Botany Department, Faculty of Science, Suez Canal University, Egypt, 1990;115.

Tewari JC. Vegetational analysis along altitudinal gradients around Nainital, Ph. D. Thesis, Kumaun University, Nainital, 1982;570.

Pielou EC. Ecological Diversity. Wiley, New York, 1975;165.

Magurran AE. Ecological Diversity and Its Measurement. Princeton University Press, Princeton, New Jersey, 1988;179.

Establishment and characterization of DNA pol β knockout human esophageal carcinoma cell line EC9706

Feng Long[1,3], Ma Yunyun[4], Zhao Guoqiang[1], Li Min[1], Sun Sajia[2], Dong Ziming[*2] , Huang Youtian[2]

[1]Department of Microbiology and Immunology, College of Basic Medical Science, Zhengzhou University, Zhengzhou 450001, Henan, China; [2]Department of Pathophysiology, College of Basic Medical Science, Zhengzhou University, Zhengzhou 450001, Henan, China; [3]Department of Pathogenic organism biology, Henan University of TCM, Zhengzhou, 450008, Henan,.China; [4]Henan Medical College for Staff and Workers, Zhengzhou, 451191, Henan, China.
dongzmzzu@126.com

Abstract- To construct a DNA polymerase β gene knockout model in human esophageal carcinoma cell EC9706 by homologous recombination for investigating its biological characterization and sensitivity upon damaging factors or chemotherapeutics. Methods: Based on the homologous recombination principle, the gene targeting vector was constructed to delete polβ gene. The vector was introduced into esophageal carcinoma cellline EC9706 by electroporation. PCR, RT-PCR and Western blot were used to detect the expression of polβ gene at DNA, mRNA and protein level in polβ knockout EC9706 cell. Flow cytometry and MTT were used to detect cell cycle and cell growth velocity. The sensitivity of the gene targeting cell line upon oxydizing agent and chemotherapeutics were detected by trypan blue anti-dyeing method. Results: In the targeting cell line, the DNA, mRNA and protein expression of polβ can not be detected and its biological characterization has marked disparation compared with the normal EC9706 cell.Conclusion: The polβ gene knockout EC9706 cell line was constructed successfully. It may lay a foundation for the further study of pol β gene. [Life Science Journal. 2010; 7(2): 13 – 18] (ISSN: 1097 – 8135).

Key Words: DNA polymerase β; gene knockout; human esophageal carcinoma.

1. Introduction

DNA polymerase β (pol β) is a key enzyme in base excision repair (BER). Its main function is to make up the short gaps generated by base excision (1). Polβ may also take part in DNA duplication, recombination, genome stability and drug resistance (2-6). Furthermore, polβ is responsible to oxidative damage (7). The vicious pol β may decrease the ability of base excision repair and increase the hypersensitity to some alkylating agents (MMS) and oxidant (H_2O_2) (8). Studies showed that there exist overexpression of polβ in many kinds of tumor cells and it may be relevant to tumor's generation (9-10). Recently, polβ mutation and abnormal expression have been found in many human carcinomas (11), such as gastric cancer (12), bladder carcinoma (13), and prostate carcinoma (14-15). Therefore, further researches of polβ on expression characteristic in tumors have been a hotspot (16).

Gene targeting via homologous recombination is a powerful means of assessing gene function in vivo (17). It has been applied to diverse organisms such as bacteria, yeast, poultry and rodents (18). In addition, human somatic cell gene targeting has also been completed successfully (19). Compared with antisense nucleotide and siRNA, gene targeting can delete aimed gene completely. In order to better understand the function of DNA polβ in esophageal carcinoma, we plan to construct the gene targeting model of polβ.

2. Materials and methods

2.1 Cell line

Human esophageal carcinoma cell line EC9706 was purchased from state key laboratory of molecular oncology of Chinese Academy of Medical Sciences and cultured in RPMI-1640 medium containing 100g/L fetal bovine serum, at 37℃ in a 5% CO_2 humidified atmosphere. It was established in 2002, and separated from the well differentiated esophageal squamous carcinoma tissue of a Chinese male patient (20).

2.2 Construction of targeting vector

The targeting vector was created by cloning strategy. The upstream (1.2kbp) and downstream (1.8kbp) homologous sequences were obtained from the genome of esophageal carcinoma EC9706 cell by PCR. The two fragments were cloned into pcDNA3.1 which contains a neomycin resistance cassette for G418 selection. PCR and restriction enzymes digestion were used to identify the positive recombinant (pOUT-polβ). Then the targeting vector pOUT-polβ was linearized with EcoR V. 2.3 2.3 Electroporation 2×107 cells/ml EC9706 cells suspended in PBS (phosphate buffered saline) and 50μg lineared plasmids were prepared. Electroporation was performed on the Gene Pulser (Bio-Rad, Hercules, CA, USA) in 0.4cm cuvettes (Bio-Rad) at the following conditions: 250 Volts, 1000μF, 7s, ∞resistance. Then the cells were planted on 10cm culture capsule, 24 hours later the medium were replaced by RPMI-1640 with 800μg/ml G418. The positive monoclone was picked for expanded culture in RPMI-1640 with 200μg/ml G418.

2.3 PCR analysis

Total DNA were isolated from the gene targeting cells and the normal EC9706 cells (employed as the control group) using DNA extraction kit according to the manufacturer's protocol (Qiagen, USA) respectively. The primers for polβ (5'AAAGGATTCCAGATAAACAC 3' , 5'

GCTGGAAGGA AAGAAGAAAG 3’）were used to identify whether polβ gene had been knocked out. PCR conditions were: initial denaturation at 94°C for 3 min, 35 cycles of amplification (94°C for 45s, 55°C for 45s, 72°C for 45 s), final extension at 72°C for 2 min, and then cooling to 4°C. The PCR products were separated on 15g/L agarose in 1×TAE and visualized by ethidium bromide staining.

2.4 RT-PCR analysis

Total cellular RNA was extracted by Trizol (Invitrogen, Carlsbad, CA). Reverse transcription was performed by AMV (Promega, USA).PCR was performed with DNA pol β and β actin (as ento-standard) specific primers, and the products were analyzed with 15g/L agarose gel electrophoresis. The primers were as follows: polβ (5’GAGAAGAACGTGAGCCAAGC3’, 5’CATCCATGTCACCACTGGAC3’), β-actin (5’ACACTGTGCCCATCTACGAGG3’, 5’CTTTG CGGATG TCCACGTC3’).

2.5 Western blot analysis

Cells were washed with cold PBS, harvested and resuspended at a cell density of 106 cells/20μl in buffer I (10mM Tris-Cl, PH7.8, and 200mM KCl). An equal volume of buffer II (10mM Tris-Cl, PH7.8, and 200mM KCl, 2mM EDTA, 40%glycerol, 0.2% Nonidet P-40, 2mM dithiothreitol, 0.5mM phenylmethylsulfonyl fluoride, 10μg/ml aprotinin, 5μg/ml leupeptin, 1μg/ml pepstain) was added. Then, the cell suspension were transferred to microcentrifuge tubes and sonicated for 10s. After centrifugation of the sonicated suspension at 10000×g for 10 min, at 4℃, the supernatant was collected. The protein concentration was determined by coomassie brilliant blue. Equivalent amounts of protein (25 μg) were separated by SDS-PAGE and then transferred to polyvinylidene difluoride membranes. Membranes were then incubated for 1 h at room temperature with the blocking reagent [5% milk, 2% BSA, 40 ml Tris-buffered saline-0.5% Tween-20 (TBST) pH 7.6], and then incubated overnight at 4℃with the primary antibody. The membranes were washed in TBST and incubated with anti-rabbit secondary antibody for 45 min at room temperature. After washing the membranes with TBST, they were visualized by the protein a peroxidase-linked process (Amersham Biosciences, Little Chalfont, and UK).

2.6 Cytotoxicity assay

Cells were seeded into 24-well plates (1×105 cells/well).48 hr later when they were approximately 90% confluent, the cells were treated with different concentration of cisplatin, bleomycin, H2O2 and methylene blue respectively(Doses are shown in Table.1).2 days later the death rates were detected by trypan blue anti-dyeing method.

2.7 Cell Proliferation Assay

5×103 cells in logarithmic growth phase were seeded in 96-well plates (200μl/well) and allowed to grow for 7 days. Each group made seven blanket wells. Absorbance was measured at 490nm everyday. Four hours before stop culturing, 20 μL of 5 mg/mL MTT (Sigma) was added to the culture medium. After incubation, the culture medium was removed and 200 μL of dimethylsulphoxide (DMSO) was added to resolve the crystal. The cell proliferation curves were drawn according to the absorbance.

2.8 Flow Cytometry Assay

Blood-serum starvation method was used to synchronize cells in G0 phase. A total of 1×106 cells were trypsinized and washed with PBS twice. Then cells were fixed with prechilled 75% ethanol at 4℃ overnight. After three times of wash, cells were digested with 0.1% RNase at 37℃ for 20 min and stained with 10 μg/mL propidium iodide (PI, Sigma) for 1 hr at 4℃. Samples were assayed by flow cytometer and data were analyzed at 488nm.

2.9 Statistical Analysis

All data were analyzed with SPSS 13.0 Software, and conducted with single factor variance analysis (ANOVA). P-values<0.05 were considered statistically significant.

3. Results

3.1 Existence and expression of pol β gene in targeting cell

The existence, mRNA and protein expression of polβgene in the targeting cells and normal untreated EC9706 cells were detected by PCR, RT-PCR and western-blot respectively. The PCR result showed that in the control group (normal EC9706) there was a marked band located in 499bp but there is no existence of polβin the targeting cell (Figure 1). RT-PCR and Western-blot both revealed that there was no expression of polβin the polβknockout cells (Figure 2, Figure 3).

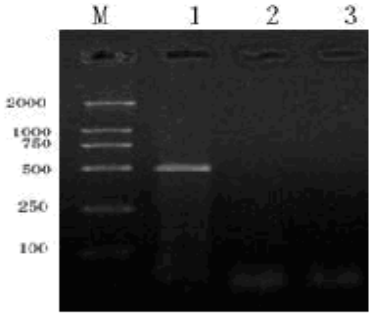

Figure 1. Agarose Gel Electrophoresis of PCR Products

Extract both of the normal EC9706 cells and the targeting cells genomes, then amplified by PCR. The results showed that in the control group (normal EC9706) there was a marked band located in 499bp but there is no existence of polβin the targeting cells. M: DNA Marker;

lane1: Control cells (EC9706); lane 2 and 3: polβ knockout EC9706 cells

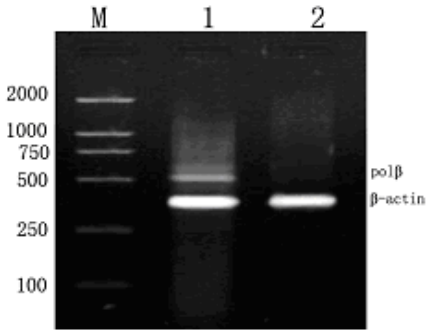

Figure 2. Agarose Gel Electrophoresis of RT-PCR Products

Extract both of the normal EC9706 cells and the targeting cells mRNA, and then amplified by PCR. There was no expression of polβ in the polβknockout cells. M: Marker; lane1: Control cells (EC9706); lane2: polβknockout EC9706 cells

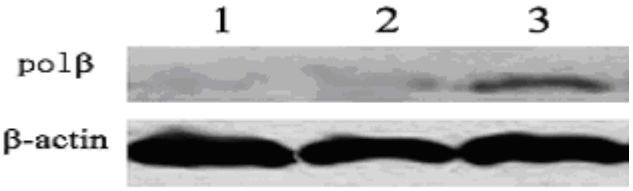

Figure 3. Western Blot Result

The whole cells proteins were prepared as described above in material and method, and samples (25 μg) subjected to Western blotting with polβ (SC-48819, Santa Cruz Biotechnology) and β-actin (SC-130656, Santa Cruz Biotechnology) antibodies. Lane1 and 2: polβ knockout EC9706 cells, there was no expression of polβ in the polβknockout cells; 3: Control cells

3.2 Cell sensitivity to DNA-damaging agents

Trypan blue anti-dyeing method was used to observe the sensitivity to DNA-damaging agents such as cisplatin, bleomycin, H2O2 and methylene blue of targeting cells and control cells. As shown in Figure4(A),4(B),4(C), beginning from the primary concentration, the death rates of the targeting cells to cisplatin, bleomycin and methylene blue were higher than that of control cells($P<0.05$). It means that the sensitivities of the polβ knockout EC9706 cell to these drugs were increased. In sensitivity to H2O2, there is no difference between the two groups when the concentration of H2O2 is below 160μmol/L ($P>0.05$). See in Figure4 (D). While the concentration of H2O2 is higher than 160μmol/L, the sensitivity of the polβ knockout EC9706 cell was increased.

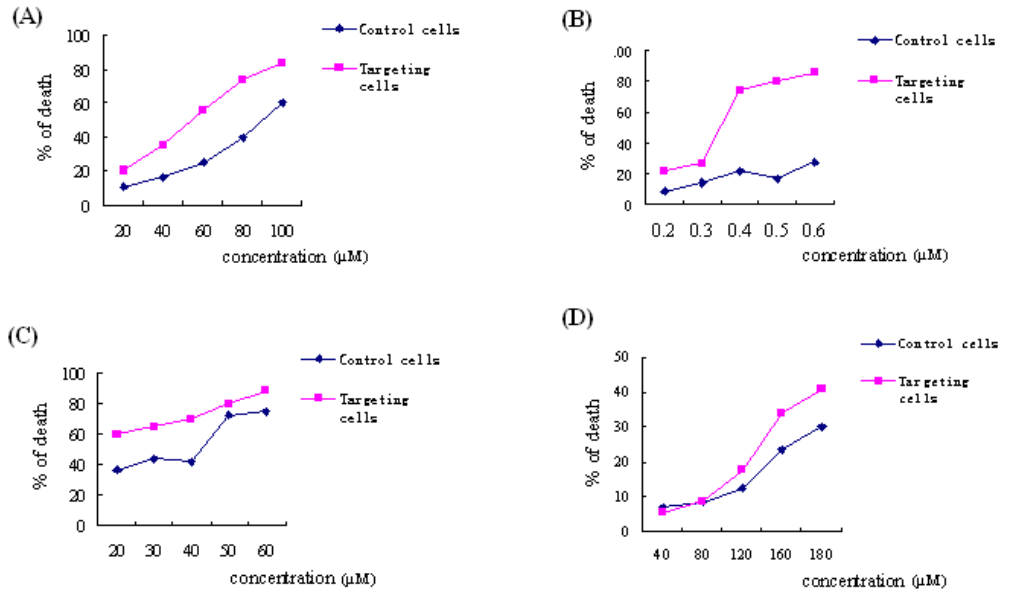

Fig.4 Cell sensitivity to DNA-damaging agents

3.3 biological behaviour of targeting cells

3.3.1 Cell growth curve

Proliferation of targeting cells was evaluated using the MTT assay (Figure.5). The absorbance-time curves showed that the growth velocity of targeting cells was significantly lower than that of control cells.

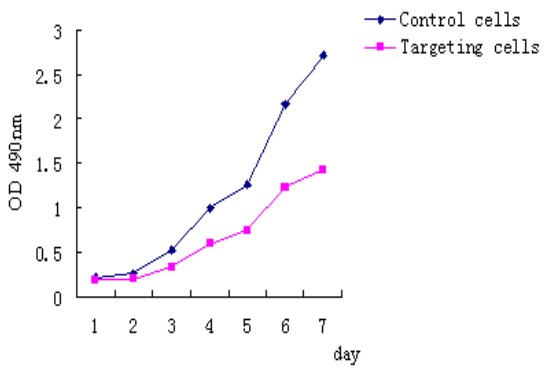

Fig.5 Proliferation curve of targeting cells and control cells

The absorbance-time curves showed that the growth velocity of targeting cells was significantly lower than that of control cells.

Trypan blue anti-dyeing method was used to observe the sensitivity to DNA-damaging agents of targeting cells and control cells. (A) Cisplatin (B) Bleomycin (C) Methylene blue (D) H2O2. As shown in Figure4(A), 4(B) and 4(C) were beginning from the primary concentration, the death rates of the targeting cells to cisplatin, bleomycin and methylene blue were higher than that of control cells ($P<0.05$). Figure4 (D) The sensitivity to H2O2, there is no difference between the two groups when the concentration of H2O2 is below 160μmol/L ($P>0.05$). While the concentration of H2O2 is higher than 160μmol/L, the sensitivity of the polβ knockout EC9706 cell was increased.

Table 1. Concentration of drugs

Drug	Final concentration（μmol/L）				
cisplatin	20	40	60	80	100
bleomycin	0.2	0.3	0.4	0.5	0.6
methylene blue	20	30	40	50	60
H2O2	40	60	80	160	200

3.3.2 Cell cycle

The cell cycle distribution of targeting cells and control cells was shown in Table 2. There have significant differences between targeting cells and control cells in G2~M phase and S phase ($P<0.05$). While no differences in G0-G1 phase.

Table.2 Cell cycle（%,$\bar{x}\pm s$）

Group	G0～G1(%)	S (%)	G2～M（%）
targeting cells	54.877±6.374	35.700±9.43	9.426±4.206
Control cells	46.673±1.616	53.403±1.504	0

4. Discussion

4.1 Construction of DNA pol β gene targeting vector

Based on homologous recombination principle, gene targeting was performed on many organisms which aim to exchange the gene between recipient cells' and the exotic gene, set the interesting gene at right site and alter the cells' emphytic character (21). As it was affected by many factors, design and construct of gene targeting vector will be the main points for gene targeting (22). In this research, we meant to replace part homologous sequences of polβ gene, finally, destroy the biological function of DNA polβ. The whole sequence was about 7.8kb (the upstream is 1280bp and the downstream is 1756bp). If occured, polβ gene core promoter will be replaced, as well as its first, second and third exons, first and second introns and bulk of the third intron. Finally, it may lead to loss of polβ gene function.

4.2 Influence on targeting cell cycle and proliferation

The cell cycle and proliferation rate of targeting cells changed compared with that of the control group (EC9706). For the targeting cells, the S phase rate decreased obviously and the proliferation was also step down ($P<0.05$). According to these results, we found that the proliferation of polβ gene targeting cells were affected, mainly displayed depressant effect. However, overexpression of polβ gene may lead to continuous malignant transformation and accelerated growth velocity (23). Therefore, polβ gene targeting can slow down tumor cell proliferation which will apply for the biotherapy of human carcinoma.

4.3 Cell sensitivity to DNA-damaging agents

The main function of polβ is base excision repair (BER) which is the major repair system for oxidative (H2O2, methylene blue) as well as alkylation damage (24). At present, induction of polβ while responding to oxidative stress has been shown in cultured cells and in organisms (25-26). In our research, polβ gene targeting cells were more sensitive to cisplatin, bleomycin and methylene blue, compared with control cell (EC9706). According to reference reports (27), polβ knockdown cells performed by RNAi technique were more sensitive to cisplatin, methylene blue and H2O2; the sensitivity to cisplatin, methylene blue was the same as that of polβ targeting cells while bleomycin was absolutely different. That may due to different expression level of polβ (polβwas deleted completely in targeting cells while there is very low level expression of polβin knockdown cells).

In conclusion, we constructed polβ gene targeting model in human esophageal carcinoma cellliwash basin (EC9706) and the deleting of polβ gene from background could remove the interference on experimental data. It provides important data for the further study of DNA polβ mutation and abnormal expression in human esophageal carcinoma.

Acknowledgments

We are grateful to Professor Guoqiang Zhao for helpful comments and suggestions during all stages of the project. This work was partially supported by the National Natural Science Foundation of China (No.39870287).

Corresponding author:
Dong Ziming. PhD.
Department of Pathophysiology, College of Basic Medical Science, Zhengzhou University,
100 Kexue Road, Zhengzhou, Henan 450001, China.
+86 13673662571; dongzmzzu@126.com

References

1. Hu DL, Zhuang ZX, Liu YM, He Y. Vector-mediated RNA interference of DNA polymerase beta in human bronchial epithelial cells. Wei Sheng Yan Jiu. 2006 Mar; 35(2):143-145.

2. Trivedi RN, Almeida KH, Fornsaglio JL, Schamus S, Sobol RW. The role of base excision repair in the sensitivity and resistance to temozolomide-mediated cell death. Cancer Res, 2005, 65 (14): 6394-6400.

3. Bu D, Cler LR, Lewis CM, Euhus DM. A variant of DNA polymerase beta is not cancer specific. J Invest Surg, 2004, 17(6): 327-331.

4. Miyamoto H, Miyagi Y, Ishikawa T, Ichikawa Y, Hosaka M, Kubota Y. DNA polymerase beta gene mutation in human breast cancer. Int J Cancer, 1999, 83(5): 708-709.

5. Iwanaga A, Ouchida M, Miyazaki K, Hori K, Mukai T. Functional mutation of DNA polymerase beta found in human gastric cancer--inability of the base excision repair in vitro. Mutation Res, 1999, 435(2):121-128.

6. Maria V. Sukhanova, Svetlana N. Khodyreva, Natalia A. Lebedeva, Rajendra Prasad, Samuel H. Wilson and Olga I. Lavrik. Human base excision repair enzymes apurinic/apyrimidinic endonuclease1 (APE1), DNA polymerase b and poly (ADP-ribose) polymerase 1: interplay between strand-displacement DNA synthesis and proofreading exonuclease activity. Nucleic Acids Res,2005,33 (4) :1222-1229.

7. Haitham T. Idriss, Osama Al-Assar, Samuel H, Wilson. DNA polymerase beta. Int J Biochem Cell Biol, 2002, 34:321-324.

8. Canitrot Y, Cazaux C, Fréchet M, Bouayadi K, Lesca C, Salles B, Hoffmann JS. Overexpression of DNA polymerase beta in cell results in a mutator phenotype and a decreased sensitivity to anticancer drugs. Proc Natl Acad Sci USA, 1998, 95:12586-12590.

9. Xu XC, el-Naggar AK, Lotan R. Differential expression of galectin-1 and galectin-3 in thyroid tumors. Potential diagnostic implications. Am J Pathol. 1995,147 (3): 815-822.

10. Kenneth C. Suen. Fine-needle aspiration biopsy of the thyroid. CMAJ. 2002, 167(5):491-495.

11. Akinari Iwanaga, Mamoru Ouchida, Kohji Miyazaki, Katsuji Hori and Tsunehiro Mukai. Functional mutation of DNA polymerase β found in human gastric cancer–inability of the base excision repair in vitro. Mutat Res, 1999, 435(2): 121-128.

12. Marian E. Eydmann and Margaret A. Knowles. Mutation analysis of 8p gene POLB and PPP2CB in bladder cancer · Cancer Res, 1997, 93(2):167-171.

13. Bergerheim US, Kunimi K, Collins VP, Ekman P. Deletion mapping of chromosomes 8, 10, and 16 in human prostatic carcinoma. Gene Chromosom Cancer, 1991, 3:215.

14. Dobashi Y, Shuin T, Tsuruga H, Uemura H, Torigoe S, Kubota Y. DNA polymerase beta gene mutation in human prostate cancer. Cancer Res, 1994, 54(9): 2827.

15. Ulrich Hübscher, Heinz-Peter Nasheuer and Juhani E. Syväoja. Eukaryotic DNA polymerases, a growing family.TIBS,2000,25(3):143-147 ·

16. Ziming Dong. Study of DNA polymerseβ. Journal of Zhengzhou University (Medical sciences), 2003, 38(4): 477- 480.

17. Manu Kohli, Carlo Rago, Christoph Lengauer, Kenneth W. Kinzler and Bert Vogelstein. Facile methods for generating human somatic cell gene knockouts using recombinant adeno-associated viruses. Nucleic Acids Res, 2004, 32(1): e3.

18. Bunz,F. Human cell knockouts. Curr. Opin. Oncol, 2002,14: 73-78.

19. John M. Sedivyand Annie Dutriaux. Gene targeting and somatic cell genetics: a rebirth or a coming of age? Trends Genet, 1999, 15: 88-90.

20. Han Y, Wei F, Xu X, Cai Y, Chen B, Wang J, Xia S, Hu H, Huang X, Han Y, Wu M, Wang M. Establishment and comparative genomie hybridization analysis of human esophageal carcinomas cell line EC97O6. Zhonghua YiXue Yi Chuan Xue Za Zhi. 2002, 19(6): 455-457.

21. Xiujie Sheng. Strategy and development of gene targeting.Journal of foreign medice, 2001, 24(1):8-10.

22. M Kozak. Effects of intercistronic length on the efficiency of reinitiation by eucaryotic ribosomes. Mol Cell Biol, 1987, 7:3438-3445.

23. Yamada NA, Farber RA. Induction of a low level of microsatellite instability by overexpression of DNA polymerase beta. Cancer Res, 2002, 62:6061-6064.

24. Lindahl T, Barnes DE. Repair of endogenous DNA damage. Cold Spring Harb Symp Quant Biol. 2000; 65:127-133.

25. Cabelof DC, Raffoul JJ, Yanamadala S, Guo Z, Heydari AR. Induction of DNA polymerase beta-dependent base excision repair in response to oxidative stress in vivo. Carcinogenesis. 2002 Sep; 23(9):1419-1425.

26. Chen KH, Yakes FM, Srivastava DK, Singhal RK, Sobol RW, Horton JK, Van Houten B, Wilson SH. Up-regulation of base excision repair correlates with enhanced protection against a DNA damaging agent in mouse cell lines. Nucleic Acids Res. 1998 Apr 15; 26(8):2001-2007.

27. Polosina YY, Rosenquist TA, Grollman AP, Miller H. 'Knock down' of DNA polymerase beta by RNA interference: recapitulation of null phenotype. DNA Repair (Amst). 2004 Nov 2; 3(11):1469-1474.

3/2/2010

The Impact of Silicone Frontalis Suspension with Ptosis Probe R for the Correction of Congential ptosis on the Asian Eyelids in Taiwan

Chi-Ting Horng[1,2], Han-Yin Sun[3], Ming-Liang Tsai[4], Shang-Tao Chien[5] , Feng-Chi Lin[1*]

[1]Department of Ophthalmology, Kaohsiung Armed Force General Hospital, Kaohsiung, 802, Taiwan ROC ；[2]Department of Pharmacy, Tajen University, Pintung, 907, Taiwan ROC;[3]School of Optometry, Chung-Shan Medical University, Taichung, 402, Taiwan ROC;[4]Department of Ophthalmology, Tri-Service General Hospital, Taipei, 114, Taiwan ROC ;[5]Department of Pathology, Kaohsiung Armed Force General Hospital, Kaohsiung, 802, Taiwan ROC

h56041@ gmail.com

Abstract — To evaluate the basic technique of Ptosis probe [R] and the impact of ptosis repair by silicone rod frontalis sling on the Asian eyelid. A retrospective interventional study including 30 patients (49 eyelids) who underwent silicone rod frontalis suspension by the same surgeon between 2005 and 2008. Cosmetic outcomes , marginal reflex distance (MRD), chin-up head posture and recurrence rate were evaluated. In all patients, MRD increased an average of 1.2 ± 1.5 mm after the operation ($P < 0.05$). The score of cosmetic outcomes was 0.6 ± 0.4.(the most of the operated eyelids achieved to good-to-excellent final lid height). The rate of chin-up head posture deceased from 33.3% to 6.6% ($P < 0.05$). Transient punctate keratopathy without corneal infection occurred postoperatively in 9 (18%) of 49 eyes. Extrusion of the sling node with or without infection occurred in 2 forehead. With a mean follow-up of 20.73 months (range：6-41 months), no recurrence of the ptosis was found. Silicone rods is an effective material in frontalis suspension for the treatment of severe ptosis with poor levator function. It may increase the MRD of operated eyelid and decreased the rate of chi-up head posture. The procedure with Ptosis probe [R] is easy, fast, and leads to less tissue trauma on the Asian eyelids. . [Life Science Journal. 2010; 7(2): 19 – 24] (ISSN: 1097 – 8135).

Key words: blepharoptosis, frontalis slings, silicone rod.

I. Introduction

Children with unilateral or bilateral congenital ptosis may have problems about crawling, walking and can not achieve other development milstones. It is not only healthy but also social problems.

The ideal surgical treatment and age of intervention were controversial in the management of congenital ptosis **[1]**. Factors including the severity of ptosis, degree of head posture, presence or absence of levator muscle function, patient age and the presence of amblyopia. Children with severe congenital ptosis are at risk of developing amblyopia. For this reason, repair of ptosis is in indicated as soon as the diagnosis is made. Frontalis suspension of the upper lid is an effective and simple method of treatment **[2]**.

Levator function is probably the most important eyelid measurement in term of surgical planning as the effectiveness of certain procedures rests solely on the integrity of levator muscle function. Frontalis suspension surgery is now well-accepted as the procedure of choice for patients (congenital or acquired etiologies) with severe ptosis and poor levator function **[3]**. This surgery treats the sequence of a variety of diseases, but certain entities present more different treatment challenges. For example, patients with cranial nerve III palsy and myasthenia gravis may be at greater risk for development of exposure keratopathy after surgery because of poor ocular mobility. Patients with MG may also have weak orbicularis muscles which may induce the poor closure of the eyelids and incompletely blink, thus resulting in exposure keratopathy **[4]**. Some progressive eyelid disorders may need adjustment of eyelid height after the initial surgical intervention because of a progressive decrease in levator strength.

For these reasons, many suspension materials have been used. These include autogenous and preserved fascia lata **[4]**, sclera **[5]**, non-absorbable sutures **[6]**, suture reinforced sclera, temporalis fascia **[7]**, Gore-Tex strips **[8]** and silicone bands and rods. Our purpose of this study was to evaluate the efficacy and outcomes of silicon frontalis suspension by double pentagon. In this report, we also describe our experience using silicone sling for the correction of ptosis in Asian eyelid in Taiwan and the basic technique of Ptosis probe [R]..

II. Patients and Methods

Charts of all eyes that had undergone a silicone rod frontalis sling procedure with Ptosis probe [R] for correcting congenital ptosis between Feb.2005 and Dec.2008 at Department of Ophthalmology, Kaohsiung Armed Forces General hospital, Kaohsiung, Taiwan (ROC) were retrospectively reviewed. The inclusion criteria was ptosis with poor levator function (5mm or less). In total, 49 lids of 30 patients met the above criteria. All patients were victims of congenital ptosis of children. Patients selected for surgery either had ptosis obscuring the visual axis, evidence amblyopia or fixation preference, or extreme chin-up posture. All experiment protocols were conducted in accordance with the Declaration of Helsinki. Ethical approval for this study were obtained from their parents.

The data were collected including age, gender, diagnose, preoperative and postoperative marginal reflex distance. The visual acuity, cosmetic outcomes, chin-up head posture (abnormal chin-up head posture is frequently

present in infant with congenital ptosis), recurrence rate and related complications were observed in the same time.

The surgeries were all performed under general anesthesia in all patients by the same surgeon(Dr. Horng). Six skin incisions were made using a No.15 blade. Three skin incisions were made 2 mm above lash line of the upper eyelid, medially, laterally, and centrally. Two incisions, down to the level of periosteum, were made in the superior brow hair. A forehead incision approximately 1.0cm above the brow, down to periosteum, was placed midway between the two brow incisions. The Ptosis probe package contains 2 polished stainless steel guide needle probe 0.8mm in diameter and 80mm in length extended with silicone tubing 0.8mm in diameter (Fig 1). One probe was passed from the lateral brow incision to the central lid incision, posterior to the orbital septum, then to lateral lid incision at a pre-tarsal level, and back to lateral brow incision to complete a triangle (Fig 2). The other probe was passed between the medial brow and eyelid incisions in similar fashion to form a second triangle. Tie the ends of the silicone rod with a square knot and adjust the tension to reproduce a normal eyelid contour. Place the height at the limbus or just 1mm below the limbus. The two probe ends were passed to central forehead incision. The probes were then cut off. Tie the two residual silicone rods together at the forehead incision. Adjust the tension to maintain the eyelid margin contour (Fig 3). Nylon 6-O thread was used to close the six skin incisions (Fig 4).

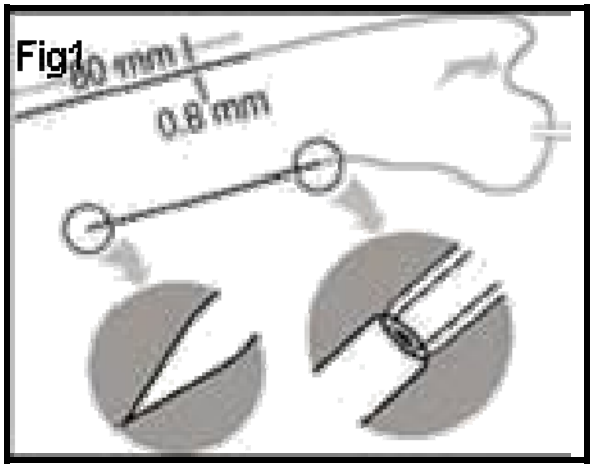

Fig 1. Ptosis probe+ silicone tubing(FCI, France)

Fig. 2. Silicone frontalis sling repair of ptosis :triangle passing of silicone rod by guide needle probe from lateral brow incision to central lid incision, then lateral lid incision and back to brow incision

Fig. 3. Silicone frontalis sling repair of ptosis: final adjustment of lid position at frontal incision

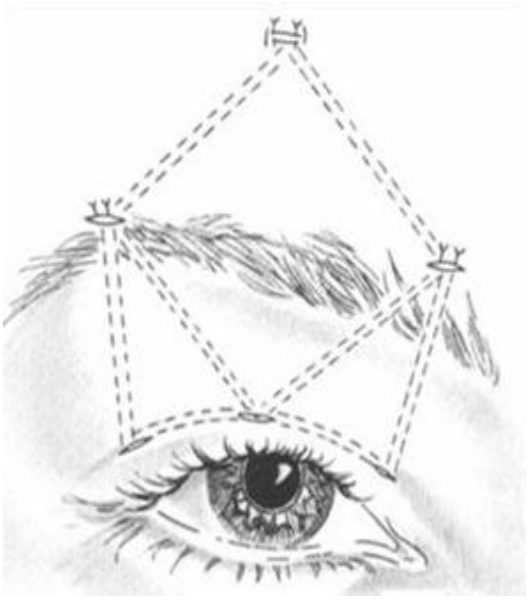

Figure 4. This figure shows the shape of the silicone loop after complete passage of silicone rod

Postsurgical evaluation were performed at 1 week, 2 week, 1 month after operation and then every three months.. The define appropriate surgical goals, a classification system was designed to assess the feature relevant to ptosis surgery, which are upper eyelid height and symmetry. Marginal reflex distance(MRD) elevation of 2 mm or greater was considered satisfactory. MRD was defined as the vertical distance measured from the corneal light reflex in primary gaze to the upper eyelid margin. The postoperative eyelid symmetry was calculated as the difference between MRD of the surgical and fellow eyelid, and was considered satisfactory if it was 1mm or less.

Postoperative cosmetic outcome was graded on a 0 to 2 scale, with 0 score indicative of excellent results, 1 as good, and 2 as poor. Outcome was defined as excellent if the eyelids were within 1 mm height between the eyelids with an acceptable crease and contour, good if there was ＞ 1mm difference in eyelid height and/or asymmetric crease, and poor if there was poorly defined eyelids crease and contour asymmetry **[9]**. All patients underwent cosmetic grading of outcome. The pre- and postoperative photographs were reviewed by the same observer.

Amblyopia was defined as best-correct visual acuity of less than 20/40, and greater than 2 Snellen lines of difference between the 2 eyes. In younger patients(such as our study) amblyopia was defined by a lack of fixation in the ptotic eye compared with the nonptotic one.

In addition to lid height, the cornea was examined postoperatively for the presence or absence of a punctate keratopathy, confluent epithelial defect, corneal scar, or corneal ulcer. If any complications such as prior sling revisions, visible sling migration, infection, extrusion, suture granulomas, lagophthalmos or poor cosmetic results happened, we should record in detail.

Statistical ayalyses:

Statically analysis was performed with Microsoft Excel (Microsoft Corporation with Excel 2003) and SPSS (Version 1.3；SPSS Inc, Chicago, Illinois , USA). The independent t test is used to evaluate the data. If the $P < 0.05$，it means significantly.

III. Results

Forty-nine eyelids of thirty patients (24 males and 6 females) were operated for upper eyelids ptosis by silicon frontalis suspension (Table1). Patient age range for 20 months to 40 months old (The mean operative age is 28.77 months old.) Amblyopia was found in 16.8%(5/30), associated with strabismus was found in 10%(3/30). With a mean follow-up of 20.73 months, the final lid height was rated as cosmetic outcomes. The mean score was 0.6 ± 0.4. In all patients, MRD increased an average of 1.2 ± 1.5 mm, from a mean preoperative 0.1 ± 0.7 mm. The rate of chin-up headache posture from preoperative 10 cases (33.3%) to postoperative 2 cases (6.6%) (Table2).

Transient punctate keratopathy occurred immediately postoperatively in 9 (18%) of 49 eyes. The keratopathy

Table 1
Demographics of study population 30 patients (49 eyelids), who Underwent Frontalis Suspension Surgery

Case	Age(Months) /Sex	Ptosis Etiology	Follow-up Time (month)	Lid Height (right/left)	Complications
1	26M/M	Congenital OU	14	good/good	Transient keratopathy, OD
2	25M/M	Congenital OU	16	good	None
3	40M/F	Congenital OU	18	good/good	None
4	24M/M	Congenital OD	18	good	Wound infection with rod exposure
5	22M/F	Congenital OD	30	good	None
6	38M/M	Congenital OU	12	good/good	Transient keratopathy, OD
7	36M/F	Congenital OU	16	good/good	None
8	36M/F	Congenital OD	20	good	Transient keratopathy, OD
9	37M/M	Congenital OU	20	good/good	None
10	30M/F	Congenital OU	34	good/good	Transient keratopathy, OS
11	40M/M	Congenital OU	20	good/good	Transient keratopathy, OS
12	24M/M	Congenital OU	22	good/good	None
13	24M/M	Congenital OS	16	good	Transient keratopathy, OS
14	30M/F	Congenital OD	22	good	None
15	32M/M	Congenital OD	20	good	None
16	27M/M	Congenital OU	40	good/good	Transient keratopathy, OD
17	26M/M	Congenital OU	16	good/good	Transient keratopathy, OD
18	28M/M	Congenital OU	18	good/good	Transient keratopathy, OS
19	30M/M	Congenital OU previous ptosis repair OD	20	good/good	good/good
20	24M/M	Congenital OU	18	good/good	None
21	20M/M	Congenital OU	24	excellent/excellent	None
22	22M/M	Congenital OU	20	excellent/excellent	Extrusion of sling, OS
23	28M/M	Congenital OU	16	good/good	None
24	26M/M	Congenital OU	16	good/good	None
25	26M/M	Congenital OU	24	good/good	None
26	36M/M	Congenital OU	18	poor/poor	None
27	27M/M	Congenital OD	22	good	None
28	28M/M	Congenital OD	24	good	None
29	25M/M	Congenital OD	18	poor	None
30	26M/M	Congenital OU; previous ptosis repair OS	24	good	uneven crease, OD

was managed with artificial tear drops and, if needed, a bandage contact lens. The epithelial disease did not result in corneal ulcers in any patient. Extrusion of the sling with or without infection occurred in two cases. During the whole follow-up time, no recurrence of ptosis was found.

Table 2
Pre- and Post-operative data in 49 eyelids

Data	Preoperative	Postoperative	P value
MRD(mm)	0.1 ± 0.7	1.2 ± 1.5	<0.05
Chin-up head posture	10 (33.3%)	2 (6.6%)	<0.05
Recurrence rate		0	
Cosmetic outcome		0.6 ± 0.4	

IV. Discussion:

The incidence of amblyopia associated with congenital ptosis in some retrospective chart studies were about 17-23% **[10, 11, and 12]**. Children younger than 3 years of age with congenital ptosis and developmental delay or possible amblyopia can undergo frontalis suspension to achieve good visual results.

Refractor errors including astigmatism and anisonetrooia, and strabismus are also coexisting congenital ptosis **[13]**. Many previous seports had ever proved that corrective surgery may increase the MRD, lower the rate of chin-up head posture and decrease the incidence of amblyopia in children **[14,20].** Our reports matched the same results.

Since 1977, repair of ptosis by frontalis muscle and fascia lata were first developed by Crawford et al. **[15]**. Unfortunately, the fascia lata has a more permanent nature and induces scarring and loss of mobility of the upper eyelid. Some opthalmologists tried to develop a new method of frontalis suspension to resolve the problem. The technique of correction of ptosis with poor levator function were first adopted by Tillettn et al in 1966 **[16]**. They used silicon band in frontalis suspension correction of ptosis. 6 patients who underwent silicon sling with good result after 19-24 months follow-up. They first enumerated the advantages of using solicon in frontalis slings. Silicon rod is readily available, easily adjustable and well tolerated by the surrounding tissues. The elasticity if silicon permits good upper lid height, as well as closure.

Lately Rowan et al. **[17]** found the use of 0.8mm silicon rod fixed with a Watzke silicon sleeve to be less bulky than the no.40 band in 1977. In the same time, they reported no incidence of infection, rejection of silicone, or recurrence of ptosis after one silicone sling placement in 12 patients with up to 2 years of follow-up.

In 1978, Leone et al. **[18]** described the suture fixation of one end of the band to the tarsus medially and one laterally. The two ends then were passed subcutaneously in a pentagonal shape to meet in the central brow region. The new method reduced the bulk of the silicon band in the lid. In 1981, Leone et al **[19]** further altered his procedure by using silicon rod in a pentagonal fashion with a full-lid crease incision. The same procedure as Leone in our study was adopted. The surgical procedure can performed to address ptosis easily. The mechanism of operation may create a linkage between the frontalis muscle and the tarsus of the upper eyelid, which allows for a better eyelid position in primary gaze.

Till now, silicon frontalis suspension is the first choice of surgery for congenital ptosis in younger children. In addition, the surgery is also used in cases of poor levator palpebrae superioris muscle function, neuromuscular diseases, and where linkage between the muscle and the eyelid is abnormal (such as Marcus Gunn jaw-winking phenomenon) **[6]**.

Although many nature or artifact material had been well developed and used in the repair of ptosis, everyone all had their own week-point. Jeong et al. **[21]** had stiffed on form histopathological study that autologous fascia lata showed less inflammation and better incorporation with surrounding structures than the silicon. However, the silicone band showed a great deal of inflammatory reaction at 2 weeks, but the reaction gradually disappeared by 8 weeks after implantation. The elasticity of silicon permits a good upper lid aperture, as well as closure. The collagenous tissues surrounding silicon band did not have incorporation or tight bond with the implant. So the silicon rod is readily available, easily adjustable, and well-tolerated by the surrounding tissues. Silicon rod remain a reasonable material choice for frontalis suspension surgery, especially for young children, because they may easily revised or replaced in comparison to other materials.

Silicone rods also remained a safe choice in patients risk for keratopathy **[20]**. Meanwhile, Jeong et al. **[21]** found that the silicon is not incorporated with the surroundings tissue, it is best used as temporal material. Fresh autologous fascia appears to be the most suitable suspenision.

Every surgery has its own gold periods. If Children < 3 years old was victim of severe ptrosis, early surgery (even < 1 year old) were suggested by Saunder et al. Because of the autofascia lata was not harvesting, silicon rod frontalis suspension was prefer. Until 3.5 years of age, Crawford et al. **[22]** were favorable fascia lata. Should they consider the gold time for treating amblyopia？ To the most of ophthalmologists' concepts, the exact of time in plan to repair ptosis may be about 3 year of age in children.

Katowitz et al and Anderson et al. **[29,30]** had stated that severe unilateral and bilateral congenital ptosis may result in development delay due to abnormal head posturing or amblyopia secondary to occlusion of the visual axis. For this reason, Carter **[25]** had strongly suggested that surgery to correct the ptosis often needs to be performed at a younger age. Frontalis suspension ptosis repair is indicated for severe ptosis with poor levator function. Fascia lata has been harvested to serve as the suspensory materials for children 3 years or older with great success. However, postoperative recurrence rate, infection and the formation of granuloma have been reported higher than silicon rod **[31]**.

In our experiences, we prefer the use of the silicon sling in Taiwan for its versatility and for its lesser tendency to induce scar tissue around the sling **[23]**. The ease of adjusting silicone rod slings makes it an excellent suspensory material in cases of blepharoptosis that more frequently require adjustment postoperatively. For these reasons, it become the newer material of choice for patients with MG, Cranial nerve III palsy, et al in many studies **[24,25]**. Postoperative results are unpredictable in patients with ptosis associated with a poor Bell's phenomenon such as chronic progressive external ophthalmoplegia (CPEO), MG, cranial nerve III palsies. The best benefit of the silicone sling is that it can be adjusted easily through the central forehead incision to reverse under-correction or over-correction.

Although the rate of complications were relatively and seldom permanent, adequate initial observation is important. The incidence of exposure keratopathy following silicon frontalis suspension can be not omitted. Van Sorge et al. **[24]** had reviewed 101 eyelids receiving silicon frontalis suspension and their cohort study demonstrated a 26 % risk of exposure keratopathy following operation. In the same time, the risk of major corneal complications, such as ulceration, was low (3%). They used the intensive lubrication therapy, eye packing

at night, partial conjunctival auto-grafting covering the inferior one-third of the cornea, even removal of sling. The conclusion is that the elasticity of the sling certainly is important in the prevention of corneal complication, even when putative risk factor are present. In our study, 30% (9/30) patients showed temporary punctuate epithelial defect, and all the lesions improved only by lubrication therapy.

Van Sorge et al. also suggest that transient superficial punctate staining was the rule for the first postoperative week or two. Even with careful postoperative use of lubricants every one to two hours, corneal abrasion may occurred sometimes. However, some previous reports showed that patients with keratitis may progress into true corneal ulceration in the complication of overcorrection. Although lagophthalmos and corneal exposure are really unavoidable with any suspension procedure, in time, the exposed corneal epithelium in young children appears to adjust, provided there is careful support with lubricant drops and/or ointment during day and night **[26]**. The possible complications of exposure keratopathy should be keep in mind in all ophthalmologists.

The other complications of repair of ptosis were under-or over-correction. No cases of under-and over-correction were encountered in our study. Lelli Jr et al. had ever reported that their cases needed to adjust or replace of silicon rod sling because of under-correct(50%) and over-correction(10%). However, their patients were all victims of high risk non-congenital blepharoptosis(such as CN 3 palsy, MG and CPEO). Leone demonstrated that the advantages of the use of silicon for frontalis suspension under local or general anaesthesia. It may enable the surgeon to judge the eyelid position during operation. Silicon sling are well tolerated by the surrounding tissues and allow eyelid closure because of their elasticity. Shortening of the sling allows for adjustment of eyelid position in the case of under-correction. Although the general anaesthesia were all adopted in our study, we can easily to set the optimum position (the lower eyelid just cover the 1/4 upper cornea) according to our experience. Thus no extra-procedure about under-correction or over-correction were necessary.

The elasticity and ease of adjustment of the silicon rod are ideal characteristics for suspensory material used to correct severe ptosis. The ability counld achieve excellent cosmetic outcome and functional outcome **[27]**. The elasticity of the silicone also allows the patients to close their upper lids with greater ease. Preoperative patients education regarding to delicate balance required between elevation the eyelid height enough to allow acuity vision, but not so high as to cause excessive exposure keratitis should help the patient accept an eyelid height that may be cosmetically suboptimal.

A pattern of gradual droop of the eyelid operated on became most obvious several years postoperatively in some literatures reviews, so call “recurrence” **[28]**. These findings suggests that this suture material is a poor alternative to fascia lata for permanent frontalis suspension in patients with congenital ptosis. Traditionally, the Wright fascia needle is used to thread the silicone rod.

In our study, no recurrence rate was noted after 21 months follow up in Taiwan children. In the same time, Ben Simon et al. **[27]** mentioned the recurrence rate about 26% in Los Angles, USA, and . Lell Jr at al. found the recurrence of ptosis is almost 10 % in Michigan, USA. We want to investigated why the results showed the fluctuation and what is the different follow-up time as well as the region factor and race factor. We know the thicknesses of eyelids of Asian Children are thinner in USA. If the subcutaneous tissues layer of ptosis patients were thinner in Taiwan, the inflammatory reaction around the silicon should be severe (may be due to different collagen types). The biochemistry of stable scar is easy to form in children in Taiwan. It can easily explain that the more stable fixed scars may contracture the surrounding tissues and induced the postoperative lower recurrence rate in Asian eyelid. .

Only two severe complications in our study were found. In case 1 , a 24 months old child, signs of wound infection with rod exposure developed four months after surgery. We arranged to remove the sling right now. In case 2, a 22 months old , extrusion of the sling developed spontaneously. However, there was no evidence of infection was found. Therefore, the end of silicone rod was cut shorter and passed deep to the frontalis muscle. Finally the patient did not have evidence of recurrence and the problem of infection postoperatively.

With good elasticity and ease of postoperative adjustment, silicone rods is an ideal suspensory material. During our follow-up period, 46 lids (94%) had good-to-excellent final lid height. No eyelids became more ptotic, suggesting that the silicone rods had not lost their tensile strength or migrated out of position. Whether or not Ptosis probe ^{R} is preferable to traditional Wright fascia needle can not be assessed by the study. With our procedure, we used a Ptosis probe ^{R} to the silicone rod. The procedure with Ptosis probe ^{R} is easy and fast. Compared with traditional Wright fascia needle 2mm in diameter, the Ptosis probe ^{R} 0.8mm in diameter facilitates less tissue trauma. However, we still prepared the Wright fascia needle standby. If detachment the sling from the probe or bending of probe tip happened during insertion, the Wright fascia needle can be used to thread the sling.

Congenital ptosis may result in developmental delay due to abnormal head posturing or amblyopia secondary to occlusion of the visual axis, necessitating corrective surgery at a very young age. In our experience, the silicon rod frontalis suspension surgery may play a important role in congenital ptosis on Asian eyelids because of its efficacy and good outcome.

V. Conclusion

This is an important advantage if early correction helps alleviate associated functional, developmental and cosmetic problems of congenital ptosis. Recent studies have identified a 3 to 10% incidence of amblyopia with severe congenital ptosis.

Congenital ptosis may result in developmental delay due to abnormal head posturing or amblyopia, necessitating corrective surgery at a very young age 3-5. . Silicone rods is an effective material in frontalis suspension for the treatment of severe ptosis with poor levator function. The procedure with Ptosis probe R is easy, fast, and leads to less tissue trauma on the Asian eyelid.

References

1. Oral Y, Ozgur OR, Akcay L, Ozbas M, Dogan OK.(2010)Congenital ptosis and Amblyopia. *J Pediatric Ophthalmol Strabismus ;* 47(2): 101-4
2. Morris CL, Buckley EG, Enyedi LB, Stinnett S, Freedman SF.(2008)Safety and efficacy of silicone rode frontalis suspension surgery for childhood ptosis repair. *J Pediatr Ophthalmol Strabismus* ;45:280-8.
3. Lelli Jr. GJ, Musch DC, Fruech BR, Nelson CC.(2009)Outcomes in silicon rod frontalis suspension surgery for high-risk non-congenital blepharoptosis. *Ophthal Plast Resconstr Surg*; 25:361-5.
4. Wilson ME, Johnson RW.(1991)Congenital ptosis. Long-term results of treatment using lyophilized fascia lata for frontalis suspensions. *Ophthalmology* ; 98:1234-7
5. Bodian M.(1968)Repair of ptosis using human sclera. *Am J Ophthalmol*; 65:352-8.
6. Saunders RA,(1991)Grice CM. Early correction of severe congenital ptosis. *J Pediatr Ophthalmol Strabismus*;28:271-3.
7. Neuhaus RW, Shorr N.(1982)Use of temporal fascia and muscle as autograft. *Arch Ophthalmol*; 101:262-4.
8. Steinkogler FJ, Kuchar A, Huber E, Arocker-Mettinger E,(1993)Gore-Tex soft-tissue patch frontalis suspension technique in congenital ptosis and in blepharophimosis-ptosis syndrome. *Plast Reconstr Surg*; 92:1057-60.
9. Lee V, Konrad H, Bunce C. et al.(2002)Aetiology and surgical treatment of childhood blepharoptosis. *Br J Opthalmol*; 86: 1282-6
10. Harrad RA, Graham CM, Collin JR.(1988) Amblyopia and strabismus in congenital ptosis. *Eye(Lond)*. 2 (Pt6): 625-7.
11. Hornblass A, Kass LG, Ziffer AJ.(1995)Amblyopia in congenital ptosis. *Ophthalmic Surg* ; 26(4):334-7.
12. Dray JP, Leibovitch I.(2002)Congenital ptosis and amblyopia: a retrospective study of 130 cases. *J Pediatr Ophthalmol Strabismus*; 39(4): 222-5.
13. Stark N, Walther C.(1984)Refractive errors, amblyopia and strabismus in congenital ptosis. *Klin Monbl Augenheilkd*; 184(1):37-9.
14. Lin LK, Uzcategui N, Chang EL.(2008)Effect of surgical correction of congenital ptosis on amblyopia. *Ophthal Plast Reconstru Surg*; 24(6): 434-6
15. Crawford JS.(1977)Repair of ptosis using frontalis muscle and fascia lata: a 20-year review. *Ophthalmic Surg*; 8(4): 31-40.
16. Tillett CW, Tillett GM.(1966)Silicon sling in the correction of ptosis. *Am J Ophthalmol*; 92: 521-3.
17. Rowan PJ, Hayes GS.(1977)Silicon sling for ptosis. *South Med J*; 70: 68-9
18. Leone CR, Jr, Rylander G.(1978)A modified silicon frontalis sling for the correction of blepharoptosis. *Am J Ophthalmol*; 85: 802-5.
19. Leone CR Jr, Shore JW, Van Gemert JV.(1981) Silicon frontalis sling rod for the correction of blepharoptosis. *Ophthalmic Surg* ; 12: 881-7
20. Morris CL, Buckley EG, Enyedi LB, Stinnett S. Freedman SF.(2008)Safely and efficacy of silicon rod frontalis suspension surgery for children ptosis repair. *J Pediatric Ophtahlmol Strabisms*; 45:289-8.
21. Jeong S, Ma YR, Park YG.(2000)Histopathological study of frontalis suspension materials. *Jpn J Ophthalmol*; 44:171-86.
22. Saunders RA, Grice CM.(1991)Early correction of severe congenital ptosis. *J Pediatr Ophthalmol Strabismus*; 28:271-3.
23. Bernardini FP, de Conciliis C, Devoto MH.(2002)Frontalis suspension sling using a silicon rod in patients affected by myogenic blepharoptosis. *Orbit*; 21:195-8.
24. Van Sorng AJ, Devoglaere T, Sotodeh M, Wubbels R. Paridaens D.(2010)Exposure kerapopathy following silicon frontalis suspension in adult neuro- and myogenic ptosis. *Acta Ophthalmol*; 8: 1 -5.
25. Carter SR, Meecham WJ, Seiff SR.(1996)Silicon frontalis slings for the correction of blepharoptosis: indication and efficacy. *Ophthalmology*; 103:623-30.
26. Katowitz JA.(1979)Frontalis suspension in congenital ptosis using a polyfilament, cable-type suture. *Arch Ophthalmol*; 97:1659-1663.
27. Ben Simon GJ, Macedo AA, Schwarcz RM, Wang DY, Mccann JD, Goldberg RA.(2005) Frontalis suspension for upper eyelid ptosis: evaluation of different surgical designs and suture material. *Am J Ophthalmol*; 140:877-85.
28. Older JJ, Dunne PB.(1984)Silicone slings for the correction of ptosis associated with progressive external ophthalmoplegia. *Ophthalmic Surg*; 15:379-381.
29. Katowitz JA. (1979) Frontalis suspension in congenital ptosis using a polyfilament, cable-type suture. *Arch Ophthalmol* ; 97:1659-63.
30. Anderson RL, Baumgartner SA.(1980)Amblyopia in ptosis. *Arch ophthalmol*;98:1068-9.
31. Hersh D, Martin FJ, Rowe N.(2006)Comparison of silastic and backed fascia lata in pediatric frintalis suspension. *J Pediatric Ophthalmol strabisum* ; 143:212-8.

4/1/2010

SusMiRTrain: ab initio SVM classifier for porcine microRNA precursor prediction

Peng-Fang Zhou, Fei Zhang, Zhen-Hua Zhao, Wen-Qian Zhang, Wen-Chao Lin, Yang Zhang, De-Li Zhang*

Investigation Group of Molecular Virology, Immunology, Oncology & Systems Biology, Center for Bioinformatics, and Research Laboratory of Virology, Immunology & Bioinformatics, College of Veterinary Medicine, Northwest A & F University, Yangling 712100, Xi'an City, Shaanxi Province, P.R.China

zhangdeli@tsinghua.org.cn

Abstract: MicroRNA (miRNA), which is short non-coding RNA, plays important roles in almost all biological processes examined. Several classifiers have been applied to predict humans, mice and rats precursor miRNAs (pre-miRNAs), but no classifier is applied to classify porcine pre-miRNAs only based on the porcine pre-miRNAs because of the little known miRNA component in the porcine genome. Here, we developed a novel classifier, called SusMiRTrain, to predict porcine pre-miRNAs. Trained on 60 porcine pre-miRNAs and 65 pseudo porcine hairpins, SusMiRTrain achieved 86.4% (5-fold cross-validation accuracy) and 0.9144 (ROC score). Tested on the remaining 14 porcine pre-miRNAs and 1000 pseudo hairpins, it reported 100% (sensitivity), 87.3% (specificity) and 87.5% (accuracy),respectively. Furthermore, a Java package, called SusMiRPred, was developed to filter out the short sequences which have not the pre-miRNAs structure features and to extract features for porcine pre-miRNAs prediction. . [Life Science Journal. 2010; 7(2): 25 – 27] (ISSN: 1097 – 8135).

Key words: MicroRNA; Swine; SVM

1. Introduction

MicroRNAs (miRNAs) are short RNAs (~20-22nt) that can regulate gene expression by binding to the mRNAs at the post-transcriptional level in eukaryotes **[1, 2]**. These short RNAs are generally derived from long, primary transcripts (pri-miRNA) which are processed into fold-back precursor miRNA (pre-miRNAs) with characteristic stem-loop RNA structures **[3]**. The pre-miRNAs are cleaved into ~22 nt duplexes which then unwind, leaving the mature miRNA sequence preferentially incorporated into RNA-induced silencing complex (RISC) to regulate protein-coding gene expression **[4,5]**, To date, miRNAs have been shown to play critical roles in almost all biological processes examined, such as control of developmental timing, cell fate specification, limb development, apoptosis, angiogenesis, fat metabolism, insulin secretion, and even cancer **[6, 2]**.

Many miRNA families are conserved among the vertebrate animals. However, many of the new miRNAs recently discovered are not conserved beyond mammals, and ~10% are taxon specific **[7]**. Comparative approaches suffer lower sensitivity in detecting novel pre-miRNAs without known homology pre-miRNAs **[8]**. But all of the porcine miRNA sequences in the latest miRBase were computationally predicted on the basis of sequence homology to known miRNAs from other species **[9, 10, 11]**. The current release of miRBase contains only 72 porcine miRNA sequences while 718 human miRNAs, 595 mouse miRNAs, and 330 rat miRNAs have been identified **[12]**.

Here, we developed a Java package: SusMiRPred, to filter out the short sequences according to the pre-miRNA structure features and to convert the structures to triplet-SVM features **[13]**. Then, we trained a SVM model called SusMiRTrain based on porcine pre-miRNA using libSVM package. Trained on 60 pre-miRNAs in miRBase and 65 pseudo pre-miRNAs, the SusMiRTrain achieved 86.4% (5-fold cross-validation accuracy) and 0.9144 (ROC score).

2. Materials and Methods

We downloaded all 77 porcine miRNA sequences from miRBase version 14.0. Genomic sequences were from NCBI of June 2009 and were downloaded from the Ensemble FTP site**[14a]**. The protein coding regions (CDS) sequences were downloaded from the Ensemble FTP site **[14b]**. We also used RNAfold **[15]** version 1.7 with default parameters to predict RNA secondary structures.

Three datasets were built to train SVM and to evaluate the classifier performance. One was training set called it as the "TRAINING-SET", and two were test sets named as the "CDS-SET" and "MIRBASE-SET" according to the ways we collected. The porcine pre-miRNAs whose secondary structures do not contain multiple loops were considered, which gave us 74 pre-miRNAs, covering more than 96% of all the reported porcine pre-miRNAs. We extracted 60 pre-miRNAs from

them as one part of "TRAINING-SET" set and the remaining 14 pre-miRNAs composed of the "MIRBASE-SET" set.

We filtered the CDS sequences keeping the length distribution of the extracted segments with that of porcine pre-miRNAs. The criteria for selecting the pseudo-miRNAs from the segments are: minimum of 18 base pairings on the stem of the hairpin structure (included the GU wobble pairs), maximum of -15 kcal/mol free energy of the secondary structure, and no multiple loops. These criteria ensured that the extracted pseudo pre-miRNAs were similar to real pre-miRNAs according to the widely accepted characteristics. As most of reported miRNAs are located in the un-translated regions or intergenic regions, we took the hairpins collected from CDS as examples of pseudo pre-miRNAs. Totally, 8494 pre-miRNA-like hairpins (pseudo pre-miRNAs) were collected in this dataset. We randomly selected 65 pseudo pre-miRNAs from them as the other part of the "TRAINING-SET" set, and 1000 pre-

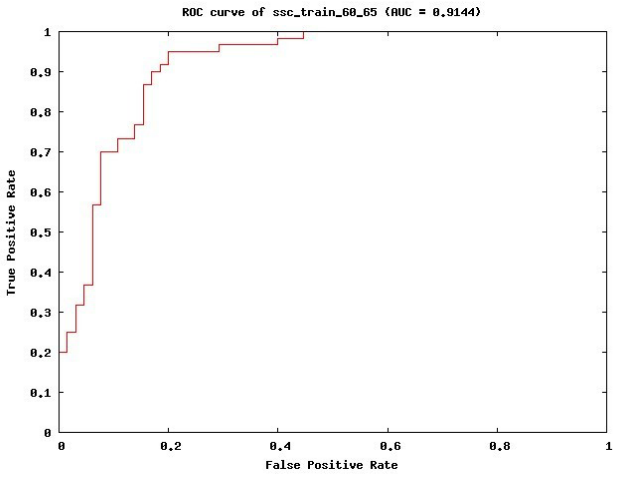

Fig. 1. ROC score

miRNA-like hairpins from remaining pseudo pre-miRNAs were extracted as "CDS-SET" set.

Trained on "TRAINING-SET" set using libSVM package with triplet features(Xue, Li et al. 2005), a training model called "SusMiRTrain" was achieved for porcine pre-miRNA prediction. Then, we used "CDS-SET" and "MIRBASE-SET" set to evaluate the SusMiRTrain performance.

We scanned for the genome sequences using a 100-nt query window with 10-nt increments at a time. Sequences with potential hairpin-like structures were extracted as candidate miRNA precursors. A GC content requirement of 30% to 75% for the 100-nt query sequences was applied. Additionally, low-complexity

3. Results and Discussion

Trained on the "TRAINING-SET" set, SusMiRTrain achieved 86.4% (5-fold cross-validation accuracy) and 0.9144 (ROC score) (Fig. 1). Tested on the "CDS-SET" set and "MIBASE-SET" set, it reported 100% (sensitivity), 87.3% (specificity) and 87.5% (accuracy), respectively. The good performance of SusMiRTrain showed that it was available for the prediction of porcine pre-miRNAs. Since the little number of porcine pre-miRNAs in miRBase, researchers predicted porcine pre-miRNAs on basis of porcine pre-miRNAs and other species pre-miRNAs, which also was on the basis of sequence homology to known miRNAs from other specie**[13]**. Here, we proposed an ab initio method for porcine pre-miRNAs prediction without known homology pre-miRNAs.

There are four layers in the SusMiRPred. First, SusMiRPred filtered short sequences with mfe >= -15kcal/mol and stem < 18. Second, it filtered the multiloop sequences. Then, the sequences with the length of inter < 9nt; the length of bulge < 6nt; the numbers of inter and bulge < 10; the numbers of inter < 8 and the numbers of bulge < 6 was remained. At last, triplet features were extracted from the remaining sequences to predict pre-miRNAs.

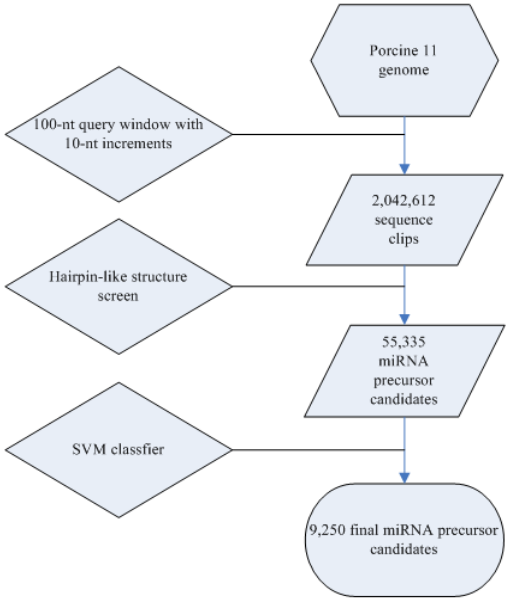

Fig.2. Flowchart of the porcine pre-miRNA prediction procedure

sequences, such as those with dinucleotides repeated >= 4 times (for example, ATATATAT), trinucleotides repeated >=3 times (for example, ATGATGATG), or any single nucleotide repeated >6 times (for example, AAAAAAA), were removed using a repeat filter. Such sequences have been observed little in known miRNAs.

The resulting candidate miRNA precursors were analyzed with the program RNAfold for secondary structure prediction. Then, we used the SusMiRPred to filter the pre-miRNAs structures. Using the SVM classifier of SusMiRTrain to predict the candidate hairpins, we got the predicted candidate results of the porcine pre-miRNAs. 9250 porcine pre-miRNAs candidates were found by scanning the whole porcine genome using SusMiRPred and SusMiRTrain (Figure 2).

4. Conclusions All of porcine microRNAs were computationally predicted on the basis of sequence homology to known miRNAs from other species. There were no ab initio approaches to predict the porcine pre-microRNAs. In this article, we proposed a Java package: SusMiRPred, and a training model: SusMiRTrain to predict the species specific pre-microRNAs. Only trained on porcine pre-microRNAs, SusMiRTrain achieved the accuracy about 87.5% for distinguishing real vs. pseudo porcine pre-miRNAs. The good performance showed that SusMiRTrain was available for porcine pre-miRNAs prediction.

Acknowledgement:

This item is supported by the NorthwestA & F University Foundation for Attracting Foreign Personnel (No. 01140406) from the“985”Project for Higher Educationand and the National Natural Science Foundation of China (No.30270342).

References

1. Bartel, D. P. (2004). "MicroRNAs: genomics, biogenesis, mechanism, and function." Cell 116(2): 281-97.
2. Mendell, J. T. (2008). "miRiad roles for the miR-17-92 cluster in development and disease." Cell 133(2): 217-22.
3. Lee, Y., M. Kim, et al. (2004). "MicroRNA genes are transcribed by RNA polymerase II." EMBO J 23(20): 4051-60.
4. Khvorova, A., A. Reynolds, et al. (2003). "Functional siRNAs and miRNAs exhibit strand bias." Cell 115(2): 209-16.
5. Schwarz, D. S., G. Hutvagner, et al. (2003). "Asymmetry in the assembly of the RNAi enzyme complex." Cell 115(2): 199-208.
6. Lee, R. C., R. L. Feinbaum, et al. (1993). "The C. elegans heterochronic gene lin-4 encodes small RNAs with antisense complementarity to lin-14." Cell 75(5): 843-54.
7. Berezikov, E., G. van Tetering, et al. (2006). "Many novel mammalian microRNA candidates identified by extensive cloning and RAKE analysis." Genome Res 16(10): 1289-98.
8. Berezikov, E., V. Guryev, et al. (2005). "Phylogenetic shadowing and computational identification of human microRNA genes." Cell 120(1): 21-4.
9. Wernersson, R., M. H. Schierup, et al. (2005). "Pigs in sequence space: a 0.66X coverage pig genome survey based on shotgun sequencing." BMC Genomics 6(1): 70.
10. Huang, T. H., M. J. Zhu, et al. (2008). "Discovery of porcine microRNAs and profiling from skeletal muscle tissues during development." PLoS One 3(9): e3225.
11. McDaneld, T. G., T. P. Smith, et al. (2009). "MicroRNA transcriptome profiles during swine skeletal muscle development." BMC Genomics 10: 77.
12. Griffiths-Jones, S., H. K. Saini, et al. (2008). "miRBase: tools for microRNA genomics." Nucleic Acids Res 36(Database issue): D154-8.
13. Xue, C., F. Li, et al. (2005). "Classification of real and pseudo microRNA precursors using local structure-sequence features and support vector machine." BMC Bioinformatics 6: 310.
14. a. ftp://ftp.ncbi.nlm.nih.gov/genomes/Sus_scrofa b. ftp://ftp.ncbi.nlm.nih.gov/genomes/Sus_scrofa/RNA
15. Reddy, A. M., Y. Zheng, et al. (2009). "Cloning, characterization and expression analysis of porcine microRNAs." BMC Genomics 10: 65.

3/5/2010

Analysis of Pulmonary Infection of Hospitalized Patients Injured in the Wenchuan Earthquake in China

Jing Xu[1,2], Zi-Gui Liu[1,2], Xia Zhu[1,2], Xue-Bing Chen[1,2], and Hong Tang[1,2*]

[1] CENTER OF INFECTIOUS DISEASES, WEST CHINA HOSPITAL, SICHUAN UNIVERSITY, CHENGDU, CHINA; [2] DIVISION OF INFECTIOUS DISEASES, STATE KEY LABORATORY OF BIOTHERAPY, SICHUAN UNIVERSITY, CHENGDU, CHINA.

htang6198@hotmail.com

Abstract-*Background:* On 12 May 2008, a devastating earthquake measuring 8.0 on the Richter scale hit Wenchuan County, Sichuan in China, and resulted in the casualties of thousands of people. Some of the hospitalized earthquake victims can occur pulmonary infection. However, few studies have been conducted on the clinical features of pulmonary infection in hospitalized casualty after Wenchuan Earthquake. *Methods*: To analyze retrospectively the clinical data of 115 pulmonary infection patients among wounded inpatients in West China Hospital of Sichuan University after the Wenchuan earthquake. *Results*: In our report, 76 cases (66.1%) of 115 hospitalized earthquake victims with pulmonary infection were patients with age > 60 years; 74 cases (64.3%) of them with long-term hospitalization(> 20 days); 23 cases (20.0%) of them with traumatic brain injury; 71 cases (61.7%) with torso trauma; 58 cases (50.4%) of them were patients with underlying disease; 25 cases(21.7%) of them were the patients treated with mechanical ventilation. A total of 143 nonduplicate clinical isolates from sputum specimen of 115 pulmonary infection patients were analyzed. Gram-negative bacilli were the most commonly isolated pathogens (73.4%). Only 7.7% of total isolates were gram-positive bacteria; 18.9% of total isolates were fungi. There were high rates of multiple drug resistance in most bacteria isolates. The detection rates and resistance rates of Acinetobacter baumannii were higher than others and 81.8% of all Staphylococcus aureus detected from sputum culture were resistant to antibiotics but vancomycin in this group patients. There were 98 cases of recovery, 17 death cases due to lung infection. *Conclusions*: Most of earthquake inpatients with pulmonary infection were patients with age > 60 years, longer hospital stay or severe trauma. These factors might increase the risk of pulmonary infection in earthquake inpatients. Gram-negative bacilli play the most important role in these pulmonary infection patients. Pandrug-resistant Acinetobacter baumannii and Methicillin resistant S.aureus in this study might increase the risk of nosocomial infection. The prevention and control of pulmonary infection are crucial for earthquake survivors during hospitalization. . [Life Science Journal. 2010; 7(2): 28 – 34] (ISSN: 1097 – 8135).

Key Words: Wenchuan earthquake; Pulmonary infection; Pathogen; Drug sensitivity

INTRODUCTION

On 12 May 2008, an earthquake measuring 8.0 on the Richter scale hit Wenchuan County, Sichuan Province in southwest China. According to the official reports, the earthquake disaster caused more than 374171 injuries and 69185 deaths, and more than ninety-six thousand people were hospitalized after earthquake. Infection is a frequent and severe complication occurring in the earthquake victims with severe trauma in the course of rescue and treatment. Of these, pulmonary infection is common and serious one that affect the prognosis of the earthquake wounded. Therefore, pulmonary infection of the wounded in the follow-up hospitalization can not be neglected in the medical rescue after earthquake. However, few studies have been conducted on the analysis of pulmonary infection in hospitalized casualty after Wenchuan Earthquake. In this study, we retrospectively reviewed the clinical data on 115 hospitalized earthquake victims with pulmonary infection in West China Hospital of Sichuan University.

MATERIALS AND METHODS

General data and diagnosis

A retrospective analysis was performed on the collected data on 115 pulmonary infection patients in hospitalized earthquake victims admitted to our hospital from 14 May to 22 June 2008. Data sources include death certificates and medical records. The following data were collected: age, gender, type of injury, length of stay, mechanical ventilation, underlying disease and the pathogen data on culture of sputum specimens.

Pulmonary infection was confirmed by the hospital final diagnosis and were defined according to the Guidelines of Pneumonia Diagnosis and Treatment (draft) issued by Chinese Society of Respiratory Diseases in 1999 and the diagnostic criteria of nosocomial infection issued by Minist ry of Health of the People's Republic of China.[1,2]

Treatment

Pulmonary infection should always prompt antimicrobial therapy. De-escalation of antibiotic therapy could be performed in infection cases of the pathogen remains elusive. All pulmonary infection patients after admission took deep sputum for germiculture. Sputum samples should be consecutively taken to determine the types of infections. According to the results of sputum culture, antimicrobial therapy should be adequate (i.e. cover the causative pathogen) and effective (i.e. adequately administered and dosed).

Bacterial identification and antimicrobial susceptibility testing

The pathogen data were collected by department of laboratory medicine in West China Hospital of Sichuan University. The identification of microorganisms and susceptibility testing were followed the performance standards for antimicrobial susceptibility testing as defined by the Clinical and Laboratory Standards Institute (CLSI).[3] Duplicate isolates of the same organism from the same patient were eliminated, and calculation of resistance rates were performed on all isolates.

RESULTS

General information

In our report, the mean age of 115 hospitalized earthquake victims with pulmonary infection (53 males, 62 females) was 67 years. 76 cases (66.1%) of 115 pulmonary infection patients were patients with age > 60 years; 74 cases (64.3%) of them were patients with long-term hospitalization(> 20 days). Categorization of the earthquake injury was based on the final diagnosis of 115 pulmonary infection patients from hospitalized earthquake casualty: 23 cases (20.0%) of them were patients with traumatic brain injury; 71 cases (61.7%) with torso trauma and 21 cases(18.3%) with others trauma. Fifty eight cases (50.4%) were patients with underlying disease. (Table 1) Of these, 23 cases were patients with chronic obstructive pulmonary disease, 15 of hypertension, 10 of diabetes, 9 of brain infarction, 2 of lung cancer and 13 cases were patients who suffered from more than two kinds of diseases.

Clinical manifestation

The onset of occult, atypical symptoms and no specific pulmonary signs were the features of most pulmonary infection patients from the earthquake. In this report, the main symptoms of these patients were cough, fever, chest tightness and shortness of breath; Chest pain and chills were rare. Of these, cough (33 cases) was one of common respiratory symptoms; stethocatharsis weakness, dry cough or less sputum were frequent. Twenty eight cases were patients with Chest tightness and shortness of breath; 29 cases were patients with dyspneic respiration. There were 21 cases in fever, including 16 cases of low or moderate fever, and only 5 cases of high fever. Twenty five cases were patients treated with mechanical ventilation, accounting for 21.7%.

The lung auscultation were mostly low breath sounds of two lungs, and moist rales could be heard in some parts of lungs but dry rales were rare. All the patients took chest photography or CT and the results showed pulmonary infections. Of them, pleural effusion (32 cases) was more common pulmonary sign, 11 cases had pulmonary atelectasis.

Table 1. The Information of 115 Hospitalized Earthquake Victims with Pulmonary Infection in West China Hospital (case, %) Pathogen characteris

Factors	Infection cases	Proportion (%)
Age（years）		
≤60	39	33.9
> 60	76	66.1
Gender		
male	53	46.1
female	62	53.9
Length of stay（days）		
≤20	41	35.7
> 20	74	64.3
Mechanical ventilation		
Yes	25	21.7
No	90	78.3
Underlying disease		
Yes	58	50.4
No	57	49.6
Torso trauma		
Yes	71	61.7
No	44	38.3
Traumatic brain injury		
Yes	23	20.0
No	92	80.0

There were 48 cases of with positive pathogens from sputum culture in 115 pulmonary infection patients. The positive rate of sputum culture was 41.7%. Pulmonary infection was mostly due to various bacteria(43 cases), 15 cases of one single bacteria, 11 cases of complex bacteria and 17 cases of complex fungi; 5 cases only by fungus. A total of 143 nonduplicate clinical isolates from sputa of 115 pulmonary infection patients were analyzed. Gram-negative bacilli (G-bacillus) were the most commonly isolated pathogens (105 isolates,73.4%). Only 11 isolates (7.7%) of total isolates were gram-positive bacteria (G+ cocci); 27 isolates (18.9%) of total isolates were fungus (Table 2).

Drug sensitive test results of some common pathogenic bacteria to antibiotics in sputum culture of 115 pulmonary infection patients from hospitalized earthquake victims are shown in Table 3.

Table 2. Microorganisms Isolated from 115 Hospitalized Earthquake Victims with Pulmonary Infection

Organism	Isolates number	Proportion（%）
Kinds of bacterium		
Pseudomonas aeruginosa	24	16.8
Klebsiella oxytoca	3	2.1
Enterobacter cloacae	4	2.8
Haemophilus influenzae	1	0.7
Acinetobacter baumannii	34	23.8
Klebsiella pneumoniae	14	9.8
Escherichia coli	6	4.2
Stenotrophomonas maltophilia	6	4.2
Burkholderia cepacia	3	2.1
Enterobacter aerogenes	2	1.4
Proteus mirabilis	3	2.1
Other gram-negative bacilli	3	2.1
Bacillus prodigiosus	2	1.4
Staphylococcus aureus	11	7.7
Kinds of fungi		
Candida albicans	11	7.7
Yeast-like fungus	4	2.8
Aspergillus	5	3.5
Candida tropicalis	4	2.8
Candida glabrata	3	2.1
Total	143	100.0

Treatment and Outcome

The third generation cephalosporin antibiotics, carbapenems and/or quinolones were applied to treat bacteria infections; Fluconazole and Itraconazole were applied to treat fungal infections; Combination therapy were applied to treat mixed infections. Tuberculosis infection should be performed in standard anti-tuberculosis program. Among 115 pulmonary infection patients from hospitalized earthquake casualty, 98 were discharge after recovery (85.2%), 17 died (14.8%). One was diagnosed as subacute hematogenous pulmonary tuberculosis by CT and etc, and was recovered by normal ntituberculotic treatment. Four patients were developed for acute respiratory distress syndrome (ARDS), three of them were recovered and one died. Eight of death cases were patients with multiple organ failure(MOF) and one died of cerebrovascular accident.

Table 3. Drug Sensitive Test Results of Some Common Pathogenic Bacteria in 48 Sputum Cultures of 115 Pulmonary Infection Patients in Hospitalized Earthquake Victims. [a] (sensitivity, %)

Antibiotics	Strains						
	Acinetobacter baumannii (n=34)	Pseudomonas aeruginosa (n=24)	Klebiella pneumoniae (n=14)	Escherichia coli (n=6)	Enterobacter cloacae (n=4)	Staphylococcus aureus (n=11)	Stenotrophomonas maltophilia (n=6)
Gentamycin	20.6	37.5	42.9	66.7	25.0	0.0	16.7
Ampicillin	2.9	—	14.3	0.0	0.0	0.0	—
Cefazolin	—	—	14.3	0.0	0.0	18.2	—
Cefoxitin	—	—	64.3	66.7	0.0	—	—
Cefotaxime	17.6	12.5	28.6	0.0	25.0	—	0.0
Ceftazidime	20.6	33.3	28.6	0.0	50.0	—	83.3
Ceftriaxone	17.6	16.7	28.6	0.0	25.0	—	0.0
Cefepime	26.5	41.7	28.6	0.0	50.0	—	0.0
Levofloxacin	50.0	25.0	64.3	16.7	75.0	0.0	100.0
Vancomycin	—	—	—	—	—	100.0	—
Imipenem	32.4	45.8	92.9	66.7	100.0	0.0	0.0
Amikacin	32.4	87.5	78.6	83.3	75.0	—	16.7
Aztreonam	23.5	20.8	28.6	0.0	25.0	—	0.0
Gatifloxacin	11.8	—	57.1	16.7	75.0	—	16.7
Tobramycin	29.4	37.5	64.3	66.7	50.0	—	0.0

Note: a: Drug sensitivity (%) = sensitive isolates / n (isolates number)

DISCUSSION

The magnitude 8.0 earthquake that struck Wenchuan County of Sichuan Province on 12 May, 2008, was the strongest earthquake China has experienced in over 50 years. Earthquakes are among the most devastating disasters that cause mass casualties. Because of gathering of a large number of the wounded and lower population immunity caused by stress and malnutrition in the earthquakes, respiratory infection became a major infection after earthquake; Some statistics showed that 6.4 percent of hospitalized earthquake victims developed pulmonary infection and most of them were hospital-acquired infections(HAI).[4,5] In this study, we retrospectively reviewed the clinical data on 115 hospitalized earthquake victims with pulmonary infection in West China Hospital. Previous study revealed that infection was the second most common reason which caused death in hospitalized earthquake casualty and pulmonary infection was frequent and serious one. [4-6] More consistently, pneumonia is known to increase medical consumption in terms of antibiotic use and length of hospital stay. [7,8]Therefore, correct understanding and effective control of pulmonary infection of earthquake inpatients are of great significance to minimize the disability and death of earthquake victims.

It is well known that trauma patients are at high risk of developing infections and the mortality which is associated with HAI is increased in the presence of trauma. [9-11] In this study(Table 1), we observed that the earthquake inpatients with age > 60 years, long-term hospitalization(> 20 days) or torso trauma were very prone to the development of pulmonary infection. The patients with torso trauma or traumatic brain injury were accounted for 61.7% and 20.0%, respectively. These patients were suffered from severe injury which affected breathing and expectoration, or the old as well as organ dysfunction, which caused immunocompromised; Furthermore, longer hospital stay increased the probability of pulmonary infection, thus, many earthquake inpatients suffered from lung infection and most of them might be nosocomial infection. Recently, Magnotti observed that pulmonary infection was an independent factor for death in trauma patients. [12] Our data showed that the case fatality of pulmonary infection was as high as 14.8% and was similar with the report of

Tanaka about Hanshin-Awaji earthquake; [13]The pulmonary infection patients easily led to MOF(7.0%,8/115) in the clinical late-phase. Catania analyzed that immunological changes following trauma cause an increase in the HAI rate which then results in higher morbidity and mortality.[14]The mechanisms such as auto-oxidative receptor injury or changes in natural killer activity associated with stress might be responsible for these changes.[15,16]

After earthquakes, the pathogens of pulmonary infection assume multiplicity. Bacterium is mostly responsible and fungus are also involved. However, mixed infections are in the majority.[17] Yorsaengrat[18] found that the respiratory tract infection was mostly due to non-fermentation and ESBL-producing G-bacillus after earthquake and tsunami. In our study, G-bacillus was the mainly responsible for pulmonary infections of hospitalized earthquake victims, accounting for 73.4%, G+ cocci accounted for 7.7%, fungal accounted for 18.9% mainly due to Candida albicans. The results were roughly consistent with the reports of Yorsaengrat[18] and Weihua Wang et al.[19] Moreover, Acinetobacter baumannii (A. baumannii) in this report was the most frequently pathogen of lung infections, accounting for 23.8%, followed by Pseudomonas aeruginosa and Klebsiella pneumoniae, accounting for 16.8% and 9.8%, respectively. Similar findings were published in Oncul 's study. [20] Their results showed that most nosocomial infections were caused by A. baumannii, Staphylococcus aureus (S.aureus) and Klebsiella pneumoniae after earthquake. Also, Oncul reported that 4.7 percent of hospitalized earthquake casualty suffered from nosocomial pneumonia after the Marmara earthquake. Thus, we considered that some patients with pulmonary infection in this study might be nosocomial infection cases. Several possible factors could be responsible for A. baumannii infection. In trauma patients, injured and ischaemic tissues make it easier for colonization of A. baumannii. A. baumannii is an increasingly important opportunistic pathogen and a relatively common cause of nosocomial infections in areas of natural disaster. [21,22]

Oncul [20] analyzed the information about disaster-associated infection after the Marmara earthquake, it indicated that all strains of S.aureus were methicillin-resistant and multiresistant strains of A. baumannii and Pseudomonas aeruginosa emerged. Our data showed that there were high rates of multiple drug resistance in most bacteria isolates, but there were different drug resistance rates to different antibiotics. According to Table 3, the resistance rates of A. baumannii and Pseudomonas aeruginosa were higher than others. It is worth noting that 81.8% of all S.aureus detected from sputum culture were resistant to antibiotics but vancomycin in this group patients. This indicated that the S.aureus infections were mostly due to Methicillin resistant S.aureus (MRSA). The above analysis showed that most of pathogens of pulmonary infection in this study were serious drug resistance and pandrug-resistant A. baumannii and Methicillin resistant S.aureus might increase the risk of nosocomial infection. This was not only because of many transferred patients admitted to our hospital as a referral center of medical rescue for severely injured patients after earthquake, but also because of many focused hospitalized patients. Thus, multi-drug resistant microorganisms could be transferred by patients from other hospitals. Moreover, inappropriate empiric antibacterial therapy has been found to cause the spread of highly virulent microorganisms such as Pseudomonas spp and Acinetobacter spp.[23-25]

In summary, most of hospitalized earthquake victims with pulmonary infection were patients with age > 60 years, longer hospital stay or severe trauma. These factors might increase the risk of pulmonary infection in earthquake inpatients. The pathogen distribution isolated from these patients was wide; Gram-negative bacilli play the most important role in these pulmonary infection patients and the resistance of antibiotics was serious. Further expansion of case studies are also needed to address the relationship between earthquake victims and pulmonary infection. We believe that the prevention and control of pulmonary infection are crucial after earthquake survivors were rescued, especially during hospitalization. Inspecting pathogens and using antibiotics reasonably according to susceptibility testing result are very important in reducing pathogenic bacteria resistant and improving the prognosis of pulmonary infection patients after earthquake. Acknowledgements

This work was supported by the National Key Technologies Research and Development Program of China during the 11th Five-Year Plan Period (No.

2008ZX10002-006 and 2008ZX10002-004）and Key Technologies Research of Sichuan Province (No. 2008SZ0039). The authors would like to thank all staff of Medical Records and Statistics Room in West China Hospital of Sichuan University for extracting data.

Correspondence to

Professor Hong Tang

Center of Infectious Diseases, West China Hospital, Sichuan University, Chengdu, China; Division of Infectious Diseases, State Key Laboratory of Biotherapy, Sichuan University, Chengdu, China.

Abbreviations

CLSI: the Clinical and Laboratory Standards Institute
G-bacillus: Gram-negative bacilli
G+ cocci: gram-positive bacteria
ARDS: acute respiratory distress syndrome.
MOF: multiple organ failure
HAI: hospital-acquired infections
baumannii: Acinetobacter baumannii
S.aureus: Staphylococcus aureus
MRSA: Methicillin resistant S.aureus

REFERENCES

1. Chinese society of respiratory diseases. Guidelines of acquired pneumonia diagnosis and treatment (Draft). Modern Practical Medicine, 2002; 14: 158-61.
2. Ministry of Health of the People's Republic of China. Diagnostic criteria of nosocomial infection. Natl Med J China, 2001; 81: 314-320.
3. Clinical and Laboratory Standards Institute. Performance standards for antimicrobial susceptibility testing, 17th informational supplement. Wayne, PA: CLSI, 2007.
4. Lai SW, Liu CS, Li CI, et al. Post-earthquake illness and disease after the Chi-Chi earthquake. Eur J Intern Med, 2000;11: 353-354.
5. Keven K, Ates K, Sever MS, et al. Infectious complications after mass disasters : the Marmara earquake experience. Scand J Infect Dis, 2003; 35: 110-113 .
6. Watson J, Gayer M, Connolly MA. Epidemics after natural disasters. Emerg Infect Dis, 2007; 13 : 1-5 .
7. Rosenthal VD, Guzman S, Migone O, et al. The attributable cost and length of hospital stay because of nosocomial pneumonia in intensive care units in 3 hospitals in Argentina: A prospective, matched analysis. Am J Infect Control, 2005; 33: 157-161.
8. Warren DK, Shukla SJ, Olsen MA, et al. Outcome and attributable cost of ventilator-associated pneumonia among intensive care unit patients in a suburban medical center. Crit Care Med, 2003; 31:1312-7.
9. Chevret S, Hemmer M, Carlet J, Langer M. Incidence and risk factors of pneumonia acquired in intensive care units. Results from a multicenter prospective study on 996 patients. European Cooperative Group on Nosocomial Pneumonia. Intensive Care Med, 1993;19: 256-264.
10. Dinkel RH, Lebok UJ. A survey of nosocomial infections and their influence on hospital mortality rates. J Hosp Infect ,1994; 28: 297-304.
11. Bochiccio GV, Joshi M, Knorr KM, et al. Impact of nosocomial infections in trauma: does age make a difference? J Trauma. 2001; 50: 612-7.
12. Magnotti LJ, Croce MA, Fabian TC. Is ventilator-associated pneumonia in trauma patients an epiphenomenon or a cause of death? Surg Infect. 2004; 5:237–242
13. Tanaka H, Oda J, Iwai A, et al. Morbidity and mortality of hospitalized patients after the 1995 Hanshin-Awaji earthquake. Am J Emerg Med. 1999; 17:186-91.
14. Catania RA, Chaudry IH. Immunological consequences of trauma and shock . Ann Acad Med Singapore. 1999; 28: 120-132.
15. Inoue-Sakurai C, Maruyama S, Morimoto K. Posttraumatic stress and lifestyles are associated with natural killer cell activity in victims of the Hanshin-Awaji earthquake in Japan. Prev Med. 2000; 31: 467-473.

16. Simms HH, D'Amico R. Posttraumatic auto-oxidative polymorphonuclear neutrophil receptor injury predicts the development of nosocomial infection. Arch Surg. 1997; 132: 171-177.

17. Uçkay I, Sax H, Harbarth S, et al. Multi-resistant infections in repatriated patients after natural disasters: lessons learned from the 2004 tsunami for hospital infection control. J Hosp Infect. 2008; 68: 1-8.

18. Yorsaengrat W, Chungpaibulpatana J, Tunki B, et al. Respiratory complication of tsunami disaster victims in Vachira Phuket Hospital. J Med Assoc Thai. 2006; 89: 518-520.

19. Wei-hua W, Yi-hua Z. Drug Resistance and Pathogens in Critically Ill Patients with Pulmonary Infection. Chin J Nosocomiol Vol . 2007; 17: 227-229.

20. Oncul O，Keskin O，Acar HV，et al. Hospital-acquired infections following the 1999 Marmara earthquake. J Hosp Infect, 2002; 51: 47-51.

21. Caricato A, Montini L, Bello G, et al. Risk factors and outcome of Acinetobacter baumanii infection in severe trauma patients. Intensive Care Med. 2009; 8:1582-1585.

22. Joly GM. Clinical impact and pathogenicity of Acinetobacter. Clin Microbiol Infect. 2005; 11: 868–73.

23. Mulin B, Talon D, Viel JF, et al. Risk factors for nosocomial colonization with multiresistant Acinetobacter baumannii. Eur J ClinMicrobiol Infect Dis. 1995;14: 569-576.

24. Scerpella EG, Wanger AR, Armitige L, et al. Nosocomial outbreak caused by a multiresistant clone ofAcinetobacter baumannii: results of the case-control and molecular epidemiologic investigations. Infect Control Hosp Epidemiol. 1995; 16: 92-97.

25. Bowton PL. Nosocomial pneumonia in the ICU-year 2000 and beyond. Chest. 1999; 115: 28S-33S.

4/1/2010

Differential Sensitivity Of Saggital Otolith Growth And Somatic Growth In *Oreochromis Niloticus* Exposed To Textile Industry Effluent

Adeogun A.O. and Chukwuka A.V

DEPARTMENT OF ZOOLOGY, FISHERIES AND HYDROBIOLOGY UNIT,UNIVERSITY OF IBADAN, IBADAN, NIGERIA.

ABSTRACT-A 30-day sublethal bioassay was carried out to investigate the relative sensitivity of saggital otolith and somatic growth indices in juvenile *Oreochromis niloticus* to textile factory effluents. Somatic indices (body weight, standard length, and condition index) were measured and saggital otoliths were extracted for morphometric (length, breadth and weight) examinations. Data were subjected to one-way ANOVA which showed a significant decrease ($p<0.05$) between the weight ($7.00x10^{-3}\pm4.05x10^{-3}$g, $6.44x10^{-3}\pm9.3x10^{-3}$ g) of the right saggita of the control fish and that of the exposed fish respectively. There were no significant differences in somatic indices and left saggita measurements for all experimental groups. Allometry as indicated by correlation analysis showed a stronger ($p< 0.05$) coupling of the right saggital growth with increase in standard length unlike the left saggita. The observed differences in otolith weight have probable implications on the choice of saggital otolith that may be suitable for daily growth-ring analysis. Also implied is the fact that otolith weight show earlier sensitivity to environmental stressors than somatic indices. Otolith morphometry holds the potential for an objective and more sensitive physiological indicator of stress in *O. niloticus* than somatic indices. [Life Science Journal. 2010; 7(2): 35 – 41] (ISSN: 1097 – 8135).

Key words: toxicity of heavy metals

I. INTRODUCTION

The sustained intensity of industrial activity has inevitably increased the levels of heavy metals in nearby land and natural waters (Tarras-Wahlberg *et al*., 2001; Jordao *et al*., 2002; Vijayakumari, 2003) and textile industries have been implicated for such practices (Akif et al.,2002; Vijayakumari, 2003; Ramadevi et al, 2006).

The toxicity of heavy metals present in process water from textile industries and other industries in its category to wild life has been proven. High mortality rate during early stages as a result of such is considered one of the major factors causing stock fluctuations. The resultant disequilibria in the ecosystem may further lead to increased environmental vulnerability hence paving way for a decline in organism population. (Laws, 1981).

Measures of growth and condition of young fishes have been used to assess the effects of environmental alterations on individuals (e.g. Karakiri *et al*, 1989, Suthers *et al*, 1992). The search for a relatively sensitive index for evaluating organism or ecosystem health have been investigated including the use of otoliths (Gibson, 1994; Able *et al*, 1999; Adams, 2002)

The potential use of otoliths as an individual record of size and growth has been recognized by some workers (Campana and Nelson, 1985; Boehlert, 1985; Reznichet et al, 1989; Pawson, 1990; Fletcher, 1995; Hare and Cowen, 1995; Agostinho, 1999; Cardinale *et a*l, 2000; Pilling *et al*, 2003) and underlying this potential is the positive relationship between otolith growth and somatic growth (Campana, 1990; Francis, 1990; Waessle *et al*., 2002). The use of otoliths in toxicology experiments has also been reported by (Zhou *et al*., 2005). Otoliths are valid structures for growth evaluation of many freshwater fish species and often are preferred over spines and scales (Hining *et al.* 2000). Fagade (1979) described in detail the structure of the otolith of *Tilapia guineensis* (Dumeril) and their use in age determination and growth evaluation.

The study investigates the relative sensitivity of morphometric measurements of saggital otoliths and somatic indices to exposures of textile factory effluents.

II. METHODOLOGY

Effluent collection and Toxicity Testing

The effluent samples for this study was collected from a textile company (Sunflag PLC) at Eric Moore, Lagos, Nigeria. Collections were made, once every week, between the months of January and March 2007 at the point of effluent discharge. These effluents were then mixed and kept in the refrigerator prior to usage.

250, 6 week old juveniles of O. *niloticus* were procured from a private fish farm in Ibadan, Nigeria. They were kept in aerated tanks and fed with Coppens® feed meal (40% crude protein) at 3% body weight for two weeks to acclimatize to laboratory conditions.

Five fishes were randomly distributed into experimental tanks and a 96hr static bioassay was conducted to determine the median lethal concentration (LC_{50}) with concentrations ranging from 0% to 40% in 2 replicates. The 96hr LC_{50} values were computed by arithmetic graphic method (Reish and Oshida, 1986).

Fractions (1/2, 12.95%; ¼, 6.47% and $1/8^{th}$, 3.24%) of the mean LC_{50} values (25.89%) were used for a 30day

exposure period. The tests were conducted in triplicates and the test media were renewed every 72hrs.

Growth Studies and Otolith Extraction

After 30days exposure period, wet weights and standard length of fishes in all experimental groups were recorded.

The otoliths of 3 fishes per replicate were removed by a deep cut into the skull above the eyes and extracted otoliths were d in 70% alcohol (Brothers, 1987). Freshly extracted otoliths (right and left) were immersed in 5% hypochlorite or bleaching solution to facilitate removal of adhered tissues.

The otoliths were weighed using an analytical weighing balance before measurement by image analysis. Image analysis techniques were used with modifications as described by Lombarte (1990) where otolith image was acquired with a high resolution scanner and measurements (length and breadth) were carried out using Adobe Photoshop® 7.

Physico-chemical Parameters

Surface water temperature was measured with Mercury-in glass thermometer (^{0}C) while pH was measured with pH meter. Dissolved oxygen (DO) was measured by Winkler's Titrimetric method. Biochemical Oxygen Demand (BOD), Chemical Oxygen Demand (COD), Total Suspended Solids (TSS), Total Dissolved Solids (TDS) and Total Solids (TS) were measured as described by APHA (1992). Effluent and exposure samples were analyzed with an Absorption Atomic Spectrometer (AAS) for Iron, Zinc, Copper, Manganese, Lead, Cadmium, Nickel, Arsenic, Chromium and Cyanide.(APHA, 1992).

Data Analysis

Data were analyzed by one-way ANOVA and differences between means were considered significant at $p<0.05$ (Zar,1996). Data on otolith morphometry were further subjected to correlation analysis using Spearman's correlation coefficient. Associations or correlations between parameters were considered significant at $p<0.05$. Allometry or growth coupling between parameters was determined by a positive correlation at $p<0.05$.

Table 1
Mean Wet Weights, Standard Lengths and Condition Indices of *O. niloticus* after 30 days exposure period (n= no of specimens=10)

Concentration (%)	Weight (g)	Standard length (mm)	Condition index (k)
0.00	12.38 ± 3.29^a	7.58± 0.71^a	2.80 ± 0.39^a
3.24	13.33 ± 3.14^a	7.85 ± 0.69^a	2.72 ± 0.21^a
6.47	12.61 ± 2.46^a	7.64 ± 0.53^a	2.80 ± 0.17^a
12.95	13.15 ± 2.93^a	7.80± 0.71^a	2.69 ± 0.30^a

Means with same superscript along the same column are not significantly different at $p< 0.05$
± indicates the standard deviation.

RESULTS

General Observations

The fishes were observed to be stunned for about 2-3 minutes. Hyperactivity (characterized by erratic swimming and short darting movements) was generally observed across all exposure concentrations (except in control experiments) and this increased with increasing concentration... Hyperventilation as evidenced by rapid opening and closure of the operculum were also observed to increase with increase in toxicant concentration.

The gills of fish used in otolith extraction were observed to have a brighter red colouration than those of control fish. The intensity of colour increased with increasing concentration.

Effect on Growth

The mean wet weights of control fishes and those exposed to varying effluent concentrations showed no

Table 2
Mean Values for left and right otolith morphometry of *O.niloticus*

CONC. (%)	LOW (g)	ROW (g)	LOL (mm)	ROL (mm)	LOB (mm)	ROB (mm
0.00	$8.33x10^{-3}$±$1.86x10^{-3a}$	$7.00x10^{-3}$±$4.05x10^{-3a}$	3.98±0.35^a	3.16±1.60^a	2.71±0.24^a	2.22±1.11^a
3.24	$9.01x10^{-2}$±$2.62x10^{-3a}$	$7.01x10^{-3}$±$2.47x10^{-3a}$	3.54±1.36^a	3.02±1.76^a	2.44±0.92^a	2.18±1.24^a
6.47	$9.33x10^{-3}$±$3.57x10^{-3a}$	$6.88x10^{-3}$±$3.0x10^{-3ab}$	3.95±0.38^a	3.46±1.37^a	2.69±0.25^a	2.39±0.93^a
12.95	$9.88x10^{-3}$±$1.36x10^{-3a}$	$6.44x10^{-3}$±$9.3x10^{-4b}$	3.98±0.24^a	3.46±1.37^a	2.70±0.09^a	2.72±0.18^a

Means with same superscript along the same column are not significantly different at $p< 0.05$
± indicates the standard deviation.

ROW=Right Otolith Weight LOW=Left Otolith Weight ROL=Right Otolith Length
ROB = Right Otolith Breadth LOL= Left Otolith Length LOB= Left Otolith Breadth

statistically significant differences after 30 days exposure. The standard length and Fulton's condition index showed no differences between the measurements obtained in all experimental groups (Table 1).

Effect on Otolith Morphometry

Morphometric measurements (otolith length and breadth) of the left and right sagittae showed no significant difference in the mean values obtained across all exposure concentrations and control. The right otolith weight however had a significantly lower weight in the highest concentration than the control exposure (Table 2).

Allometric growth

Morphometric relationships between otolith indices (weight, length and breath) and somatic indices(wet weights, standard length and condition index) for all experimental groups are summarized in Table 3. Significant associations (r= 0.376, 0.397, 0.442, $p<0.05$) were observed between all the growth dimensions (length, width and weight) of the right saggitae and standard length. Only the weight of the left saggitae had a significant relationship (r=0.477, $p<0.05$) with the standard length.

Table 5. Concentrations of As, Cd, Cu, Pb, Ni, Fe, Mn and Zn were low and within acceptable limits and although Mn showed the highest availability in effluent samples, it did not exceed acceptable limits. Cyanide and Chromium levels however had values that exceeded FMENV acceptable limits.

III. DISCUSSION

Exposure of fish to pollutants especially during early development may have a wide range of specific and non specific effects (Klumpp and Von Westerhagen, 1995), which may ultimately interfere with important developmental processes (Von Westerhagen *et al*, 1988). Loss of equilibrium and hyperventilation observed in fish could be attributed to a respiratory distress due to the presence of cyanide. Solomonson (1981) reported that cyanide is a well known inhibitor of the respiratory enzyme (cytochrome oxidase) reducing tissue respiration. Other workers have also observed that metal pollution induce changes in fish ventilation and heart physiology (Hughes and Tort, 1985; Anune *et al*, 1991; Adakole and Balogun, 2005). ???High levels of cyanide may result in asphyxia for fish in natural environments where no artificial aeration exists. Respiratory distress may impair

Table 3

Correlation Coefficient (r) Values between Otolith Indices and Somatic Indices.

Parameters	Otolith morphometry						Somatic indices		
	ROW	LOW	ROL	ROB	LOL	LOB	SL	CF	BW
ROW	1.00	0.951*	0.513	0.518	0.695	0.517	0.442*	-0.253	0.260
LOW	0.951*	1.00	0.522*	0.615*	0.617*	0.593*	0.477*	-2.14	0.345*
ROL	0.513*	0.522*	1.00	0.561*	0.611*	0.522*	0.376*	-0.120	0.399*
ROB	0.518*	0.615*	0.561**	1.00	0.431*	0.767*	0.397*	0.110	0.477*
LOL	0.695*	0.617*	0.611*	0.431*	1.00	0.565*	0.129	-0.178	0.074
LOB	0.517*	0.593*	0.522*	0.767*	0.565*	1.00	0.270	-0.236	0.345*
SL	0.442*	0.477*	0.376*	0.397*	0.129	0.270	1.00	-0.245	0.516*
CF	-0.253	-0.214	-0.120	0.110	-0.178	-0.236	-0.245	1.00	0.140
BW	0.260	0.345*	0.399*	0.477*	0.074	0.345*	0.516*	0.140	1.00

* Correlation significant at the 0.05 level (2-tailed)

ROW=Right Otolith Weight LOW=Left Otolith Weight ROL=Right Otolith Length
ROB = Right Otolith Breadth LOL= Left Otolith Length LOB= Left Otolith Breadth
SL = Standard Length CF = Condition Factor BW = Body Weight

Physicochemical Properties

The physico-chemical characteristics of effluents and exposure concentration are summarized in Table 4.Temperature values ranged from 26.02-29.00^{o}C; slightly alkaline pH values of 7.03-9.60 were recorded; dissolved oxygen content of effluent was very low (2.89mgl^{-1}) compared with all experimental groups. Other parameters like BOD, COD, TSS, TDS and TS had higher values between control and all exposure concentrations (except for control exposures). Values for BOD and COD exceeded FMENV limits in exposure concentrations (except for control exposures). The highest values for BOD, COD, TSS, TDS and TS were recorded in effluent samples and these exceeded FMENV limits.

Heavy Metal Concentrations

The mean levels of heavy metals in exposure concentrations and effluent samples are presented in

feeding ability and there has been considerable discussion on the role food in determining maximum growth rate in juvenile fish (Miller *et al*, 1991; Van der Veer and Witte, 1993; Gibson, 1994) .Underlying this factor is the concept that the quality and quantity of food are the driving forces governing size of fish as an allometric scaling factor (Brett and Groves, 1979; Reichert *et al*, 2000). The decrease in otolith weight with increasing toxicant exposure may be due to stressor induced reduction in feeding ability which may ultimately affect growth as observed by the significantly lower values between control fish and highest exposure concentration in the right sagittal otolith. Such observations were however not apparent in wet weights and standard length of fish under the same conditions. Massou et al (2004) reasoned that a variety of factors (growth rate, response lags, ontogenic transitions) may be responsible for varied relationships between otolith growth and somatic growth. Otolith weight represents an integration of the complete

growth history of a fish (Burke *et al*, 1993). This is because the 3-dimensional growth of otoliths is a function of time and probably genetic predisposition whose expression is anchored on environmental events. Labrapoulou and Papaconstantinou (2000) and Pino *et al* (2004) reported a potential advantage in the use of otolith weight as a rapid and economic method for assessment of age in both tropical and temperate fishes (Worthigton *et al*, 1995; Cardinale *et al*, 2000; Araya *et al*, 2001; Pilling *et al*, 2003)

along a radial axis, hence allowing for detection of somatic growth in any plane. This may also explain why the weight of the left and right saggital otolith showed a better relationship ($P<0.05$) with the standard length than any other otolith measurement. Since the relationships between calcareous structures and body size in fishes are tangibly linked to changes in environmental conditions (Berghahn, 2000; Massou *et al*, 2004; Kruitwagen *et al*, 2006), otolith growth may thus be able to provide sensitive information on habitat quality.

Table 4
Summary of the Physico-chemical parameters of Effluent Experimental groups compared with FMENV acceptable limits

Parameter	Control (mean values)	Exposure Concentrations (mean values)	Textile factory Effluent (mean values)	FMNEV Acceptable Limits
Temperature	26.02±1.95	26.94±3.40	29.00±1.95	29.00
pH	7.03±0.05	8.24±0.53	9.60±0.85	6.00-9.00
Dissolved Oxygen	6.72±0.25	5.17±2.95	2.89±1.50	4.00
Biochemical oxygen Demand	8.50±1.05	82.76±15.51	98.60±10.95	20.00
Chemical Oxygen Demand	10.02±0.65	124.99±14.38	308.78±35.40	80.00
Total Suspended Solids	3.02±0.25	19.05±3.20	56.63±11.87	30.00
Total Dissolved Solids	27.25±1.90	263.26±21.66	2655.30±38.96	500.00-1500.00
Total Solids	29.26±2.95	278.31±23.55	2712.90±48.76	2000.00

± represents standard deviation of the values stated

As observed from the correlation results (Table 3), the length and breadth of the right saggital otolith showed a significant growth relationship ($p<0.05$) with the length-wise growth of the fish unlike the left saggital otolith. The relatively stronger relationship of the right saggital otolith suggests a selective growth coupling. This phenomenon where somatic growth synchronizes with internal structures on a particular body axis is referred to as axial symmetry. Such events of selective coupling or differential synchrony strong enough to be detected are believed to occur in species with a strong axial symmetry (Nolf, 1985; Bori, 1986).

The presence of non-biodegradable substances may be an explanation for the high COD levels observed. Suspected textile processing stages that may contribute to such physicochemical effects may include stages like sizing and desizing, scouring, dyeing and printing. The various dyes, mordant, surfactants and soap pastes used in these stages form settleable suspended solids. The biologically resistant nature of such substances and their toxic implications has been reported by Sawyer and McCarty (1978). The high TSS detected could be attributed to the vivid colors from the various dye stuffs used in textile production and this may constitute major sources of

Table 5
Summary of Levels of Heavy metals in Effluent Experimental groups compared with FMENV Acceptable limits

Heavy metal	Control (mean values)	Exposure concentrations (mean values)	Textile factory effluent (mean values)	FMENV (acceptable limits)
Cyanide	---	---	0.223	0.1
Chromium	---	---	0.693	0.1
Arsenic	---	---	0.015	0.1
Cadmium	---	---	0.035	<1.0
Copper	---	---	0.310	<1.0
Lead	---	---	0.085	<1.0
Nickel	---	---	0.355	<1.0
Iron	---	---	0.700	20.0
Manganese	---	---	2.123	5.0
Zinc	---	---	0.870	<1.0

--- = values indeterminable

The comparisons for differential sensitivity across otolith and somatic indices (Tables 1& 2) showed no significant differences across all exposure concentrations except for the weight of the right sagitta otolith. The sensitivity of otolith weight to toxicity regimes may be due to the fact that otolith weight unlike its length and breadth increases

heavy metals especially chromium.

Increased concentrations of heavy metals in river sediments could increase concentration of suspended solids (Kambole, 2003) which holds dire consequences for primary production in the recipient water body. Also

increased suspension in the water column could result in poor visibility for organisms with high dependence on sight, hence increasing vulnerability to predation. Sessile, interstitial or surface benthic organisms are also at risk because of the increased resident time in contaminated sediments (Chukwu and Nwankwo, 2003).

The high values of heavy metals in effluent samples (cyanide, chromium and manganese) may be due to the type of dye used in the processing of the textiles. Most synthetic dyes have been implicated as sources of heavy metals observed in textile factory effluent and studies have shown that metal exposures may lead to retarded growth in fishes (Weis and Weis, 1976; Viyakumari,2003; Ramadevi *et al*, 2006). The heavy metal profile of effluent are consistent with results published by Osibanjo (1991) in a survey of heavy metal content from Nigerian textile industries where Manganese (Mn) was the highest available metal, followed by Zinc (Zn) and Iron (Fe). Chromium and Cyanide levels exceeded FMENV limits for effluents as stated in interim Effluent Guidelines for all categories of industries in Nigeria (FEPA, 1991). Chromium has been reported to potentially damage and/or accumulate in various fish tissues thereby increasing their susceptibility to infection. (DWAF, 1996b). This may lower uptake of food and food conversion in fish leading to growth reduction. The high level of Chromium reported in effluents from Sunflag industry is consistent with values reported by Yusuff and Sonibare (2005) for effluents of Kaduna textile industry. DWAF (1996b) reported that cyanide is widespread in surface and groundwater's and originates from industrial effluents from chemical industries amongst others. Although conditions which enhance cyanide toxicity were not recorded (low pH and dissolved oxygen) in exposure concentrations due to artificial aeration, clinical symptoms of cyanide poisoning (ranging from loss of equilibrium to stupor) were observed. Patho-anatomical pointers to cyanide toxicity i.e. cherry red color of gills were also observed (Leduc, 1981; DWAF, 1996a).

IV. CONCLUSION

The ability of a water-body to support aquatic life, as well as its suitability for other uses depends on the presence or absence of contaminants in the water body. Varying levels and interactions of contaminants hold in store a range of effects for the resident organisms', especially sensitive stages like juveniles. Endeavours at measuring environmental stress from a pool of bio-indicators in fish, carries with each attempt a fundamental search for sensitivity and affordability in bioindicators.

Furthermore the differential growth relationship between morphometry of the right and left saggital otolith with fish length may have implications on the choice of otoliths to be used for microstructural studies (growth rings).

We conclude that growth studies using otoliths in juvenile sized fish may be more valid if otolith in the detected growth axis i.e. right saggital otolith (in this case) is used for such evaluations. Also since otolith weight seems to be a better detector of growth changes in juvenile *O. niloticus*, a closer look should be made on its relative importance as a sensitive parameter in pollution studies.

REFERENCES

Able, K.W., J.P. Manderson & A.L. Studholme. 1999. Habitat quality for shallow water fishes in urban estuary: the effect of man-made structures on growth. Marine Ecol. 187: 227–235.

Adakole, J.A and J.K. Balogun, 2005. Effects of acute concentrations of metal-finishing waste water on haematological parameters of *Clarias gariepinus*

Adams, S.M. (ed.) 2002. Biological indicators of aquatic ecosystem stress, American Fisheries Society, Bethesda, Maryland. 621 pp.

Agostinho, C.S. (1999). Use of Otoliths to Estimate Size at Sexual Maturity in Fish. Fundacao Universidade do Tocantins- R. Luiz leite Ribeiro/ Av. Castelo Branco, Setor Aeroporto, CEP 77500-000. Porto Nacional-TO, Brazil.

Akif M, Khan A.R, Sok K, Min K.S, Hussain Z, Maal-Abrar M 2002. Textile effluents and their contribution towards aquatic pollution in the Kabul River (Pakistan). J Chem Soc Pakistan 24(2):106– 11.

APHA, 1992: Standard methods for the examination of water and waste water. 16th Ed., Amer. Publ. Health Assoc., Washington, 1268pp.

Araya, M., Cubillos, L., Guzman, M., Peñailillo, J., Sepúlveda, A., 2001. Evidence of a relationship between age and otolith weight in the Chilean jack mackerel, *Trachurus symmetricus murphyi* (Nichols). Fish. Res. 51, 17–26.

Berghahn, R., 2000. Response to extreme conditions in coastal areas: biological tags in flatfish otoliths. Mar. Ecol. Prog. Ser. 192, 277–285.

Boehlert, G.W., 1985. Variability in age estimates in Sebastesas: a function of methodology, different readers and different laboratories, California. Fish Game 70, 210±224.

Bori, C. (1986). Ana'lisis morfome 'trico comparado del otolito (saggita) de *Solea vulgarisy*, *S. senegalensis* (Teleostei: Soleidae) del Delta del Ebro. *Investigaciones Pesqueras*

Brett, L.J., Groves, T.D.D., 1979. Physiological energetics. In: Hoar, W.S., Randall, D.S., Brett, J.R. (Eds.).Fish Physiology, Vol. 8. Academic Press, New York, pp. 279–352.

Brothers, E.B., 1987. Methodological approaches to the examination of otoliths in ageing studies. In: R.C. Summerfelt and G.E. Hall, (eds), Age and Growth of Fish, lowa State University Press, Ames lowa, USA: 319–330.

Campana, S. E. 1990. How reliable are growth backcalculations based on otoliths? Canadian Journal of Fisheries and Aquatic Sciences, 47: 2219–2227.

Cardinale, M., Arrhenius, F., Johnsson, B., 2000. Potential use of otolith weight for the determination of

age-structure of Baltic cod (*Gadus morhua*) and plaice (*Pleuronectes platessa*). Fish.Res. 45, 239–252.

Chukwu, L.O. and Nwankwo, D.L; 2003. The Impact of land based pollution on the hydrochemistry and Macrobenthic community of a tropical west African creek. Diffuse Pollution Conference Dublin 2003.

Fagade, S.O. (1979). The structure of the otoliths of *Tilapia guineensis* and their usage in age determination. *Hydrobiologia* vol. 69, 1-2, pag. 169-173.

FMENV (Federal Environmental Protection Agency) (1991), Guidelines to Standards for Environmental Pollution Control in Nigeria, Lagos, Nigeria.

Francis, R. I. C. C. 1990. Back-calculation of fish length: a critical review. Journal of Fish Biology, 36: 883–902.

Gibson, R.N. 1994. Impact of habitat quality and quantity on the recruitment of juvenile flatfishes. Netherlands J. Sea Res. 32: 191–206.

Hare, J. A., and Cowen, R. K. 1995. Effect of age, growth rate, and ontogeny on the otolith size–fish size relationship in bluefish, *Pomatomus saltatrix*, and the implications for backcalculation of size in fish early life history stages. Canadian Journal of Fisheries and Aquatic Sciences, 52: 1909–1922.

Hining, K. J., J. L. West, M. A. Kulp, and A. D. Neubauer. 2000. Validation of scales and otoliths for estimating age of rainbow trout from southern Appalachian streams. North American Journal of Fisheries Management 20:978–985.

Jordao CP, Pereira MG, Bellato CR, Pereira JL, Matos AT. Assessment of water systems for contaminants from domestic and industrial sewages. Environ Monit Assess 2002; 79(1):75– 100.

Kambole M.S. (2003). Managing the water Quality of the Kafue River, in: Physics and Chemistry of the Earth, Parts A/B/C, 28 (20-27), pp 1105-1109.

Karakiri, M., R. Berghahn & H. von Westernhagen. 1989. Growth differences in 0-group plaice Pleuronectes platessa as revealed by otolith microstructure analysis. Marine Ecol. Prog. Ser. 55: 15–22.

Klumpp DW, Von Westernhagen H (1995) Biological effects of pollutants in Australian tropical coastal waters: embryonic malformations and chromosomal aberrations in developing fish eggs. Mar Pollut Bull 30:158–165

Labropoulou, M., Papaconstantinou, C., 2000. Comparison of otolith growth and somatic growth in two macrourid fishes.Fish. Res. 46, 177–188.

Laws E.A. (1981). Aquatic pollution. John Wiley and Sons, New York, pp.301- 369.

Massou, A.M., Le Bail, P.Y., Panfili, J., Lae, R., Baroillers, J.F., Mikolasek, O., Fontenelle, G., and Auperin, B. (2004). Effects of confinement stress of variable duration on the growth and microincrement deposition in the otoliths of *Oreochromis niloticus* (Cichlidae)

Miller, J.M., Burke, J.S., Fitzhugh, G.R., 1991. Early life history patterns of Atlantic North American flat fish: likely (and unlikely) factors controlling recruitment. Neth. J. Sea Res. 27 (3/4), 261–275.

Nolf, D. (1985) Otolithi piscium. In *Handbook of Paleoichthyology, Vol X* (Schulze, L. & Kuhn, O., Eds), pp. 1-26. Stuttgart: Gustav Fischer Verlag.

Osibanjo, O., (1991). Physicochemical characteristics of effluents from selected Nigerian industries. Environ.Pollut. (in press)

Pawson, M.G., 1990. Using otolith weight to age fish. J. Fish Biol. 36, 521±531.

Pilling, G.M., Grandcourt, E.M., Kirwood, G.P., 2003. The utility of otolith weight as a predictor of age in the emperor *Lethrinus mahsena* and other tropical fish species. Fish. Res. 60, 493–506.

Pino C.A. , Luis A. Cubillos, Miguel Araya , Aquiles Sepúlveda ; 2004. Otolith weight as an estimator of age in the Patagonian grenadier, *Macruronus magellanicus*, in central-south Chile. *Fisheries Research 66 (2004) 145–156*

Ramadevi, S. Kokila & V Bhuvanswari, (2006): A study on mutagencity of dyeing industry effluent and genotoxicily in lymphocytes of dyeing industry workers. Poll res 25(2) 383 – 386.

Reish, D. L. and Oshida, P. S. (1986): Manual of methods in aquatic environment research. *FAO Fisheries Technical Paper* 247: 1-65.

Sawyer, C.C. and McCarty, P.L. (1978), Chemistry for Environmntal Engineers, McGraw Hill, New York. Pp 331-514

Suthers, I.M., A. Fraser & K.T. Frank. 1992. Comparison of lipid, otolith and morphometric condition indices of pelagic juvenile cod (Gadus morhua) from the Canadian Atlantic. Marine Ecol. Prog. Ser. 84: 31–40.

Tarras-Wahlberg NH, Flachier A, Lane SN, Sangfors O. (2001). Environmental impacts and metal exposure of aquatic ecosystems in rivers contaminated by small scale gold mining: the Puyango River basin, Southern Ecuador. Sci Total Environ 2001; 278(1– 3):239– 61.

Van der Veer, H.W., Witte, J.I., 1993. The 'maximum growth/ optimal food condition' hypothesis: a test for 0-group plaice *Pleuronectes platessa* in the Dutch Wadden Sea. Mar. Ecol. Prog. Ser. 101, 81–90.

Vijayakumari, B. (2003). Impact of textile dyeing effluent on growth of soyabean (Glycine max L.) *J. Ecotoxicol.Environ.Monit.* 13(1): 59-64

Von Westernhagen H (1988) Sublethal effects of pollutants on fish eggs and larvae. In: Hoar WS, Randall DJ (Eds) the physiology of developing fish; Part A: Eggs and larvae. Fish physiology. Academic, Orlando, pp 253–346

Waessle J.A., Carlos A. L., and Marco Favero. (2002). Otolith morphology and body size relationships for juvenile sciaenidae in the Rio de la Plata estuary (35-36^{o}S)

Worthington, D.G., Fowler, A.J., Doherty, P.J., 1995a. Variation in the relationship between otolith weight and age: implications for the estimation of age of two tropical damsel-fish (*Pomacentrus moluccensis* and *P. wardi*). Can. J. Fish. Aquat. Sci. 52, 233– 242.

Wright, P. J. (1991). The influence of metabolic rate on otolith increment width in Atlantic salmon parr, Salmo salar L. Journal of Fish Biology 38, 929–933.

Wright, P. J., Fallon-Cousins, P. & Armstrong, J. D. (2001). The relationship between otolith accretion and resting metabolic rate in juvenile Atlantic salmon during a change in temperature. Journal of Fish Biology 59, 657–666. Doi: 10.1006/jfbi.2001.1678.

Yusuff, R.O. and Sonibare, J.A. (2005): Characterization of Textile Industries' Effluents in Kaduna, Nigeria and Pollution Implications. Global Nest: the Int. J. Vol 6, No 3, pp212-221.

Zhou B, Liu W, Wu RS, Lam PK. 2005. Cultured gill epithelial cells from tilapia (*Oreochromis niloticus*): a new in vitro assay for toxicants. Aquat Toxicol. 71:61-72.

4/9/2010

A Modified lentiviral vector construction system

Bo Song, JingWei Liu, XiuFang Chen, YuMing Xu*

DEPARTMENT OF NEUROLOGY, THE FIRST AFFILIATED HOSPITAL, ZHENGZHOU UNIVERSITY, ZHENGZHOU, 450052, CHINA

Xuyuming@zzu.edu.cn

Abstract: Objective: To develop a lentiviral vector system, which can be used to co-express multiple genes of interest, such as siRNAs cassettes, reporter gene and resistant gene simultaneously and to facilitate to titrate lentiviral vector stock with $TCID_{50}$ method. Method: Synthesis new multiple cloning sites（MCS）to replace the original MCS of pLKO-1-puro and produced an intermediate plasmid pLKO-1-puro-MCS; Destination plasmid pLKO-M was constructed through transfering the CMV promoter-GFP-IRES element into pLKO-1-puro-MCS; The support plasmid pENTR-U6-20 was produced through transfering the siRNA-Expression cassette of pSilencer 2.0 into pENTR-U6-con. pLKO-M was cotransfected with pCMV-dR8.2 dvpr and pCMV-VSVG into 293T cells to produce lentiviral vectors. Harvest the virus 72 hours after contransfection and titrate it on Vero cells with $TCID_{50}$ method.Result: Restriction enzyme digestion analysis of pLKO-M showed that it was constructed successfully; restriction enzyme digestion analysis and sequencing result of pENTR-U6-20 indicated that it is constructed successfully. The GFP gene in pLKO-M can express normally and the titre caculated with $TCID_{50}$ method is $6.47X10^6$ IU/ml. Conclusion: The multiple gene coexpressing system which contains two plasmid, pLKO-M and pENTR-U6-20, was established and the titre of pLKO-M virus can be measured with $TCID_{50}$ method. [Life Science Journal. 2010; 7(2): 42 – 46] (ISSN: 1097 – 8135).

Keywords: gene therapy; lentiviral vector; siRNA; titration method.

1. Introduction

Lentiviral vectors has many advantages, such as the ability to infect dividing and nondividing cells, the ability to integrate with host cell genome and express transgenes stably, and triggering elicit little or no immune reactions1- 5. (Lentiviral vectors can efficiently deliver genes to postmitotic neuronal cell types offering long-term expression, can be generated in high titers, and do not give immunological complications. Various animal studies have demonstrated the effectiveness of these vectors to deliver therapeutic genes into the nervous system, as well as to model human diseases6.

The study results of its application in neurological disordes, especially Parkinson's disease is encouraging[7-11]. But there are two important issues that should have reaserchers' attentions, one issue is that the pathogenesis of neurological disorder involves more than one single gene.The other one is that we lack rapid and stable titration method of lentiviral vector stock. A new lentiviral vector should be reconstruct ed, which can co-express more than one gene and contains an more direct reporter gene tol simplify the titration procedure.

For this purpose, the research developed a multiple gene co-expressing lentiviral vector construction system which consists of two plasmid, pENTR-U6-20 and pLKO-M .Using this system, we planed to construct lentiviral vectors that could co-express more than one single siRNA, GFP and gene of interest and construct a standard titrate method based on GFP expression, with $TCID_{50}$ method. We hope that this system would be a useful tool to study neurological disorders.

2. Materials and Methods

2.1 Plasimids. Lentiviral backbone plasmid pLKO-1-puro(figure 1),helper plasmid pCMV-dR8.2 dvpr and pCMV-VSVG, pENTR-U6-con (figure2), pGFP-IRES and pSilencer 2.0 are all kindly provided by proffessor ZhiQiang Han from ZhengZhou university and propagated in E.coli strain DH5α.

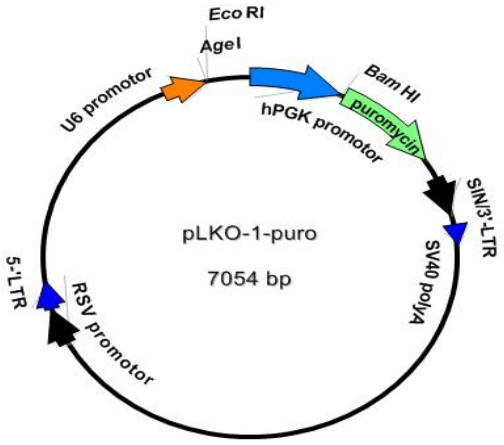

Figure 1: The map of pLKO-1-puro plasmid

2.2. Cell culture. 293T cells and Vero cells were purchased from ShangHai cell bank and cultured in Minimum Essential Medium (Invitrogen) supplemented with 10% (v/v) fetal bovine serum (FBS) and 2 mM glutamine (Invitrogen), 5% CO_2, humidified atmosphere at 37 ^oC in an incubator (SanYo, Japan)

2.3. Construction of intermediate plasmid pLKO-1-puro-MCS: Design and synthesis the following two oligonucleotides which is complimentary to each other at the restriction enzyme recognition sites:

MCS1: 5'CCGGTGAATTCTCTAGAGTCGACACGCGT3' (with a sticky end attached to the 5' end whch is complementary with AgeI digested end, it contains the following restriction sites: 5' MluI、SalI、XbaI、EcoRI and AgeI '3.)

MCS2 ： 5‘AATTACGCGTGTCGACTCTAGAGAATTCA3’ (with a sticky 5’ end that is complementary with EcoRI digested end, it contains the following restriction sites: 5’AgeI、EcoRI、XbaI、SalI and MluI ‘3).

Annealing the two strands and ligate it with AgeI and EcoRI digested plasmid pLKO-1-puro with T4 DNA ligase (Takara) to produce pLKO-1-puro-MCS. Then transform E.coli strain DH5α with traditional Calcium chloride transformation method, screen positive clonies with EcoRI、XbaI、SalI、MluI plus BamHI digestion analysis.

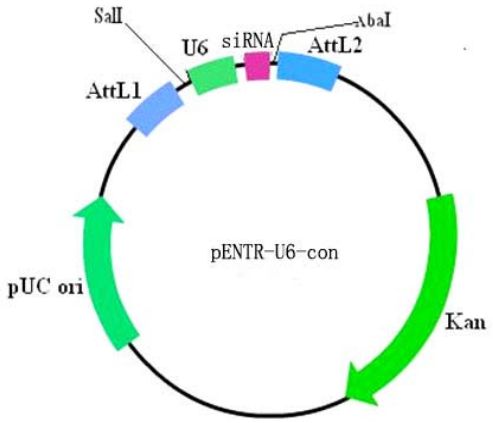

Figure 2: The map of pENTR-U6-con

2.4. construction of destination plasmid pLKO-M: Design primers that is specific to the CMV promotor-GFP-IRES-MCS element of the pGFP-IRES:

GXbaI: 5‘GCTTCTAGATCAATATTGGCCATTAGCCATATTA’3 (with a XbaI restriction site and 3 protective base attached to the 5’ end)

GSalI：5‘ACTGTCGACGATCCCGGGTTGTGGCAAGCT’3 (with a SalI restriction site and 3 protective base attached to the 5’ end) Amplify the element with PrimeStar HS polymerase (Takara), the PCR parameters used in this step is:94 ºC 4 min-***94*** ºC ***30 sec -58*** ºC ***30sec-72*** ºC ***2min*** - 72ºC 5 min - 4ºC indefinite .Perform electropheresis in 1% agarose gel, harvest the 2.4kb PCR product. Digest the PCR doduct and pLKO-1-puro-MCS with XbaI and SalI, then ligate them to construct pLKO-M. Transform DH5α, screen positive clonies with XbaI and SalI digestion.

2.5. Construction o support plasmid pENTR-U6-20: Design primers that is specific to the siRNA expression cassette of pSilencer2.0:

INPTEN1:5‘CAAGTCGACGAATTCCCCAGTGGAAAGACGCGC 3’ (with a SalI restriction site and 3 protective base attached to the 5’ end).

INPTEN2: 5‘ACCTCTAGACCAAGCTTTTCCAAAAAACTACCG 3’ (with a XbaI restriction site and 3 protective base attached to the 5’ end)

Amplify the siRNA expression element which with PrimeStar HS polymerase (Takara), the PCR parameters used in this step is: 94 ºC 4 min-***94*** ºC ***30 sec -58*** ºC ***30sec-72*** ºC ***30 sec***-72ºC, 5min-4 ℃ indefinite. The siRNA expression cassette is about 421bp，Harvest the 421bp PCR product , digest the PCR product and pENTR-U6-con with SalI and XbaI, then ligate them to produce pENTR-U6-20. Transform DH5α, screen positive clonies with XbaI and SalI digestion analysis. Select one positive colony and sequence with hU6 Forward sequencing primer 5’TGGACTATCATATGCTTACCGT 3’, align the sequencing result with original siRNA expression cassette of plasmid pSilencer2.0.

2.6. Production of lentiviral vectors. Grow 293T cells in a 100 mm culture dish .When the cells is about 90% confluence ,Cotransfect 3 microgram pLKO-M、22.67μg helper plasmid pCMV-dR8.2 dvpr and 0.33μg envelope plasmid pCMV-VSVG(the proportion between three plasmid is: pLKO-M : pCMV-dR8.2 dvpr : pCMV-VSVG =9:8:1) with lipofectin 2000 (Invitrogen) following the protocols provided in the user’s manual. 48 hours after cotransfection, observe green fluorescence under inverted fluorescent microscope (Nicon) to estimate transfection efficiency. 72 hours after cotransfection, transfer the culture medium from the culture dish into a 15ml tube. Centrifuge at 3000 rpm, 4 ºC for 10 minutes and filtrate with a 0.45 μm filter(Millipore) to clarify the viral stock solution. Then concentrate it through centrifuging at 4℃，25000rpm for 90 minutes in an ultraspeed centrifuger(Beckman). Remove supernant and resusspensed with fresh medium. Store the viral solution at -80 ℃。

2.7. Titration of viral stock solution with $TCID_{50}$ method: The method used here is derived from $TCID_{50}$ method that is used to titrate adenoviral stock solution[12]. Briefly , grow Vero cells in two 96-wells culture plates with 10^4 cells in each well. Serially dilute vector stock solution with fresh medium in 1.5 ml EP tube, from 10^{-1} to 10^{-10} . Infect the Vero cells in each well with 100 μl of the last 8 serial dilutions. Incubate at 37℃ for 48 hours, then observe green fluorescence under inverted fluorescent microscope, count positive wells in each plates and calculate the titre in each 96-well culture plates use this formula $T = 10^{1+1+d(S-0.5)}$IU/ ml, and the mean of two culture plates is the final titre of the stock solution.

3. Result

3.1. Construction of intermediate plasmid pLKO-1-puro-MCS: Digest pLKO-1-puro-MCS with EcoRI、XbaI、SalI、MluI plus BamHI produced four 750bp segments, as showed in the electropherogram of digestion product, which indicated that it was constructed successfly(see figure 3).

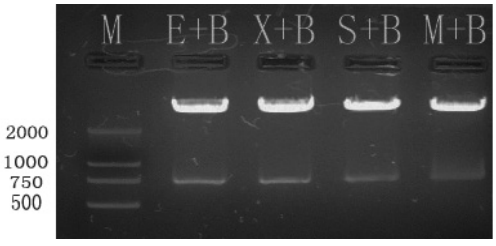

Figure 3: Electropherogram of digestion product of pLKO-1-puro-MCS；M：Marker DL2000；B：BamHI；X：XbaI；S：SalI；M：MluI.

3.2. Construction of plasmid pLKO-M: Digestion of pLKO-M with XbaI and SalI produced a 2.4kb segment which should be the CMV promotor-GFP-IRES-MCS element. Electropheresis of digestion product showed that pLKO-M was successfully (see figure 4). The recombinant lentiviral vector pLKO-M have some new features that was shown in figure 5.

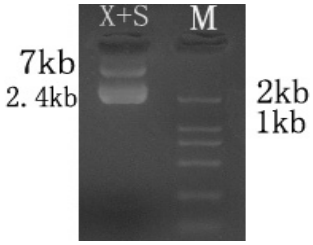

Figure 4: Electropherogram of XbaI and SalI digestion product of pLKO-M

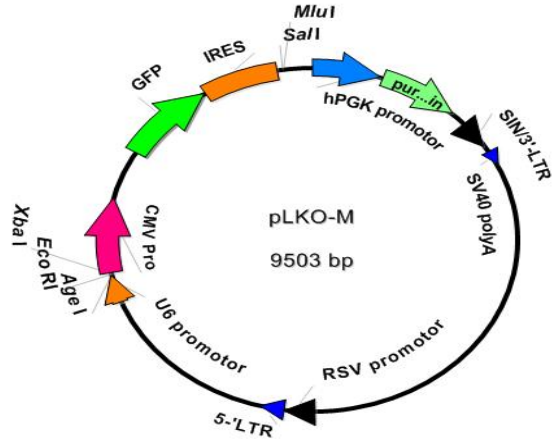

Figure 5: The map of recombinant lentiviral vector pLKO-M.

3.3. Construction of support plasmid pENTR-U6-20: The siRNA expression cassette of pSilencer2.0 was successfully amplified and cloned into plasmid pENTR-U6-CON, and confirmed by restriction digestion analysis and sequencing. Electropheresis of XbaI and SalI digestion product of pENTR-U6-20 produced a 421bp DNA segment(see figure 6) which should be the siRNA expression cassette of pSilencer2.0, and it is confimed by sequencing result. The features of pENTR-U6-20 was showed in figure 7.

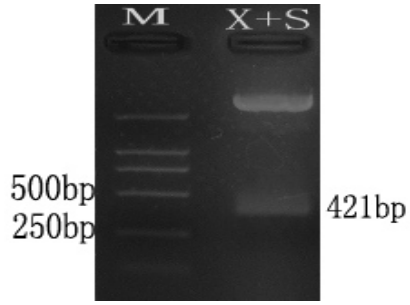

Figure 6: Electropherogram of XbaI and SalI digestion product of pENTR-U6-20.

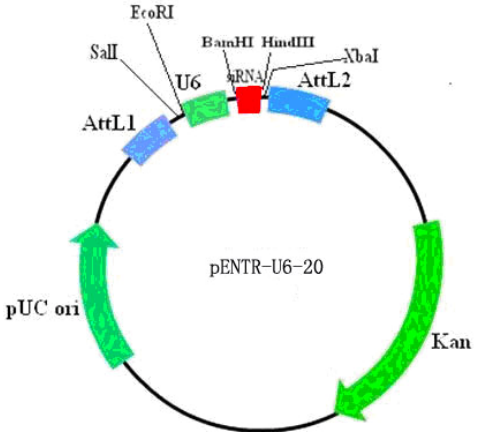

Figure 7: The map of pENTR-U6-20.

3.4. Production of lentiviral vectors. 36 hours after contransfection of 3 plasmid into 293T cells, green fluorescence appeared; 48 hours later, the green fluorescence became very obvious and bright （see figure 8）. 72h after transfection, about 9ml of virus was harvested. After centrifugation at 4℃，25000 rpm for 90 minutes, remove the supernant and and resuspensed the pellet with 900 μl of fresh medium.

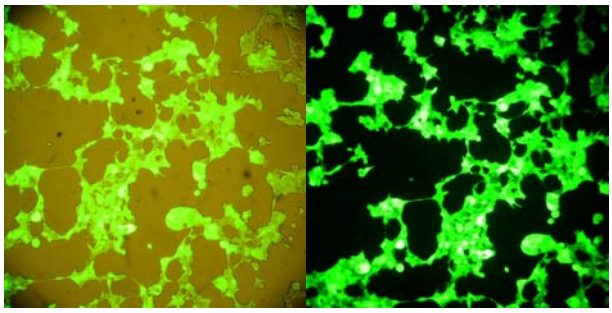

A:(×100) B:(×100)

Figure 8: 48 houres after contransfection into 293T cells.figure A is dark field, figure B is light field.

3.5 Titration of viral stock solution with $TCID_{50}$ method. Green fluorescence appeared 48 hours after infection Vero cells in 96-well culture plates with serial dilutions of lentiviral stock. GFP- positive wells can be determined and counted without difficulty. According to the formula provided above, the titre calculated on one culture plate ≈$7.94X10^6$IU/ml and the other one≈$5.01X10^6$IU/ml. The final mean titre of lentiviral stock solution was $6.47X10^6$ IU/ml.

Discussion

Multiple gene co-expression lentiviral vectors had been used in the study of neurological disorders, but there is no report of multiple siRNA co-expression or siRNA and gene of interest coexpression lentiviral vectors[13-19]. This kind of vectors are more useful than single gene expressing vectors. we developed this system that can be used to construct multilple siRNA, GFP and gene of interest co-expression lentiviral vectors. This system has the following features:

1): Features of pLKO-M: As shown in figure 1 and figure5, pLKO-M was derived from pLKO-1-U6-puro, it contains U6 promotor-(AgeI-EcoRI-XbaI) element and CMV promoter-GFP-IRES-(SalI-MluI) element. U6 promotor can initiate siRNA expression and IRES element can mediate translation of two proteins from one mRNA. So it is possible to clone a siRNA into the AgeI-EcoRI-XbaI site to down-regulate a target gene and clone the CDS of a gene of interest to up-regulate it. Down regulation and up regulation of specific genes are two most important strategies of gene therapy which involves different mechanisms, apply those two strategies simultaneously may produce synergistic effect which is more effective than using either strategy alone. Lentiviral vector pLKO-M can be used to apply those two strategies simultaneously throught one vector. The GFP gene is driven directly by CMV promoter and as a reporter gene to facilitate researches. So, this vector itself is a siRNA, GFP and gene of interest coexpression lentiviral vector.

2)Fetures of support plasmid pENTR-U6-20: As indicated in figure 2 and figure 7, the support plasmid pENTR-U6-20 and its precursor pENTR-U6-Con are derived from the pENTR-U6 which is the entry plasmid of Gateway cloning system. The plasmid pENTR-U6 is a linear ready-to-use plasmid easier to use, but not reproducible. However, pENTR-U6-Con is a circular and reproducible plasmid that can be used repeatedly. The restriction sites in pENTR-U6-20 is compatible with pSilencer2.0 and pSilencer3.0, so siRNAs of target genes can be designed directly using Ambion's online siRNA design program, which made siRNA designing became more simple and easier, and also decreased the probabilities of making mistakes greatly. Support plasmid pENTR-U6-20 maintained the Gateway cloning elements attL1 and attL2, so siRNAs in this plasmid can be transferred directly to any destination plasmid of Gateway cloning system. Because the restriction sites(EcoRI and XbaI) flanking the U6 promotor-siRNA element is compatible with pLKO-M, so siRNA expression cassettes in pENTR-U6-20 can be transferred directly into pLKO-M and other vectors that have EcoRI and XbaI sites.

Titration method of lentiviral vectors derived from pLKO-M. The tritration method for lentiviral vectors can be divided into functional and non-functional methods. Nonfuntional method is usually based on detection of viral RNA or viral proteins and will detect inactivated and defective virus can not accurately reflect the functional units; The functional method is usually based on detection of reporter gene product, such as neomycin, puromycin or GFP, it will reflect the quatity of infectious viral particles[20-22]. $TCID_{50}$ method is functional method and had became the standard titration method of adenoviral vectors. Titration of adenoviral vectors with $TCID_{50}$ method is based on observing cytopathic effect (CPE). Cytopathic effect (CPE) is an infection marker of adenoviral vectors, through observing CPE and count positive wells of a 96-well culture dish, we can calculate the titre of adenoviral vectors. But lentiviral vector does not produce cytopathic effect, so we should find other infection marker to count positive wells and calculate the final titre. The GFP gene in vectors derived from pLKO-M is driven directly by CMV promoter and can express GFP 48 hours after infection of host cells, so it is an excellent infection marker that can be used to titrate lentiviral vectors. This experiment proved that GFP can be used to determine positive wells in 96-well culture dish directly under an inverted fluorescent microscope. As an infection marker to titrate lentiviral vector, GFP is more labour-saving than other kinds of reporter genes and more timesaving than observing CPE because standard $TCID_{50}$ method requires observing CPE for at least ten days[11].

Lentiviral vectors have been widely used in the study of neurologic disorders, and researchers are now developing more useful vectors and strategies of gene therapy. This research presented a strategy to construct multiple gene coexpression lentiviral vectors and provided a optional tool to study neurological disorders.

References

1. Naldini L, et al.In vivo gene delivery and stable transduction of nondividing cells by a lentiviral vector. Science 272, 263-7 (1996).
2. Naldini L, Blomer U, Gage FH, Trono D, Verma IM.Efficient transfer, integration, and sustained long-term expression of the transgene in adult rat brains injected with a lentiviral vector. Proc Natl Acad Sci U S A 93, 11382-8 (1996).
3. Kafri T, van Praag H, Ouyang L, Gage FH, Verma IM.A packaging cell line for lentivirus vectors. J Virol 73, 576-84 (1999).
4. Abbas-Terki T, Blanco-Bose W, Deglon N, Pralong W, Aebischer P.Lentiviral-mediated RNA interference. Hum Gene Ther 13, 2197-201 (2002).
5. Abordo-Adesida E, et al.Stability of lentiviral vector-mediated transgene expression in the brain in the presence of systemic antivector immune responses. Hum Gene Ther 16, 741-51 (2005).
6. Gene therapy for neurodegenerative diseases based on lentiviral vectors. Prog Brain Res. 175: 187-200(2009).
7. Dowd E, et al.Lentivector-mediated delivery of GDNF protects complex motor functions relevant to human Parkinsonism in a rat lesion model. Eur J Neurosci 22, 2587-95 (2005).
8. Kordower JH, et al.Neurodegeneration prevented by lentiviral vector delivery of GDNF in primate models of Parkinson's disease. Science 290, 767-73 (2000).
9. Brizard M, Carcenac C, Bemelmans AP, Feuerstein C, Mallet J, Savasta M.Functional reinnervation from remaining DA terminals induced by GDNF lentivirus in a rat model of early Parkinson's disease. Neurobiol Dis 21, 90-101 (2006).
10. McCoy MK, Ruhn KA, Martinez TN, McAlpine FE, Blesch A, Tansey MG.Intranigral lentiviral delivery of dominant-negative TNF attenuates neurodegeneration and behavioral deficits in hemiparkinsonian rats. Mol Ther 16, 1572-9 (2008).
11. Matsukawa N, et al.Overexpression of D2/D3 receptors increases efficacy of ropinirole in

chronically 6-OHDA-lesioned Parkinsonian rats. Brain Res 1160, 113-23 (2007).

12. Zhang XZ, et al.[Quality control of clinical-grade recombinant adenovirus used in gene therapy]. Zhonghua Yi Xue Za Zhi 84, 849-52 (2004).
13. Yu X, et al.Lentiviral vectors with two independent internal promoters transfer high-level expression of multiple transgenes to human hematopoietic stem-progenitor cells. Mol Ther 7, 827-38 (2003).
14. Jones S, et al.Lentiviral vector design for optimal TCR gene expression in the transduction of PBL and TIL. Hum Gene Ther (2009).
15. Yang S, et al.Development of optimal bicistronic lentiviral vectors facilitates high-level TCR gene expression and robust tumor cell recognition. Gene Ther 15, 1411-23 (2008).
16. Semple-Rowland SL, Eccles KS, Humberstone EJ.Targeted expression of two proteins in neural retina using self-inactivating, insulated lentiviral vectors carrying two internal independent promoters. Mol Vis 13, 2001-11 (2007).
17. Khare PD, et al.Durable, safe, multi-gene lentiviral vector expression in feline trabecular meshwork. Mol Ther 16, 97-106 (2008).
18. Chen HH, et al.Detection of dual-gene expression in arteries using an optical imaging method. J Biomed Opt 9, 1223-9 (2004).
19. Azzouz M, et al.Multicistronic lentiviral vector-mediated striatal gene transfer of aromatic L-amino acid decarboxylase, tyrosine hydroxylase, and GTP cyclohydrolase I induces sustained transgene expression, dopamine production, and functional improvement in a rat model of Parkinson's disease. J Neurosci 22, 10302-12 (2002).
20. Geraerts M, Willems S, Baekelandt V, Debyser Z, Gijsbers R.Comparison of lentiviral vector titration methods. BMC Biotechnol 6, 34 (2006).
21. Jin D, et al.CD38 is critical for social behaviour by regulating oxytocin secretion. Nature 446, 41-5 (2007).
22. Delenda C, Gaillard C.Real-time quantitative PCR for the design of lentiviral vector analytical assays. Gene Ther 12 Suppl 1, S36-50 (2005).

4/20/2010

Some Biochemical and Organoleptic changes due to Microbial growth in Minced Beef packaged in Alluminium polyethylene trays and Stored under Chilled condition

Agunbiade, Shedrach Oludare; Akintobi, Olabiyi A. and Ighodaro, Osasenaga Macdonald

DEPARTMENT OF BIOCHEMISTRY AND MICROBIOLOGY, LEAD CITY UNIVERSITY, IBADAN, OYO STATE, +234, NIGERIA.

macigho@yahoo.com

Abstract -Changes in the quality of minced beef were studied under two refrigerated conditions (1-2^{0}C and 5-7^{0}C) using some biochemical organoleptic and bacterial assays during a six-day period. Meat's crude protein concentration remained constant (19.7-19.8%) in 4 days and 3 days at 1-2^{0}C and 5-7^{0}C respectively. There was an increase of only 0.4 to 0.6% and 0.9 to 1.4% during the 6 day period at 1-2^{0}C and 5-7^{0}C respectively. Between the 4th-6th day under both chill temperatures the meat has spoilt turning dark brown, slimy and putrid. This period coincided with meat's bacteria log number of 8.6/g and above, increased alkalinity from 0.5 in fresh meat to between 4.3 and 5.7 ml of 0.02N HCl/g sample and increased total volatile nitrogen (TVN) from 12.6mgN/100g protein in the fresh state to between 23.8 and 39.8 mgN/100g protein under the two chill temperatures. The gradual increase of meat's pH from 5.4 in fresh state to 5.8 at 1-2^{0}C in 5 days and 5.7 at 5-7^{0}C in 3 days, and its subsequent pronounced increase to between 6.1 and 6.9 may be ascribed to proteolysis on one hand. Increased TVN may also be responsible for the elevated meat's pH and alkalinity in the spoiling meat. Minced meat for use in hamburger, corn beef, hotdog and other meat products may enjoy a shelf stability of only 3 day holding period under chill temperatures otherwise it is deemed unsafe for human consumption. [Life Science Journal. 2010; 7(2): 47– 51] (ISSN: 1097 – 8135).

Keywords: Beef, organoleptic, bacterial, chill temperatures,biochemical, volatile nitrogen, alkalinity,protein, pH

1. Introduction

Meat (beef) owes its perishability to its high water content and preponderance of nutrients such as high molecular proteins, low molecular substances such as glucose, free amino acids, peptides and very minute amount of glycogen (Koutsoumanis *et al*., 2006, Jay, 2000, Ingram and Dainty, 1971). The quality of beef depends, among other factors, upon the pre-slaughter handling, care and state of animal, age, sex, species, hygiene precautions in the slaughter house and meat pH (Anon, 2001).

In a situation when a cow is well rested before slaughter, its post-rigor pH of 5.4 is achieved (Ingram and Dainty, 1971). Further changes (chemical, microbial and organoleptic), depending upon prevailing or storage temperature, relative humidity, bulkiness of meat, degradation of low molecular substances by the activity of the dominant indigenous microorganisms, are also overt (Ellis and Goodacre, 2001; Koutsoumanis *et al*., 2006; Labadie, 1999). The main bacteria implicated in the spoilage of refrigerated beef include *Brochothrix hermosphacta, Lactobacilli spp., Leuconostoc spp., Carnobacterium spp., Pseudomonas spp.* and Enterobactriaceae (Borch *et al*., 1996, Nuchas *et al.,* 2008).

Lactic acid bacteria (LAB) have been reported to play a role in the spoilage of refrigerated raw meat (Labadie, 1999). Spoilage signs are often attributed to the undesirable growth of microorganisms to unacceptable levels. In meat, microbial spoilage leads to the development of off-odours and often slime formation (Hilario *et al*. 2004, Huis in't Veld, 1996, Jackson *et al.,* 1997). Meat's organoleptic changes may vary according to the microbial association contaminating the meat and to the conditions under which the meat is stored (Danilo *et al.*, 2006).

It has also been reported that development of organoleptic spoilage is related to metabolization of meat's low molecular substances, such as sugar and free amino acids and the release of undesirable volatile metabolites. As soon as the glucose present in aqueous phase has been exhausted other substrates are consequently utilized by metabolizing microorganisms to produce odoriferous nitrogenous compounds, the most predominant of which is ammonia (Pearson and Muslemuddin, 1968, Stanbridge and Davis, 1998). Microbial loads from 10^7 cfu/cm^{-2} have been associated with occurrence of off-odours when the loads increased to as high as 10^9 cfu/cm^{-2} when the meat becomes putrid (Dainty *et al*., 1985, Jay, 2000).

Several devices have been shown to influence increased shelf life of meat at refrigeration conditions without the use of chemical additives (Brody, 1996, Fiber, 1991, Ilario, 2009, Danilo *et al.*, 2006). Vacuum packaging of raw meat under chill conditions has proved to be effective in extending the shelf life and preventing

growth of pathogens (Labodie, 1999). The main objective of this study was to assess the quality and to determine the optimum storability of minced beef packaged in polyethylene trays within one week period at chill storage temperatures.

2. Materials and Methods

Freshly cut stewing steaks, from the same meat muscle (*Longissimus dorsi*) were bought at a local abbatoir. The steaks were aseptically trimmed of visible fat, minced in the laboratory, packaged in portions of 60g in polyethylene trays with interior covered with multilayer barrier film.

To study the effect of storage temperature and storage period (days) on biochemical and organoleptic changes and bacteriological growth (counts), a factorial design was used. There were two levels of storage temperatures (1-2^0 and 5-7^{0}C) and six (6) levels of storage periods (0, 1, 2, 3, 4, 5 and 6 days). Three replicates were performed for each experiment for a total of 42 samples/packages) and the standard error was calculated. All samples were stored in cold room at lower (1-2^{0}C) and upper (5-7^{0}C) chill temperatures. By mincing, the natural microflora of the meat were thoroughly mixed with sterile spatula.

2.1. Analytical Procedures

2.1.1. Crude Protein

Kjeldahl method of analysis (AOAC, 1990) was used to determine crude nitrogen, multiplied by 6.25 to obtain crude protein.

2.1.2. Total Volatile Nitrogen (TVN)

Total Volatile Nitrogen was determined by modified Lucke and Geidel macro distillation at atmospheric pressure (Pearson, 1975).

The TVN was released by boiling the flesh directly with magnesium oxide, which prevents volatile acids from distilling from the protein.

2.1.3. Amino acid

Amino acid was determined by formol potentiometric titration to pH 9.0 end point as specified by Pearson, (1975).

2.1.4. Degree of alkalinity and pH

Titrimetric method was used to determine the degree of alkalinity and pH of meat by the technique of Shelef and Jay (1970).

2.1.5. Total bacterial count (TBC)

Samples (10g) arising from each tray were aseptically weighed after mixing thoroughly with sterile spatula and blended with 40ml sterile ringer's solution for 2 minutes in a stomacher at room temperature. Decimal dilutions were spread in triplicate in nutrient agar, incubated at 35 ± 2^{0}C for 48h. Results were calculated as the means for 3 determinations.

3. Results

Table 1 reports the changes in crude protein, amino acid and total volatile nitrogen (TVN) during chill storage. Crude protein in beef stored at 1-2^{0}C for the first 4 days and at 5-7^{0}C for the first 3 days remained identical and constant being 19.7-19.8%. Crude protein increased from 19.7 at zero day to between 20.1 to 20.3% in 5 days at 1-2^{0}C and to between 20.1 to 21.1% in 4-5 days at 5-7^{0}C. Fresh beef with formol value (amino acids) 17.5 decreased gradually from 17.2 to 15.6 and from 17.1 to 16.2 at 1-2^{0}C and 5-7^{0}C respectively from day 1-day 6.

After consistent decrease in amino acid from day 1 to day 5, an increase in amino acid value on the 6th day in each storage environment was observed. Conversely TVN increased consistently in meat samples stored in both media. Rate of increase in TVN was apparently higher at 5-7^{0}C than at 1-2^{0}C. On the 4th day of storage at both storage temperatures their TVN values were about doubled the TVN value of fresh sample. During the last 2 days TVN rose to between 27.3 and 29.1 at 1-2^{0}C and between 34.3 and 39.8 mgN/100g protein at 5-7^{0}C. TVN values of 14.2-16.9 at 1-2^{0}C in 3 days and 15.1-17.5 at 5-7^{0}C in 2 days corresponded to periods in storage at which bacterial log number were 7.0 and 6.6 respectively.

Fig 1 shows the changes in pH levels, degrees of alkalinity and bacterial log number in meat stored under the two storage conditions. pH values from 5.4 in fresh state increased within narrow limits of 5.4-5.8 in meat stored for 5 days at 1-2^{0}C and 5.4-5.7 in meat stored for 3 days at 5-7^{0}C. Under the latter condition, pH has increased tremendously to between 6.1 – 6.9 as found between 4 and 6 days. Although the degrees of alkalinity were identical at both refrigeration temperatures they showed constant increase from day 1 to day 6. The bacteria log number of fresh beef was 5.5 per gram. Bacteria log number has increased to 5.6 and 6.0 per gram at 1-2^{0}C and 5.9 and 6.6 per gram at 5-7^{0}C within two days. Bacteria log number per gram and titration values showed a remarkable increase from the third day at both 1-2 and 5-7^{0}C.

Table 2 shows the changes in bacterial population and organoleptic signs in beef under storage condition with bacteria log of number of 5.6 and 5.9 per gram meat retained the bright red colour above these levels i.e. 6-6.6 Cfu/g beef colour has turned pale red but odourless. During 3rd and 4th day storage periods at 1-2^{0}C with bacteria log number 6.9 and 8.1 per gram and 7.7 per gram on 3rd day at 5-7^{0}C all samples have changed to dark red but remained odourless. On the 5th day at 1-2^{0}C and on the 4th day at 5-7^{0}C beef colour has turned brownish with about 8.6 per gram bacterial log number per gram and off odour. Bacteria log number of 9.2 and above at both storage conditions meat has turned dark brown (6th day at 1-2^{0}C and days 5th day at 5-7^{0}C) and became starky, slimy and putrid.

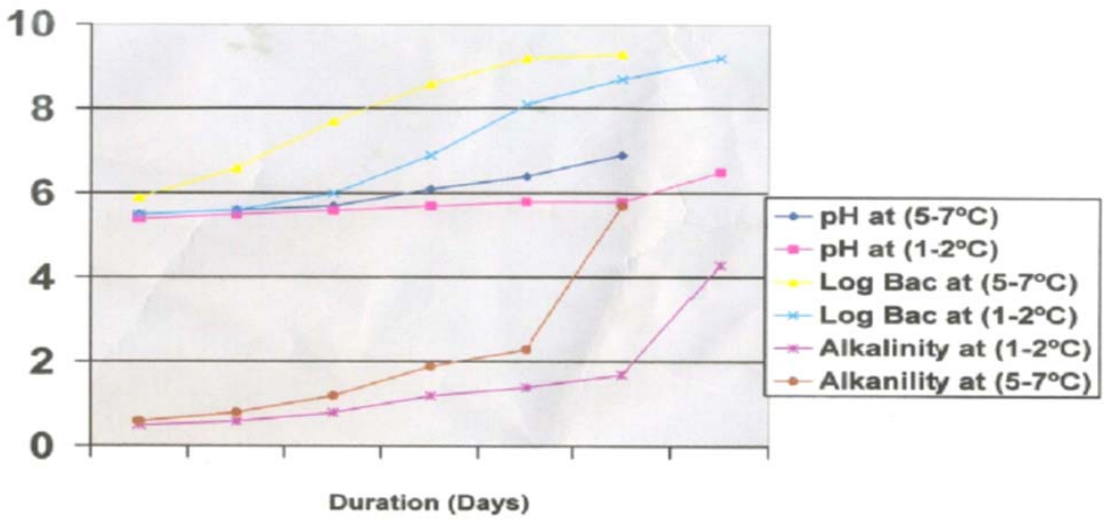

Figure 1: Changes in Bacteria log numbers, pH and Alkalinity (ml 0.1 Hcl /g Sample)

Table 1

Changes in crude protein amino acid and total volatile nitrogen during chill storage temperatures

Storage Temp.	Storage Time (days)	Crude Protein %	Amino acid ml o.IN NaoH	Total Volatile Nitrogen (TVN) mgN/100g Protein
Fresh	Zero	19.7 ± 0.8	17.5 ± 1.2	12.6 ± 0.1
1-2^{0}C	1	19.7 ± 0.8	17.2 ± 1.1	14.2 ± 0.2
"	2	19.7 ± 0.7	17.0 ± 0.2	16.4 ± 0.6
"	3	19.7 ± 0.7	16.2 ± 0.2	16.9 ± 0.5
"	4	19.8 ± 0.8	15.4 ± 0.1	23.8 ± 0.7
"	5	20.1 ± 0.9	15.0 ± 0.1	27.3 ± 0.7
"	6	20.3 ± 1.0	15.6 ± 0.3	29.1 ± 0.7
5-7^{0}C	1	19.7 ± 0.8	17.1 ± 1.2	15.1 ± 0.4
"	2	19.7 ± 0.7	16.4 ± 1.4	17.5 ± 0.6
"	3	19.8 ± 0.7	15.1 ± 1.5	20.9 ± 0.8
"	4	20.1 ± 0.9	14.4 ± 1.2	26.1 ± 1.0
"	5	20.6 ± 1.0	14.8 ± 0.8	34.3 ± 1.0
"	6	21.1 ± 1.1	16.2 ± 1.2	39.8 ± 1.1

Values are means ± of triplicate determinations

Table 2
Bacterial loads and subjective orgalonoleptic signs during chill storage

Storage temp. ^{0}C	Duration (days)	Bacterial log Nos	Colour	Slime growth	Smell
Fresh	Zero	5.5	Bright red	-	Odourless
1-2^{0}C	1	5.6	Bright red	-	"
	2	6.0	Pale-red -		"
	3	6.9	Dark red-		"
	4	8.1	Dark red-		Odourless
	5	8.7	Brown	-	Off odour
	6	9.2	Dark brown	Slimy	Putrid
5-7^{0}C	1	5.9	Bright red	-	Odourless
	2	6.6	Pale red -		Odourless
	3	7.7	Dark red	-	Odourless
	4	8.6	Brown	-	Off odour
	5	9.2	Dark brown	Slimy	Putrid
	6	9.3	Dark brown	Slimy	Putrid

Values are means of log numbers of bacterial

4. Discussion

The crude protein, 19.7% of meat as determined fresh from abbatoir and periodically verified frozen at -18^{0}C was constant. The crude protein value apparently remained constant for 4 and 3 days when stored at 1-2 and 5-7^{0}C respectively. The increase of 0.4-1.4% during these periods in storage as found in the two media is seemingly insignificant. This increase, however, may be due to synthesis of protein from non-protein nitrogenous substances by resident microorganisms in agreement with previous reports (Jay & Kontou, 1967; Ellis and Goodacre, 2001). The proliferating microorganisms in meat ecological niche at growth and death phase, being themselves proteinaceous, may also cause increase in crude protein in the spoiling meat. Further investigation is however needed to get this latter assertion established.

Amino acid concentration, decreasing gradually from fresh state of the meat to spoilt state at both storage temperatures is not accidental. This may be indicative of the metabolization of free amino acids by spoilage organisms resident in the spoiling meat (Dainty, 1985, Jay, 2000, Ellis and Goodcre, 2001, Labadie, 1999). The increased bacterial log no. as high as 9.0/g and the observed off-odour, slimeness and putrid stance resulting from free amino acid metabolization has been confirmed by previous reports (Ercolini *et al*., 2006, Jackson*, et al*., 1997, Huis in't Veld, Hilario *et al*., 2004).

The slight increase in amino acids on the 6th and 5th days at 1-2^{0}C and 5-7^{0}C respectively, may result from proteolysis of some kind by meat's microflora, particularly *Pseudomonas*, commonly implicated in the spoilage of beef at chill temperatures (Dainty *et al*., 1975, Ercolini *et al*., 2006).

The gradual but consistent rise in the degree of meat's alkalinity as storage and spoilage progressed may be due to production and accumulation of odoriferous nitrogenous compounds, most predominantly ammonia (Pearson and Muslemuddin, 1968, Standbridge, 1998, Dainty *et al*. 1985). Ammonia, determined as TVN, may be used as an index of meat quality under chill temperature according to the scheme of Pearson (1975) showing meat's fresh TVN to be 13 and its acceptable value to be ≤ 17. In this report it was evident that beef storage for 4 days at 1-2^{0}C and barely 3 days at 5-7^{0}C is acceptable for human consumption. However, in four days TVN values of 23.8 at 1-2^{0}C in 2 days and 20.9 with bacteria log nunmber 8.1/g and TVN 20.9 with bacteria log no 7.7/g are adjudged fit for human consumption being odourless, non-slimy and non-putrid.
All the parameters used to determine the wholesomeness of meat under chill conditions seem to have worked in consonance. The narrow limit within which pH changes occur makes pH measurement in spoiling meat restrictive (limiting). However, pH measure is useful for detecting proteolysis in spoiling meat when a sharp increase in post rigor pH is observed. Both TVN and degree of alkalinity accurately measure meat spoilage as they consistently increased as spoilage advanced and bacteria log number increased with increasing storage time.

Meat colour changes with passage of time in fresh state from bright red, through pale red to dark red during chill storage when the meat was odourless and still acceptable. With a change in colour to brown or dark brown, the meat has become slimy and putrid at high

bacterial log numbers of between 8.6-9.3 cfu/g. from this study it is obvious that the maximum holding period for minced beef to keep under chill conditions is about four days pending use in meat products.

5. Conclusion

Meat preservation by freezing or refrigeration coupled with good packaging materials, has proved to be of a greater advantage than other alternative preservation methods such as dry salting or wet curing. In dry salting or salt curing, the amounts of salt used depend upon the end product desires. High levels of salt in meat or meat products may be fraught with danger. High dietary salt content is linked with hypertension. Application of nitrites on meat has been widely acknowledged for their functionalities as retainer of meat's reddish colour and their bacteriostatic effect on *Clostridium botulinum*. Reactions of meat's amines with nitrites have been implicated in information of nitroso- compounds, a carcinogen due to uncontrolled application of nitrites. This work has, however, predicted the maximum period of time it takes minced meat, without additive, to spoil under chilled storage. This holding period will give a meat processor a relief from having to be passing through labour intensive processing on daily basis.

Correspondence to: Ighodaro O.M. Department of Biochemistry, Lead City University, Ibadan, Oyo State,

References

ANON, Ingredients in Processed Meat Product: Montana Meat Processors Convertion April 27-29, 2001. Basic Chemistry of Meat

AOAC. 1990 "Official Methods of Analysis (14th edn.) Association of Official Analytical Chemist, Washington, DC.

Body, A.L., 1996. Integrating aspect and modified atmosphere packaging to fulfil a vision of tomorrow. *Food Technol,* 50: 56-66

Borch, E. Kant-Muermans, M. L. Blixt, V. (1996) Bacterial spoilage of meat and cured product. *Int. J. Food Microbiol* 33: 103-120

Dainty, R.H., Edwards, R.A. and Hibbard, C.M. 1985. The Time Course of Volatile Compounds Formation during refrigerated storage of naturally contaminated beef in air. *J. Appl. Bacteriol.* 59, 303-309

Ellis, D.L., and Goodcre, R. (2001) Rapid and quantitative detection of the microbial spoilage of muscle foods: Current status and future trends. *Trends Food Sci. Technol*. 12: 414-424

4/21/2010

Ercolini, D. Russo, F., Torrieri, E. Masi P. and Villani, F. (2006). Changes in the spoilage-related microbiota of beef during refrigerated storage under different packaging conditions. *Appl. Environ. Microbiology. 4663-4671*

Hilario, F., Burkley, T. R. and Young, J.M. (2004), Improved resolution of the phylogenetic relationships among *Pseudomonas* by the combined analysis of atPD, CarA, recA and 16S rDNA. *Antone Leeuwenhoek* 86: 51-64

Huis in't Veld, J.H.J. 1996. Microbial and biochemical spoilage of foods an overview. *Int.J. Food Microbiol*. 33: 1-18

Ingram, M. and Dainty, R.H. (1971). Changes caused by microbes in spoilage of meats. *J. appl. Bact*. 34: 21-22

Jackson, T.C., Acuff, G.R. and Dickson, J.S. (1997). Meat, poultry, and seafood, p. 83-100. In M.P.Doyle and T.J. Beuchal (ed). Food microbiology: Fundamentals and frontiers. ASM Press, Washington, D.C.

Jay, J.M. (2000). Food preservation with modified atmospheres, p. 283-295. In D.R. Heldman (ed.), Modern food microbiology. Aspen Publishers, Inc. Gaithersburg, Md.

Jay, J.M., and Kontou, S.S. (1967). *Appl. Microbiol*. 15: 759-64

Koutsoumanis, K., Stamation, A., Skandamis, P. and Nychas J.G. (2006). Development of microbial model of temperature and pH on spoilage of ground beef and validation of the model under dynamic temperature conditions. *Appl. Environ. Microbiol*. 72: 124-134

Labadie, J.(1999). Consequences of packaging and bacterial growth. Meat is an ecological niche. *Meat Sci*. 52: 299-305

Nychas, G.J.E., Skandamis, P.N., Tassau, C.C., Koutscumanis, K.P. (2008) Meat spoilage during distribution, *Meat Sci*. 78: 77-87

Pearson, D. (1975). Laboratory Techniques Series. Laboratory Techniques pp. 169-172 in Food Analysis, London & Boston Butterworth

Pearson, D. and Muslemuddin. M. (1968). The accurate determination of total volatile nitrogen in meat and fish reprinted from *J. of Association of Public Analysts*, 6: 117-123.

Shelef, L.A. and Jay, J.M. (1970). Use of a titrimetric method to assess the bacterial spoilage of fresh beef. *Appl. Microbiol*. 19: 902-905

Standbridge, L.H. and Davies, A.R. (1998). The microbiology of chill-stored meat, p. 175-177. In A. Davies and R. Board (ed.), Microbiology of meat and poultry. Blackie Academic & professional, London, United Kingdom.

Connectance and Reliability Computation of Wireless Body Area Networks using Signal Flow Graphs

Ali Peiravi

DEPARTMENT OF ELECTRICAL ENGINEERING, SCHOOL OF ENGINEERING, FERDOWSI UNIVERSITY OF MASHHAD, MASHHAD, IRAN

ali_peiravi@yahoo.com

Abstract: Ambulatory monitoring and health care using wireless body area networks is an active area of applied research. In this study, a new method is presented to compute the connectance and reliability of wireless body area networks based on an improved approach to the topological analysis of the network's digraph using Mason's rule. The procedure outlined is simple and fast and may be used to compute quantitative measures of a wireless body area network's reliability. [Life Science Journal 2010;7(2):52-56]. (ISSN: 1097-8135).

Keywords: Connectance, reliability, wireless body area network, signal flow graph

Introduction

The general network topology used for wireless body area networks is the star topology with the sensor nodes sending their data to a central processing node for data processing and/or fusion. Reliability of these networks is very important since they deal with human life. Reported applications to date have had performance and reliability problems. In this paper, a novel approach to compute the connectance and reliability of wireless body area networks is proposed.

Wireless body area networks are distributed systems deployed on a patient's body with wireless connectivity. They are characterized by scarce energy and computation power of individual nodes. Sensing physical quantities on various locations in the body and sending the sensed information to a central node and then possibly to a remote place via a sink node
through wireless means are two primary jobs of a wireless body area network and are usually performed for remote patient monitoring and care. These jobs must be performed with a high level of reliability because in such applications major decisions regarding human life depend on the information received from the wireless body area network. A major characteristic of wireless body area networks is that the branches formed from the sensor nodes to the sink are usually unidirectional.

Wireless body area networks (WBANs) promise ambulatory health monitoring for extended periods of time and near real-time updates of patients' medical records through the Internet or intranet. Jovanov et al. (2006) presented a WBAN as shown in Figure 1 utilizing a common off-the-shelf wireless sensor platform with a ZigBee-compliant radio interface and an ultra low-power microcontroller. The standard platform interfaces to custom sensor boards that are equipped with accelerometers for motion monitoring and a bioamplifier for electrocardiogram or electromyogram monitoring. They used TinyOS operating system to develop the software modules for on-board processing, communication, and network synchronization.

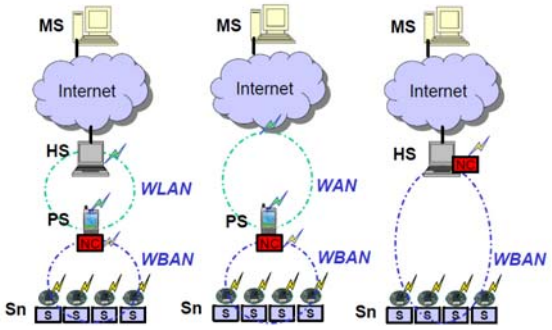

Figure 1. The Wireless Body Area Network (WBAN) for ambulatory monitoring adopted from Jovanov et al. (2006)

Motivation and Earlier Works

The main motivation of this study is to obtain the connectance and reliability of wireless body area networks. In order to compute these measures, one needs to establish an approach to quickly determine the tie-sets between the sensor nodes and the base station where the processing is done. The general trend in wireless body area networks is that the branches are directed with the flow of signals usually from the sensor nodes through the hubs and towards the base stations. Systems that result in undirected graphs can also be handled by the approach presented herein merely by replacing each undirected branch with a pair of oppositely directed branched. However, the typical sparsity of the connection matrix that makes the proposed approach so attractive would vanish in many such instances.

Much of the reported work on network reliability has made use of the minimal cutest of the underlying graphs. For example, one may cite the work of Hakimi (1983). However, that approach is restrictive since the critical elements of the network are not easily identified.

There have also been methods presented to compute reachability in social networks. Luce and Perry

(1949) applied matrix methods to the analysis of experimental data concerning group structure indicating relationships which can be depicted by line diagrams such as sociograms. They introduced the concepts of n-chain and clique, which have simple relationships to the powers of certain matrices. Using them it is possible to determine the group structure by methods which are both faster and more certain than less systematic methods.

Signal flow graphs were introduced by Mason (1953) to model the electrical behavior of amplifiers by introducing a topological structure with a set of algebraic linear equation. Later on Mason (1956) presented a topological formula for the solution of the equations. Coates (1959) extended this approach and presented the association of a linear graph called a flow graph with a set of linearly independent algebraic equations.

Desoer (1960) presented an independent derivation of the optimum formula for the gain of a flow graph by starting from the definition of a determinant and using a few of its elementary properties and reported on a simpler and independent derivation of Coates' important result.

Chen (1965) showed that a general network determinant and its cofactors can be evaluated by means of "directed trees" and "directed two-trees". He stressed that the products of such directed trees and directed two-trees will automatically give the correct signs. In case of passive networks that contain no magnetic coupling, the digraph associated with the node-admittance matrix reduces to the original network; the directed trees and directed two-trees reduce to ordinary trees and two-trees, respectively.

Interest in the reliability of wireless sensor networks has increased in recent years even though studies on the reliability of protocols used in WSN have a longer history. Bein et al. (2005) explored the reliability issues in multi-fusion sensor networks by presenting Markov models of the reliability using different types of sensors and spares that replace sensors when failed and compared these models in terms of reliability, cost and MTTF.

AboElFotoh et al. (2006) defined a reliability measure for wireless sensor networks that considers the aggregate flow of sensor data into a sink node (gateway or cluster head). Given an estimation of the data generation rate and the failure probability of each sensor, they formulated the reliability measure.

Purohit et al. (2008) addressed the issue of quantifying reliability for a wireless sensor network. They adopted the reliability block diagram approach and modeled the hardware and software modules of the wireless sensor network as a series-parallel structure. The drawback of their proposed approach is that software reliability estimation is quite different from hardware reliability estimation and cannot be treated the same way. Moreover, many of the modules which they model as independent components in series in the RBD are not actually so and may have some degree of dependency and redundancy.

Vasar et al. (2009) proposed Markov models for the reliability analysis of the wireless sensor networks with an emphasis on fault tolerant systems. They also presented a comparison between systems using dedicated replacements and universal replacements for defective nodes.

Peiravi (2009) proposed the RBD approach for the computation of the reliability of WBANs using existing databases such as manufacturer's data, the MIL-HDBK 217F or the NPRD and EPRD for estimates of the failure rates of the various parts that make up the network. In this paper, a new approach to computing connectance and reliability of wireless body area networks is proposed based on the earlier works of Mason (1956), Coates (1959), Desoer (1960) and Chen (1965) who developed signal flow graph based solutions of linear algebraic equations. The method is advanced further and is easy to use. It yields a fast method of computing the tie-sets in wireless body area networks that may be used to compute the reliability of WBAN's.

Signal Flow Graph Modeling of WBAN

There is an increasing interest in the application of Wireless Body Area Networks (WBANs) in recent years since they may be used to develop patient monitoring systems with flexibility and mobility for patients. The network topology that is generally used in wireless sensor networks for such ambulatory studies is of the star configuration [1].

Signal flow graphs were first introduced by Mason (1953), and were later modified by Coates (1959) to investigate the behavior of complex networks and control systems, particularly those involving feedback loops. The flow graph methodology is used in this study to devise some very useful connectivity properties of a digraph associated with a wireless body area network.

A wireless body area network may be modeled by a digraph G(N,B) with $n = |N|$ and $b = |B|$. To each node of a WBAN represented by a digraph G we assign a signal y_i. The branch from node i to node j is imbued with a transmission property. Let us call it a transmittance or connectance c_{ij}. The node signals y_i may be of an arbitrary nature and magnitude as long as the ratio of any two of them such as y_j / y_i has some physical or topological significance. If y_i exists at node i, and node i is connected to node j through a branch, then the presence of y_i is felt as a contribution $c_{ij} y_i$ to y_j at node j. This relationship does not in any way affect the originating signal y_j unless feedback is present that does not exist in wireless body area networks. Fig. 2 shows the concept of branch connectance and how the signals at the sensor nodes are transmitted through the branches to the upper level nodes.

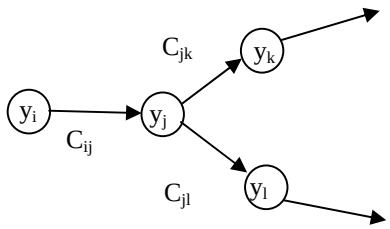

Fig 2. The concept of node to node connectance

If the connectances are assigned binary values of $c_{ij} = 0$ or $c_{ij} = 1$ depending on whether or not a branch exists that directly connects node i to j, then the graph can be thought of as a Boolean switching system. This representation is adequate when studying the connectivity and reliability properties of wireless sensor networks. In such cases, the absence of a direct branch between nodes i and j is indicated by the presence of a zero in place of c_{ij} in the graph's connection matrix.

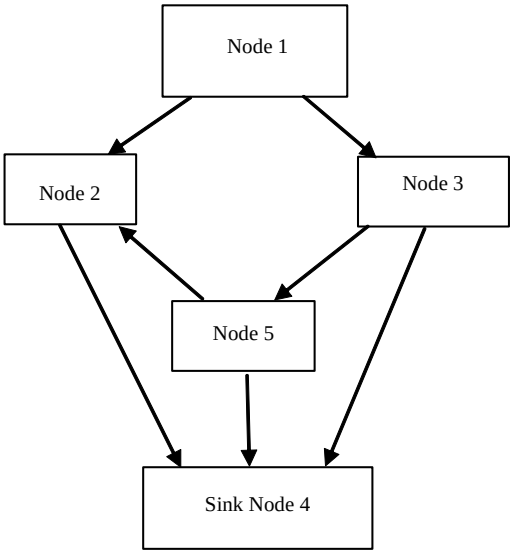

Fig 3 The schematic diagram of simple wireless body area network with node 2 as a cluster head and node

The signals at the nodes may be computed from (1) through (3) as follows:

$$y_j = c_{ij} y_i \quad (1)$$

$$y_k = c_{jk} y_j = c_{ij} c_{jk} y_i \quad (2)$$

$$y_l = c_{jl} y_j = c_{ij} c_{jl} y_i \quad (3)$$

We can find an equivalent connectance from node i to node k, or from node i to node l simply from (4) and (5):

$$y_k / y_i = c_{ij} c_{jk} \quad (4)$$

$$y_l / y_i = c_{ij} c_{jl} \quad (5)$$

The interconnections among the nodes of a wireless body area network may be represented by a connection matrix $C = [c_{ij}]$. The elements c_{ij} of the connection matrix represent the existence of a direct connection between nodes i and j. The value used for c_{ij} is usually taken to be either a zero implying no direct connections, or a 1 in case there is a connection. One may also assume other values for this parameter to indicate more sophisticated features of the link from i to j. For example, one may use $c_{ij} = R_{ij}$ to denote the reliability of the direct link connecting node i to node j, or $c_{ij} = f_{ij}$ to denote the capacity of the flow limit in the direct link from node i to node j.

For example, let us consider the simple wireless body area network shown in Fig. 3. The digraph for this network is shown in Fig. 4 with the connectances marked on the branches. The connection matrix C for this network may be written as (6):

$$C = \begin{bmatrix} 0 & C_{12} & C_{13} & 0 & 0 \\ 0 & 0 & C_{23} & C_{24} & 0 \\ 0 & 0 & 0 & C_{34} & C_{35} \\ 0 & 0 & 0 & 0 & 0 \\ 0 & C_{52} & 0 & C_{54} & 0 \end{bmatrix} \quad (6)$$

The fact that row 4 contains all zeros indicates that node 4 is a sink in this network. Similarly the zeros in column 1 indicate that node 1 is a purely source node and that it does not relay the data from other nodes.

Computing Tie-Set Connectances

Consider the digraph of a simple wireless body area network as shown in Fig. 3. By substituting the transmittance values of the branches of the WBAN in the connection matrix, we get the following matrix as (7):

$$C = \begin{bmatrix} 0 & A & B & 0 & 0 \\ 0 & 0 & C & D & 0 \\ 0 & 0 & 0 & E & H \\ 0 & 0 & 0 & 0 & 0 \\ 0 & F & 0 & G & 0 \end{bmatrix} \quad (7)$$

The signal flow graph equations for the wireless body area network shown in Fig 4 take the following form as (8):

$$\begin{aligned} y_2 &= Ay_1 + Fy_5 \\ y_3 &= By_1 + Cy_2 \\ y_4 &= Dy_2 + Ey_3 + Gy_5 \\ y_5 &= Hy_3 \end{aligned} \quad (8)$$

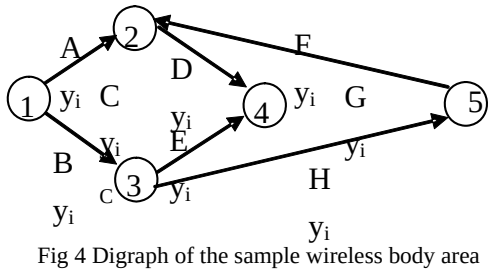

Fig 4 Digraph of the sample wireless body area network with node 4 as the sink

These equations can easily be ordered and rearranged as follows in (9):

$$\begin{aligned} -Ay_1 + y_2 - Fy_5 &= 0 \\ -By_1 + y_3 - Cy_2 &= 0 \\ -Dy_2 + y_4 - Gy_5 &= 0 \\ -Hy_3 + y_5 &= 0 \end{aligned} \qquad (9)$$

Among the five signals y_1, y_2, y_3, y_4, y_5 appearing in the four equations above, one is assumed to be given. Let it be y_1 for the moment and let us find the connectivity between node 1 and the rest of the nodes in the network. This may be found from the ratios y_2/y_1, y_3/y_1, y_4/y_1 and y_5/y_1. If any of these ratios is non-zero it indicates that the associated node is reachable from node 1. Thus we obtain full reachability information about the network. For non-zero ratios, the transmittance to the sink node is obtained which may also be used to find the tie-sets or path connectances.

Cramer's rule is proposed as a means of obtaining this information in this paper. The determinant of (9) may be computed as follows:

$$\det = \begin{vmatrix} +1 & 0 & 0 & -F \\ -C & +1 & 0 & 0 \\ -D & -E & +1 & -G \\ 0 & -H & 0 & +1 \end{vmatrix} = 1 - FCH \qquad (10)$$

The term $FCH = C_{52}C_{23}C_{35}$ in the determinant above represents a cyclic path from node 5, to node 2, to node 3 and then back to node 5 and should be assigned an equivalent connectance equal to zero.

Then we can compute the ratio y_2/y_1 as follows:

$$y_2/y_1 = \frac{1}{\det}\begin{vmatrix} +A & 0 & 0 & -F \\ +B & +1 & 0 & 0 \\ 0 & -E & +1 & -G \\ 0 & -H & 0 & +1 \end{vmatrix} = A + BHF \qquad (11)$$

Similarly one can obtain the tie set connectances from 3 to 1, 4 to 1 and 5 to 1 as follows:

$$\begin{aligned} y_3/y_1 &= B + AC \\ y_4/y_1 &= AD + BE = ACE + BHG = ACHG + BHFD \\ y_5/y_1 &= BH + ACH \end{aligned} \qquad (12)$$

It is noteworthy that the ratios above yield the equivalent connectances between the associated node pairs. Also, these connectances indicate all the path sets that exist. Using this simple procedure, one may find all the path sets between any pairs of nodes of a wireless body area network. Given the above information, one may easily use series-parallel rules of reliability to compute the pair-wise reliabilities of the WBAN. For example, the tie-set from node 1 to 2 is indicated as A+BHF. This means that the reliability of connection from node 1 to node 2 may be computed based on the equivalent RBD as shown in Fig. 5.

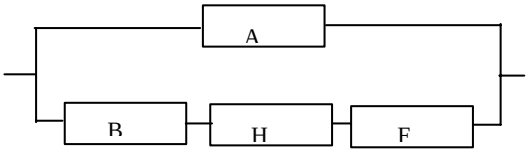

Fig 5 The equivalent reliability block diagram for

Given that we have now computed all the connectances in the network, we can compute R using the usual series-parallel rules of reliability calculations. For example, the reliability of having a connection between nodes 1 and 2 is as in (13):

$$R_{12}(t) = 1 - (1 - R_A(t))(1 - R_B(t)R_H(t)R_F(t)) \qquad (13)$$

The reliabilities of each component j may be computed using estimates of the component failure rates as mentioned before using (14)

$$R_j = e^{-\lambda_j t} \qquad (14)$$

All other pair-wise reliabilities may be computed in a similar fashion.

Conclusions

Although a lot of progress has been reported in the application of WBAN, a lot more work should be done in improving the performance and reliability of wireless body area networks used for health monitoring and care. In this paper, a simple and innovative approach for the calculation of the connectance and reliability of wireless body area networks is presented based on a modification of the signal flow graph methodology. The application of the approach to the digraph of a sample wireless body area network is presented to indicate the speed and efficiency of the proposed approach.

Acknowledgement

I would like to thank the Office of Vice Chancellor of Research and Technology of Ferdowsi University of Mashhad for the Grant Project No. 10448 dated 1388/10/2 to support the study that has resulted in the preparation of this article.

References

1 Peiravi, Ali, (2009), "Reliability of Wireless Body Area Networks used for Ambulatory Monitoring and Health Care,", Life Science Journal, Vol. 6, No. 4, pp. 5-14.

2 Jovanov, E.; Milenkovic, A.; Otto, C.; De Groen, P.; Johnson, B.; Warren, S.; Taibi, G. (2006), "A WBAN system for ambulatory monitoring of physical activity and health status: applications and challenges," 27th Annual International Conference of the Engineering in Medicine and Biology Society, 2005. IEEE-EMBS 2005. pp.3810-3813, 17-18 Jan. 2006.

3 Hakimi, S. L. (1983), "Computing the edge and vertex connectivities of graphs and digraphs," Proc. IEEE International Symposium on Circuits and Systems, pp.323-326.

4 Luce, R. D., Perry, A. D. (1949), "A method of matrix analysis of group structure," Psychometrika, vol. 14, no. 1, pp.95-116.

5 Mason, S. J. (1953), "Power gain in feedback amplifiers," Technical report no. 257, August 25, 1953, Research Laboratory of Electronics, MIT.

6 Coates, C. (1959), "Flow-graph solutions of linear algebraic equations," IRE Transactions on Circuit Theory, vol.6, no.2, pp. 170-187, Jun 1959. http://ieeexplore.ieee.org/stamp/stamp.jsp?arnumber=01086537.

7 Chen, W. K. (1965), "Topological analysis for active networks," IEEE Transactions Circuit Theory, vol.12, no.1, pp. 85-91, Mar 1965. http://ieeexplore.ieee.org/stamp/stamp.jsp?arnumber=1082396&isnumber=23385.

8 Desoer, C. A. (1960), "The optimum formula for the gain of a flow graph or a simple derivation of coates formula," Proc. of the IREE, pp.883-889.

9 AboElFotoh, H. M. F.; ElMallah, E. S.; Hassanein, H. S. (2006), "On the reliability of wireless sensor networks," Proceedings of the IEEE International Conference on Communications, 2006. ICC '06. , vol. 8, pp.3455-3460, June 2006. http://ieeexplore.ieee.org/stamp/stamp.jsp?arnumber=4025008&isnumber=4024985

10 Purohit, N.; Varadwaj, P.; Tokekar, S. (2008), "Reliability analysis of wireless sensor network," 16th IEEE International Conference on Networks,. ICON 2008, pp.1-6, 12-14 Dec. 2008. http://ieeexplore.ieee.org/stamp/stamp.jsp?arnumber=4772586&isnumber=4772559.

11 Bein, D., Jolly, V., Kumar, B., Latifi, S. (2005), "Reliability modeling in wireless sensor networks," International Journal of Information Technology, vol. 11 no. 2, pp.1-8.

12 Vasar, C., Prostean, O., Filip, I., Robu, R., Popescu, D. (2009), "Markov models for wireless sensor network reliability," Proceedings of IEEE ICCP'9, pp.323-328

4/28/2010

Role of Entophytic Microorganisms in Biocontrol of Plant Diseases

Wafaa M. Haggag

DEPARTMENT OF PLANT PATHOLOGY, NATIONAL RESEARCH CENTRE , CAIRO, EGYPT.

Wafaa_hagggag@yahoo.com

Abstract: Endophytic microorganisms are to be found in virtually every plant on earth. Endophytic microorganisms exist within the living tissues of most plant species and do so in a variety of relationships, ranging from symbiotic to slightly pathogenic. Root endophytic microorganisms are seen as promising alternatives to replace chemical pesticides and fertilizers in sustainable and organic agriculture systems. The capability of colonizing internal host tissues has made endophytes valuable for agriculture as a tool to improve crop performance. This association is often mutualistic: endophytes provide the plant with antagonism against diseases. Once inside the plant, an endophyte occupies a niche with relatively low competition from other microorganisms, provided the endophyte gets there first. Novel endophytes usually have associated with them novel secondary natural products and/or processes. Identifying, understanding and utilizing endophytes or its products to control of plant diseases and to enhance crop production are integral parts of sustainable agriculture. In this review, we addressed the major topics concerning the control of plant diseases by entophytic microorganisms mediated by specific metabolites of microbial origin. [Life Science Journal 2010;7(2):57-62]. (ISSN: 1097-8135).

Keywords: Biological control, Entophytic microorganisms, pathogens.

I. Introduction

Plant pathogens include fungi are the most visible threats to sustainable food production. Plant The decreasing efficacy of the fungicides as well as risks associated with fungicide residues on the leaves and fruit, have highlighted the need for a more effective and safer alternative control measures. In recent years, entophytes has received increasing attention as a promising supplement or alternative to chemical control. The strategic use of naturally occurring organisms to control pest populations and increase production of major crops represents a viable option to host-plant resistance and pesticide-based pest and pathogen control. Endophytic microorganisms, microorganisms that grow in the intercellular spaces of higher plants, are recognized as one of the most chemically promising groups of microorganisms in terms of diversity and pharmaceutical potential (Wagenaar and Clardy, 2001). Beneficial endophytic microorganisms comprise especially fungi and bacteria that colonize internal plant tissues without causing visible damage to their hosts (Petrini, 1991). Furthermore, the endophytic microorganisms are not considered as saprophytes since they are associated with living tissues, and may in some way contribute to the well being of the plant. Endophytes exist in a range of tissue types within a broad range of plants, colonizing the plant systemically with bacterial colonies and biofilms, residing latently in intercellular spaces, inside the vascular tissue or within cells (Ulrich *et al.* 2008). Endophytes, microorganisms that reside in the tissues of living plants, are relatively unstudied and potential sources of novel natural products for exploitation in agriculture. That is, the plant is thought to provide nutrients to the microbe, while the microbe may produce factors that protect the host plant from attack by animals, insects or microbes (Yang *et al.*, 1994). Studies on microorganisms from plant species are recently becoming more frequent, since these fungi and bacteria have been studied for biological control and production of compounds with pharmacological properties. They are different from phytopathogenic microorganisms because they are not detrimental, do not cause diseases to plants, and are distinct from epiphytic microorganisms which live on the surface of plant organs and tissues (Hallmann *et al.*, 1997). Endophytic bacteria are able to penetrate and become systemically disseminated in the host plant, actively colonizing the apoplast (Quadt-Hallmann *et al.*, 1997b), conducting vessels (Hallmann *et al.*, 1997), and occasionally the intracellular spaces (Quadt-Hallmann *et al.*, 1997a). This colonization presents an ecological niche, similar to that occupied by plant pathogens, and this endophytic bacteria can, therefore, act as biological control agents against pathogens (Hallmann *et al.*, 1997). In this sense, the suppression of plant diseases due to the action of endophytic microorganisms has been demonstrated in several pathosystems (Narisawa *et al.*, 1998). Several mechanisms may control this suppression, either directly on the pathogen inside the plant by antibiosis (Sturz *et al.*, 1998) and competition for nutrients (Mari *et al.*, 1996 and Puentea, *et al.*, 2009), or indirectly by induction of plant resistance response (M'Piga *et al.*, 1997) and more recently, their potential for enhanced degradation of several pollutants has also been investigated (Doty 2008). There are many reports demonstrating that many bioactive

compounds could be produced by endophytic microorganisms (Huang *et al*., 2001). At the same time, molecular markers provide gigantic sources of data that can assist scientists in developing tools to monitor the genetic and environmental fate of these agents.

In the present review we will focus on examples of associations between endophytic microorganisms and plants, especially those that result in diseases control. The intent of this review is to provide insights into the presence of endophytes in nature, the products that they make, and how some of these organisms are beginning to show some potential for control of plant pests and diseases .

1-What is an Endophyte?

The term endophyte refers to interior colonization of plants by bacterial or fungal microorganisms. Endophytic microorganisms, microorganisms that grow in the intercellular spaces of higher plants, are recognized as one of the most chemically promising groups of microorganisms in terms of diversity and pharmaceutical potential (Wagenaar and Clardy, 2001). Furthermore, the endophytic microorganisms are not considered as saprophytes since they are associated with living tissues, and may in some way contribute to the well being of the plant. It seems that other microbial forms, e.g., mycoplasmas and archaebacteria, most certainly exist in plants as endophytes, but no evidence for them has yet been presented. The most frequently isolated endophytes are the fungi. Endophytic bacteria colonize an ecological niche similar to that colonized by plant pathogens but do not cause damage to their hosts. It turns out that the vast majority of plants have not been studied for their endophytes. Thus, enormous opportunities exist for the recovery of novel fungal forms, taxa, and biotypes. Hawksworth and Rossman estimated there may be as many as 1 million different fungal species, yet only about 100,000 have been described (Hawksworth, 1991). As more evidence accumulates, estimates keep rising as to the actual number of fungal species. It seems obvious that endophytes are a rich and reliable source of genetic diversity and novel, undescribed species. The endophytes that we are most concerned with are the ones growing inside a turfgrass plant. Finally, in our experience, novel microbes usually have associated with them novel natural products. This fact alone helps eliminate the problems of dereplication in compound discovery.

2-Effects of entophytic microorganisms towards pathogens

Indeed, intensive work has shown that endophytic microorganisms can have the capacity to control pathogens (Duijff, *et al*., 1997 and Sturz, and Matheson. 1996), and nematodes (Hallmann *et al.*, 1998). The first record of an endophyte affecting a plant disease was that by Shimanuki (1987) who showed that timothy (*Phleum pratense*) plants infected with the choke fungus, *Epichloe typhina*, were resistant to the fungus *Cladosporium phlei*.

In some cases, they can also accelerate seedling emergence and promote plant establishment under adverse conditions and enhance plant growth and development (Lazarovits, and Nowak. 1997, and Pillay, and Nowak. 1997). Furthermore, several antagonistic entophytes bacterial species have been isolated from the xylem of lemon roots (*Citrus jambhiri*), including *Achromobacter* spp., *Acinetobacter baumannii*, *A. lwoffii*, *Alcaligenes-Moraxella* spp., *Alcaligenes* sp., *Arthrobacter* spp., *Bacillus* spp., *Burkholderia cepacia*, *Citrobacter freundii*, *Corynebacterium* spp., *Curtobacterium flaccumfaciens*, *Enterobacter cloacae*, *E. aerogenes*, *Methylobacterium extorquens*, *Pantoea agglomerans*, *Pseudomonas aeruginosa*, and *Pseudomonas* spp. against root pathogens (Araújo *et al*., 2001, and Lima *et al.*, 1994). Several bacterial endophytes have been reported to support growth and improve the health of plants (Hallmann *et al*., 1997, Stoltzfus *et al.*, 1998) and therefore may be important sources of biocontrol agents. *Erwinia carotovora*, for example, is inhibited by numerous endophytic bacteria, including several strains of *Pseudomonas* sp. ,*Curtobacterium luteum*, and *Pantoea agglomerans* (Sturz *et al.*, 1999). Furthermore, Wilhelm *et al*. (1997) demonstrated that *Bacillus subtilis* strains isolated from the xylem sap of healthy chestnut trees exhibit antifungal effects against *Cryphonectria parasitica* causing chestnut blight. Endophytic bacteria have the ability to promote growth and inhibit plant disease, and as they are in intimate contact with the plant they are an attractive choice as biological control agents. For example, Sturz *et al*. (1999) found that 61 of 192 endophytic bacterial isolates from potato stem tissues were effective biocontrol agents against *Clavibacter michiganensis* subsp. *sepedonicus*. In oak, endophytic bacteria biologically active against the oak wilt pathogen *Ceratocystis fagacearum* have been isolated (Brooks *et al.*, 1994). A number of the biologically active endophytes and root-colonizing microorganisms that have been isolated or detected belong to the actinobacterial phylum, specifically the genus *Streptomyces* (Coombs, and Franco. 2003, Sessitsch *et al*., 2001, Xaio *et al*., 2002). The first actinobacterial endophyte isolated, belonging to the genus *Frankia*, is a nitrogen-fixing actinobacterium that forms actinorhizae with eight families of angiosperms (Provorov *et al*., 2002). A number of endophytic actinobacteria were previously isolated by culture-dependent methods, with the major genera being *Streptomyces*, *Microbispora*, *Micromonospora*, and *Nocardioides* (Coombs and. Franco. 2003). A number of these isolates were capable of suppressing fungal pathogens of wheat in vitro and in planta, including *Rhizoctonia solani*, *Pythium* spp., and *Gaeumannomyces graminis* var *tritici*, indicating their potential use as biocontrol agents (Coombs *et al.*, 2003).

3-Mechanisms of diseases control displayed by endophytic

In this sense, the suppression of plant diseases due to the action of endophytic microorganisms has been demonstrated in several pathosystems (Narisawa *et al.,* 1998). Several mechanisms may control this suppression, either directly on the pathogen inside the plant by antibiosis and competition for nutrients , or indirectly by induction of plant resistance response (M'Piga *et al*., 1997). Endophytes usually occur in above-ground plant tissues, but also occasionally in roots (for example, dark septate endophytic fungi have been isolated from various plants), and are different from mycorrhizae by lacking external hyphae (Mandyam and Jumpponen, 2005 and Leho Tedersoo *et al*., 2009). Although some root endophytic fungus requires host cell death for proliferation during forming mutualistic symbiosis with plant (Deshmukh *et al.,* 2006), it is universally hypothe-sized that endophyte-host interactions involve a balance of antagonism and exhibit great phenotypic plasticity compared to plant pathogens (Schulz and Boyle, 2005). Only few documents refer to the plant secondary metabolism mediated by the fungal endophytes. Currently, endophytes are viewed as an outstanding source of bioactive natural products because there are so many of them occupying literally millions of unique biological niches (higher plants) growing in so many unusual environments. Thus, it appears that these biotypical factors can be important in plant selection, since they may govern the novelty and biological activity of the products associated with endophytic microbes. Peppermint growth and terpene production of *in vitro* generated plants (*Mentha piperita*) in response to inoculation with a leaf fungal endophyte indicate variation of the essential oil profile by fungal infection. The other study showed that the weight of roots, seedlings and terpenoid production of *Euphorbia pekinensis* increased after they were inoculated with an extensive host range endophytic *Phomopsis* sp. Meanwhile, microbial elicitor derived from some fungal endophytes also promotes biomass and induces the terpenoids (artemisinin) biosynthesis and production in plant suspension cells (Wang et al., 2006). It seems likely that both mycorrhizal fungi and fungal endophytes infection might result in specific-enhancement of the MEP pathway metabolic flux in plants. The red resin of *Dracaena cochinchinensis* is commonly used in traditional Chinese medicine for the treatment of traumatic and visceral hemorrhages. Chemical studies have revealed that the resin contains various flavonoids (Zheng *et al*., 2004). In addition, endophytic actinomycetes may also affect plant growth either by nutrient assimilation or enhanced secondary metabolites (anthocyanin) synthesis (Hasegawa *et al*., 2006). Furthermore, the production of antimicrobial substances, such as antibiotics or HCN, is an important mechanism to fight phytopathogens (Blumer, and Haas. 2000). Koshino *et al.* (1989) have described compounds, toxic to some fungi, which include sesquiterpenes, chokols, hydroxyl-unsaturated fats, phenolic glycerides and an aromatic sterol which are produced in the mycelial-choked heads of timothy. Endophytes effectively inhibits and kills certain other fungi and bacteria by producing a mixture of volatile compounds (Strobel *et al.,* 2001). The majority of these compounds have been identified by gas chromatography-mass spectrometry, synthesized or acquired, and then ultimately made into an artificial mixture. This mixture mimicked the antibiotic effects of the volatile compounds produced by the fungus. The newly described *Muscodor roseus* was twice obtained from tree species growing in the Northern Territory of Australia. This fungus is just as effective in causing inhibition and death of test microbes in the laboratory as *Muscodor albus* (Worapong *et al*., 2002). Another endophytic s*treptomycete* (NRRL 30566), from a fern-leaved *Grevillea* tree (*Grevillea pteridifolia*) growing in the Northern Territory of Australia, produces, in culture, novel antibiotics called kakadumycins (Castillo *et al.,* 2003). Each of these antibiotics contains, by virtue of their amino acid compositions, alanine, serine, and an unknown amino acid. Colletotric acid, a metabolite of *Colletotrichum gloeosporioides*, an endophytic fungus in *Artemisia mongolica*, displays antimicrobial activity against bacteria as well as against the fungus *Helminthsporium sativum* (Zou *et al*., 2000). Another *Colletotrichum* sp., isolated from *Artemisia annua*, produces bioactive metabolites that showed varied antimicrobial activity as well. Yue *et al.* (2000) have identified a number of compounds produced by cultures of *Epichloe* and *Neotyphodium* species that have antifungal activity against the chestnut blight fungus *Cryphonectria parasitica* and suggest that they may play a similar role against other pathogens, the compounds in this study which showed the greatest antifungal activity were the indole derivatives indole-3-acetic acid and indole-3-ethanol, a sesquiterpene and a diacetamide. Indirect disease control is achieved by mechanisms modulating the plant immune response, including the induction of systemic acquired resistance (van Wees *et al.* 1999).

4-Genetic and environmental modifications influencing diseases control by endophytes

Identification of endophytes has relied mainly upon cultivation-based methods (Bell *et al*., 1995). Molecular techniques based on the rRNA gene as a phylogenetic marker (Amann *et al.,* 1995) provide a powerful approach to circumvent drawbacks related to cultivation . Molecular markers provide the means to assess genetic variation in endophytes and host plants, providing an insight into the relationship between variation in endophyte and host plants and the variability of agronomic traits (Gamper *et al*., 2008). Researchers have endeavored to elucidate the molecular mechanisms during the establishment of plant-endophytic association (Bailey *et al.,* 2006). Techniques such as terminal restriction fragment length polymorphism (T-RFLP) analysis or denaturing gradient gel electrophoresis (Smalla, *et al*., 2001) in combination with sequence analysis of rRNA genes allow rapid characterization of microbial communities. Comparison with data from amplified fragment length polymorphism

(AFLP) data demonstrated that the SSR markers are informative for assessing genetic variation within and between endophyte species. Following the development of these markers for the sensitive detection of endophytes *in planta*, the assessment of endophyte diversity in a globally-distributed pool of perennial ryegrass germplasm are reported. Recently, Garbeva *et al.* (2001) monitored endophytic populations of potato by PCR-denaturing gradient gel electrophoresis, which revealed the occurrence of a range of organisms falling into several distinct phylogenetic groups. Their results also suggested the presence of nonculturable endophytes in potato.

II. Conclusion

Endophytes are a poorly investigated group of microorganisms that represent an abundant and dependable source of bioactive and chemically novel compounds with potential for exploitation in a wide variety of medical, agricultural, and industrial arenas. The mechanisms through which endophytes exist and respond to their surroundings must be better understood in order to be more predictive about which higher plants to seek, study, and spend time isolating microfloral components. This may facilitate the product discovery processes. The results presented in this review show that, as expected, great diversity has been found among endophytes isolated from plant hosts. They play important roles for protecting plants against diseases. Certainly, one of the major problems facing the future of endophyte biology and natural-product discovery is the rapid diminishment of rainforests, which hold the greatest possible resource for acquiring novel microorganisms and their products. The role of endophyes protecting plants against diseases has been quite well studied. However, Countries need to establish information bases of their biodiversity and at the same time begin to make national collections of microorganisms that live in these areas.

Referances

1. Amann, R. I., W. Ludwig, and K. H. Schleifer. 1995. Phylogenetic identification and in situ detection of individual microbial cells without cultivation. Microbiol. Rev. 59:143-169.
2. Araújo, W. L., H. O. Saridakis, P. A. V. Barroso, C. I. Aguilar-Vildoso, and J. L. Azevedo. 2001. Variability and interactions between endophytic bacteria and fungi isolated from leaf tissues of citrus rootstocks. Can. J. Microbiol. 47:229-236.
3. Bailey, B.A., Bae, H., Strem, M.D., Robert, D.P., Thomas, S.E., Crozier, J., Samuels, G.J., Choi, I.k.-Young, Holmes, K.A. 2006. Fungal and plant gene expression during the colonization of cacao seedlings by endophytic isolates of four *Trichoderma* species. Planta. 224: 1449–1464.
4. Bell, C. R., G. A. Dickie, W. L. G. Harvey, and J. W. Y. F. Chan. 1995. Endophytic bacteria in grapevine. Can. J. Microbiol. 41:46-53.
5. Blumer, C., and D. Haas. 2000. Mechanism, regulation, and ecological role of bacterial cyanide biosynthesis. Arch. Microbiol. 173:170-177.
6. Brooks, D. S., C. F. Gonzalez, D. N. Appel, and T. J. Filer. 1994. Evaluation of endophytic bacteria as potential biological control agents for oak wilt. Biol. Control 4:373-381.
7. Castillo, U., J. K. Harper, G. A. Strobel, J. Sears, K. Alesi, E. Ford, J. Lin, M. Hunter, M. Maranta, H. Ge, D. Yaver, J. B. Jensen, H. Porter, R. Robison, D. Millar, W. M. Hess, M. Condron, and D. Teplow. 2003. Kakadumycins, novel antibiotics from Streptomyces sp. NRRL 30566, an endophyte of Grevillea pteridifolia. FEMS Lett. 224:183-190.
8. Coombs, J. T., and C. M. M. Franco. 2003. Isolation and identification of actinobacteria isolated from surface-sterilized wheat roots. Appl. Environ. Microbiol. 69:5303-5308.
9. Coombs, J. T., P. P. Michelsen, and C. M. M. Franco. 2003. Evaluation of endophytic actinobacteria as antagonists of *Gaeumannomyces graminis var. tritici* in wheat. Biol. Control 29:359-366.
10. Deshmukh, S., Hückelhoven, R., Schäfer, P., Imani, J., Sharma, M., l. Weiss, M., Waller, F., Kogel, K.H. 2006. The root endophytic fungus *Piriformos-pora indica* requires host cell death for proliferation during mutualistic symbiosis with barley. Proc. Natl. Acad. Sci. 103: 18450–18457.
11. Doty S.L. 2008. Tansley review: enhancing phytoremediation through the use of transgenics and endophytes. New Phytol 179:318–333
12. Duijff, B. J., V. Gianinazzi-Pearsonand, and P. Lemanceau. 1997. Involvement of the outer membrane lipopolysaccharides in the endophytic colonization of tomato roots by biocontrol *Pseudomonas fluorescens* strain WCS417r. New Phytol. 135:325-334.
13. Hallmann, J., A. Quadt-Hallmann, R. Rodríguez-Kábana, and J. W. Kloepper. 1998. Interactions between *Meloidogyne incognita* and endophytic bacteria in cotton and cucumber. Soil Biol. Biochem. 30:925-937.
14. Hallmann, J., A. Quadt-Hallmann, W. F. Mahaffee, and J. W. Kloepper. 1997. Bacterial endophytes in agricultural crops. Can. J. Microbiol. 43:895-914.
15. Hasegawa, S., Meguro, A., Shimizu, M., Nishimura ,T., Kunoh, H. 2006. Endophytic actinomycetes and their interactions with host plants. Actinomycetologica. 20: 72–81.
16. Hawkswo, D.L. 1991. The fungal dimension of biodiversity: magnitude, significance, and conservation. Mycol. Res., 95, s. 641-655.
17. Huang Y., Wang J., L.I. G., Zheng Z., Su W. 2001. Antitumor and antifungal activities in endophytic fungi isolated from pharmaceutical plants Taxus mairei, Cephalotaxus fortunei and Torreya grandis. FEMS Immunol. Med. Microbiol., 34, s. 163-167.

18. Gamper H.A., Young J.P.W., Jones D.L., Hodge A. 2008. Real-time PCR and microscopy: are the two methods measuring the same unit of arbuscular mycorrhizal fungal abundance?. *Fungal Genetics and Biology* 45: 581–596.
19. Garbeva, P., L. S. van Overbeek, J. W. L. van Vuurde, and J. D. van Elsas. 2001. Analysis of endophytic bacterial communities of potato by plating and denaturing gradient gel electrophoresis (DGGE) of 16S rDNA based PCR fragments. Microb. Ecol. 41:369-383.
20. Koshino, H., Yoshihara, T. , Sakamura, Y. , Shimanuki, S., Sato, T. and Tajimi. A. 1989. A ring B aromatic sterol from stromata of*Epichloe typhina*.Phytochemistry 28:771-772
21. Leho Tedersoo, Pärtel, K., Jairus, T., Gates, G., Põldmaa, K. and Tamm , H. .2209. Ascomycetes associated wit ectomycorrhizas: molecular diversity and ecology with particular reference to the *Helotiales* Environmental Microbiology .11(12), 3166–3178
22. Lazarovits, G., and J. Nowak. 1997. Rhizobacteria for improvement of plant growth and establishment. Hortscience 32:188-192.
23. Lima, G., A. Ippolito, F. Nigro, and M. Salerno. 1994. Attempts in the biological control of citrus mal secco (*Phoma tracheiphila*) using endophytic bacteria. Dif. Piante 17:43-49.
24. M'piga, P., Bélanger, R.R., Paulitz, T.C. and Benhamou, N. 1997. Increased resistance to *Fusarium oxysporum* f. sp. *radicis-lycopersici* in tomato plants treated with the endophytic bacterium *Pseudomonas fluorescens* strain 63-28. Physiological and Molecular Plant Pathology, v.50, p.301-320.\
25. Narisawa, K., Tokumasu, S.and Hashiba, T. 1998. Suppression of clubroot formation in chinese cabbage by the root endophytic fungus, *Heteroconium chaetospira*. Plant Pathology, v.47, p.206-210.
26. Pillay, V. J., and J. Nowak. 1997. Inoculum density, temperature and genotype effects on in vitro growth promotion and epiphytic and endophytic colonization of tomato (*Lycopersicum esculentum* L.) seedlings inoculated with a pseudomonad bacterium. Can. J. Microbiol. 43:354-361.
27. Provorov, N. A., A. Y. Borisov, and I. A. Tikhonovich. 2002. Developmental genetics and evolution of symbiotic structures in nitrogen-fixing nodules and arbuscular mycorrhiza. J. Theor. Biol. 214:215-232.
28. Puentea, M., Ching Y. Li b,1, Yoav Bashana,C. 2009. Endophytic bacteria in cacti seeds can improve the development of cactus Seedlings. Environmental and Experimental Botany 66 (2009) 402–408
29. Schulz ,B., Boyle, C. 2005. The endophytic continuum.Mycol. Res. 109: 661–686.
30. Sherameti, I., Shahollari ,B., Venus, Y., Altschmied, L., Varma, A., Oelmuller, R. 2005. The endophytic fungus *Piriformospora indica* stimulates the expression of nitrate reductase and the starch-degrading enzyme glucan-water dikinase in tobacco and *Arabidopsis* roots through a homeodomain transcription factor that binds to a conserved motif in their promoters. J. Biol. Chem. 280: 26241–26247.
31. Shimanuki, T. 1987. Studies on the mechanisms of the infection of timothy with purple spot disease caused by *Cladosporium* (Gregory) de Vries. *In* Res. Bull. 148 Hokkaido Natl. Agric. Exp. Sta. pp 1-56.
32. Smalla, K., G. Wieland, A. Buchner, A. Zock, J. Parzy, S. Kaiser, N. Roskot, H. Heuer, and G. Berg. 2001. Bulk and rhizosphere soil bacterial communities studied by denaturing gradient gel electrophoresis: plant-dependent enrichment and seasonal shifts revealed. Appl. Environ. Microbiol. 67:4742-4751.
33. Strobel, G. A., Dirksie, E., Sears, J. and. Markworth, C. 2001. Volatile antimicrobials from a novel endophytic fungus. Microbiology 147:2943-2950
34. Sturz, A. V., and Matheson. B. G. 1996. Populations of endophytic bacteria which influence host-resistance to *Erwinia*-induced bacterial soft rot in potato tubers. Plant Soil 184:265-271.
35. Sessitsch, A., B. Reiter, U. Pfeifer, and E. Wilhelm. 2001. Cultivation-independent population analysis of bacterial endophytes in three potato varieties based on eubacterial and Actinomycetes-specific PCR of 16S rRNA genes. FEMS Microbiol. Ecol. 1305:1-10.
36. Stoltzfus, J. R., R. So, P. P. Malarvithi, J. K. Ladha, and F. J. de Bruijn. 1998. Isolation of endophytic bacteria from rice and assessment of their potential for supplying rice with biologically fixed nitrogen. Plant Soil 194:25-36.
37. Sturz, A. V., B. R. Christie, B. G. Matheson, W. J. Arsenault, and N. A. Buchanan. 1999. Endophytic bacterial communities in the periderm of potato tubers and their potential to improve resistance to soil-borne plant pathogens. Plant Pathol. 48:360-369.
38. Ulrich, K., Ulrich A. and Ewald, D. 2008 . Diversity of endophytic bacterial communities in poplar grown under field conditions. FEMS Microbiol Ecol 63:169–180
39. Worapong, J., G. A. Strobel, B. Daisy, U. Castillo, G. Baird, and W. M. Hess. 2002. *Muscodor roseus* anna. nov. an endophyte from *Grevillea pteridifolia*. Mycotaxon 81:463-475.
40. van Wees, S. C., M. Luijendijk, I. Smoorenburg, L. C. van Loon, and C. M. Pieterse. 1999. Rhizobacteria-mediated induced systemic resistance (ISR) in *Arabidopsis* is not associated with a direct effect on expression of known defense-related genes but stimulates the expression of the jasmonate-inducible gene *Atvsp* upon challenge. Plant Mol. Biol. 41:537-549.
41. Wagenaar, M.M.and Clardy, J. 2001. Dicerandrols, new antibiotics and cytotoxic dimmers produced by the fungus *Phomopsis longicolla* isolated from an endangered mint. J. Nat. Prod., 64, s. 1006-1009.
42. Wang, J.W., Zheng, L.P.and Tan, R.X. 2006. The Preparation of an elicitor from a fungal endophyte to

enhance artemisinin production in hairy root Cultures of *Artemisia annua* L. Chin. J. Biotechnol. 22: 829–834.

43. Wilhelm, E., W. Arthofer, and Schafleitner, R. 1997. *Bacillus subtilis*, an endophyte of chestnut (*Castanea sativa*), as antagonist against chestnut blight (*Cryphonectria parasitica*), p. 331-337. *In* A. C. Cassells (ed.), Pathogen and microbial contamination management in micropropagation. Kluwer Academic Publishers, Dortrecht, The Netherlands.
44. Xaio, K., L. L. Kinkel, and D. A. Samac. (2002). Biological control of *Phytophthora* root rots on alfalfa and soybean with *Streptomyces*. Biol. Control 23:285-295.
45. Yang, X., Strobel, G., Stierle, A., Hess, W.M., Lee, J. and Clardy, J. 1994. A fungal endophyte-tree relationship: Phoma sp. in Taxus wallachiana. Plant Sci., 102, , s. 1-9.
46. Yue, Q., Miller, C. J. ,White, J. F. and Richardson. M. D. 2000. Isolation and characterization of fungal inhibitors from *Epichloe festucae*. J. Agric. Food Chem. 48:4687-4692.
47. Zheng, Q.A., Li, H.Z., Zhang, Y.J., Yang, C.R. (2004). Flavonoids from the resin of *Dracaena cochinchinensis*. Helvetica Chim. Acta.87: 1167–1171.
48. Zou, W. X., J. C. Meng, H. Lu, G. X. Chen, G. X. Shi, T. Y. Zhang, and R. X. Tan. 2000. Metabolites of *Colletotrichum gloeosporioides*, an endophytic fungus in *Artemisia mongolica*. J. Nat. Prod. 63:1529-1530.

4/25/2010

Prognostic Value of Active Movement of Hemiplegic Upper Limb in Acute Ischemic Stroke

Bo Song, Shuo Li, Yuan Gao, Yuming Xu*

DEPARTMENT OF NEUROLOGY, THE FIRST AFFILIATED HOSPITAL, ZHENGZHOU UNIVERSITY, ZHENGZHOU, 450052, CHINA

Xuyuming@zzu.edu.cn

Abstract-Background and Purpose: The purpose of this study is to assess the prognostic value of active movement of affected upper limb on daily life in patients after acute ischemic stroke onset. Method: 165 consecutive patients with arm plegia in acute ischemic stroke were evaluated by four bedside tests to evaluate active movement of plegic arm (active finger extension, active finger flexion, shoulder abduction and shoulder shrug) on admission, day 14 and 30. Activity of daily life was assessed by Barthel Index on month 3, 6 and 12 after stroke onset. Result: Score of finger flexion and extension on day 30 was associated with 3 month and 12 month prognosis after stroke onset, and the expectation rate declined from 6.022 at 3 month to 2.919 at 12 month. Total score of four tests was associated with medium-term (6 month) prognosis (p=0.000). Conclusion: Active movement of hemiplegic upper limb in acute ischemic stroke has good predictive value on activity of daily life. [Life Science Journal 2010;7(2):63-66]. (ISSN: 1097-8135).

Key words: ischemic stroke; prognosis; rehabilitation

Introduction

The incidence of first-ever stroke in China ranged from 116 to 219 per 100 000 per year, and the prevalence varies from 259.86 per 100 000 to 719 per 100 000, most of stroke subtype is ischemic stroke.[1, 2,3].

Kwakkel G [4] suggested that 30%~66% of ischemic stroke patients had impaired active movement of affected upper limb after onset. Active movement of hemiplegic upper limb, especially find hand use, was directly associated with daily life activity in patients[5]. Therefore, recovery of function of the paretic arm is one of the main concerns of patients after stroke. Katrak[6,7] showed that preservation of proximal movements (shoulder adduction and shrug) after stroke was an early predictor of arm recovery. Nicola S et al[8] indicated that active finger extension was a reliable early predictor of recovery of arm function in patients with stroke. In Welmer's study[9], moderate to good correlations between fine hand use and self-care (Barthel Index), were observed from the first week to 18 month after stroke onset, although the strength of the correlations decreased from 0.69 to 0.54.

Published studies suggested good predictivity of active movement of hemiplegic upper limb on prognosis, however, these experiments had some limits, such as small sample size (less than 100 patients) and little attention on prognosis of daily life activity, et al. We did investigation on prognostic value of active movement of hemiplegic upper limb in patients with acute ischemic stroke in China.

Materials and Methods

Acute schemic stroke patients were enrolled consecutively for from August, 2007 to April, 2008 in neurology department in the first affiliated hospital of Zhengzhou University. Inclusion criteria and Exclusion criteria as follows:

Inclusion criteria:(1) ischemic stroke;(2) admission within 7 days after onset; (3)muscle strength of proximal or distal end of affected arm < 3 degree; (4)first stroke or another with full recovery from previous ones; (5)intact active movement of affected upper limb before stroke onset.

Exclusion criteria: (1) hemorrhagic stroke.; (2) some factors of this stroke would affected to judge the extent of paralysis upper limb: such as disturbance of consciousness, limb apraxia, self-neglect and sensory aphasia and so on; (3) some other factors which would affected to judge the extent of paralysis upper limb: such

as osteopathy, rheumatism and mental diseases and so on; (4) refused to participate in this study.

Patients were assessed for active movement of affected upper limb on admission, day 14 and 30. The evaluation protocol included 4 potential predictors of arm recovery from Fugl-Meyer arm subset score scale, including shoulder shrug, shoulder abduction, active finger flexion, and active finger extention (score of each test ranged from 0 to 2: 0 totally unable, 1 incompletely, 2 fully accomplish tasks without any hesitation). Prognosis of daily life activity was quantified by Barthel Index (BI score: 0 to 100) on 3, 6 and 12 month after stroke onset by telephone follow-up. BI >60 was defined as good outcome, and BI ≤60 as poor outcome.

In performing statistical analysis, we did single factor analysis in the frist step, i.e., Mann-Whitney test. We hypothesized that the single factor might associate with prognosis when it met the significance leve at $p<0.05$, Then we selected those factors with positive results in single factor analysis to put into logistic regression analysis. Data were analyzed using the SPSS statistical package, 15.0 version.

Results

165 patients which met the criteria were enrolled consecutively. During the study, we observed 19 drop-outs, including 11 deaths. The others were completed 3 months, 6 months and 1 year follow-up .

Single factor analysis: Mann-Whitney test: Mann-Whitney test was performed to assess the correlation between active movement of plegic upper limb and prognosis on activity of daily life. To specify active movement of affected upper limb, we categorized it into proximal score (shoulder shrug + shoulder abduction), distal score (active finger flexion + active finger extension), total score (proximal score + distal score). The positive results were shown in Table 1.

Table1. Single factor analysis: association between active movements of plegic upper limb and prognosis (Mann-Whitney Test)

	BI (3 months)				BI (6 months)				BI(12 months)			
	>60	≤60	z	P	>60	≤60	z	P	>60	≤60	z	P
NIHSS	97	61	-6.57	0.00	102	49	-5.49	0.00	104	42	-4.25	0.00
Total score On admission	98	61	-5.02	0.00	103	49	-4.29	0.00	105	42	-3.54	0.00
Total score day 14	98	61	-6.33	0.00	103	48	-4.83	0.00	105	41	-4.05	0.00
Total score Day 30	98	59	-7.94	0.00	103	47	-6.52	0.00	105	40	-5.06	0.00
Proximal score On admission	98	61	-4.62	0.00	103	49	-3.26	0.00	105	42	-2.34	0.02
Proximal score day 14	98	61	-5.75	0.00	103	48	-4.83	0.00	105	41	-3.19	0.00
Proximal score day 30	98	59	-7.04	0.00	103	47	-5.45	0.00	105	40	-3.92	0.00
Distal score On admission	98	61	-4.13	0.00	103	49	-3.91	0.00	105	42	-3.08	0.00
Distal score Day 14	98	60	-5.07	0.00	103	48	-4.26	0.00	105	41	-4.00	0.00
Distal score Day 30	98	59	-7.05	0.00	103	47	-6.16	0.00	105	40	-5.17	0.00

Logistic regression analysis: prognosis (Barthel Index) at 3, 6 and 12 month was set as independent variables respectively, and factors associated with prognosis at each time point as dependent variables. All above variables were put into logistic regression analysis as illustrated in Table2. It is drawn from the table that distal active movement (active finger flexion + active finger extension) of plegic upper limb on day 30 was associated with prognosis on 3 months (p=0.000) and 12 months (p=0.000) after stroke onset; The expectation rate declined from 6.022 on 3 months to 2.919 on 12 months; total score (shoulder shrug + shoulder abduction + finger flexion + finger extension) on day 30 was correlated with activity of daily life on 6 months (p=0.000).

Table 2. multiple factors analysis: active movements of plegic upper limb and prognosis (Logsic regression analysis)

	BI	B	Wald	Sig.	Exp(B)	95.0% C.I
Distal socre Day 30	3M	1.795	17.057	0.000*	6.022	2.569-14.119

	12M	1.071	13.499	0.000*	2.919	1.648-5.170
Constant	3M	5.610	10.586	0.001	273.069	
	12M	-0.280	0.831	0.362	0.756	
Total score Day 30	6M	0.730	15.824	0.000*	2.074	1.448-2.976
Constant	6M	1.039	1.458	0.227	2.827	

*p<0.05, sig.=p.

Discussion

The present study, focusing on predictable value of active movement of hemiplegic upper limb on activity of daily life (issued by Barthel index) after stroke onset, was first implemented in Han population in China. The study suggested that active movement of affected upper limb in acute ischemic stroke, especially active distal movement, predict good prognosis in short-, medium- and long-term prognosis on activity of daily life. The probable reason lie in capability of active distal movement of affected arm could help patients manage tasks on Barthel index , such as eating and dressing.

Our observation was in accordance with Smania[8] and Welmers'[9] views: Smania proposed that active distal movement could better predict early recovery of affected arm than proximal movement; while Welmer indicated that fine hand use in acute stroke was positively associated with self-care (Barthel index) on prognosis in short- and long-term run.

The present study also indicates that the strength of association between active finger movement and activity of daily life declined with time, expectation rate declined from 6.022 at 3 month to 2.919 at 12 month. This may be explained as follows: 1. the active movement of affected arm could be further recovered after acute phase; 2.patients took time to learn to use unaffected arm to perform those tasks in Barthel index, and this could compensate their inability in affected arm in daily use. It was also discussed in Welmer and Feyss'[10] researches.

There is no correlation between active proximal movement of affected arm and activity of daily life in the present study. In contrast, Katrak [7,8] showed that proximal movement, i.e. shoulder shrug and shoulder abduction, was a reliable predictor for arm recovery. However, Katrak focused on ability of active movement of plegic upper limb when evaluating prognosis, while we use Barthel index to evaluate prognosis of activity of daily life. Barthel index consists of many tasks requiring active distal movement to manage instead of proximal use, which might explain the negative result in the present study.

According to the present study, neurologists may use four simple bedside tests to evaluate active movement of hemiplegic upper arm in patients with acute ischemic stroke. It could not only help doctors to predict prognosis of patients on activity of daily life, but also ease the anxiety of patients and encourage them to better devote themselves to rehabilitation.

Conclusion

Active movement of hemiplegic upper limb in acute ischemic stroke, especially distal active movement, has promising prognostic value on activity of daily life.

References

1. National 8.5 CVD collaborative Group. Community comprehensive preventive study on cardial and cerebral vascular diseases. *Chin J Prevent Med* 1998; **32** (suppl)**:** 3–4.

2. Shi FL, Hart RG, Sherman DG, Tegeler CH. Stroke in the People's Republic of China. Stroke. 1989; 20: 1581–85.

3. Liu M, Wu B, Wang WZ, et al.Stroke in China: epidemiology, prevention, and management strategies. Lancet Neurol. 2007; 6(5): 456-64.

4. Kwakkel G, Kollen B, Wagenaar R. Therapy impact on functional recovery in stroke rehabilitation: a critical review of the literature. Physiotherapy. 1999; 13:4 57– 470.

5 Sharma N, Pomeroy VM, Baron JC. Motor imagery: A backdoor to the motor system after stroke? Stroke. 2006, 37 (7):1941-1952.

6 6 Katrak P， Bowring G，Conroy P et al.Predicting upper limb recovery after stroke the place of early shoulder and hand movement[J].Arch Phys Med Rehabil, 1998, 79(7):758-761.

7 Katrak PH. Shoulder shrug--a prognostic sign for recovery of hand movement after stroke. Med J Aust 1990;152(6):297-301.

8 Nicola S, Stefano P, Michele T et al. Active Finger Extension: A Simple Movement Predicting Recovery of Arm Function in Patients With Acute Stroke[J]. Stroke 2007;38;1088-1090.

9 Welmer AK, Holmqvist LW, Sommerfeld DK. Limited Fine Hand Use After Stroke And Its Association With Other Disabilities. J Rehabil Med. 2008; 40(8): 603-608.

10 Feys HM, De Weerdt WJ, Selz BE et al. Effect of a Therapeutic Intervention for the Hemiplegic Upper Limb in the Acute Phase After Stroke : A Single-Blind, Rando mized, Controlled Multicenter Trial[J]. Stroke 1998; 29; 785-792.

4/1/2010

Surgical treatment of esophageal cancer after subtotal gastrectomy

Pan Xue [1], Li Xiang-nan [2]

[1]The Nursing College of Zhengzhou University, Zhengzhou, Henan 450052, China.
[2]The First Affiliated Hospital of Zhengzhou University, Zhengzhou, Henan 450052, China.
lxn-2000@163.com

Abstract: OBJECTIVE: To reconstruct the digestive tract using the remaining stomach and part of the colon for the esophageal cancer after subtotal gastrectomy to investigate the surgical treatment and long-term survival. **METHODS:** 20 patients presenting with esophageal carcinoma after gastrectomy were analyzed retrospectively. Left postero-lateral thoracotomy incision was used in patients with esophageal cancer in the middle but not close to aortic arch and patients with lower thoracic segment. The digestive tract was reconstructed by the remaining stomach. Right postero-lateral thoracotomy, upper abdominal and left neck incisions were used in patients with upper thoracic segment lesions and esophageal cancer in the middle but close to aortic arch. Transverse and descending colon were used for the digestive tract reconstruction. **RESULTS:** All cases had successful operation and no serious postoperative complications, no death. **CONCLUSIONS:** Residual stomach and colon can be used for reconstruction of digestive tract, the key lies in the choice of appropriate surgical methods for different patients. [Life Science Journal 2010;7(2):67-68]. (ISSN: 1097-8135).

Key words: subtotal gastrectomy; esophageal cancer

Introduction

Surgery is still the first choice for the esophageal cancer after subtotal gastrectomy, but how to rebuild the digestive tract is very important. In our department, 20 patients presenting with esophageal carcinoma after gastrectomy between 2002 and 2008 were analyzed retrospectively. We reconstruct the digestive tract using the the remaining stomach and part of the colon to investigate the surgical treatment and long-term survival .

Clinical data:

This study included a total of 20 patients, male 15 cases and female 5 cases, the average age of 60 (52 to 76) years old, the incidence of gastric ulcer in 16 cases, four cases can not clear the history of the disease. Preoperative gastroscopy confirmed that subtotal gastrectomy with the stomach being reconstructed in a Billroth-II fashion. The interval between gastrectomy and the diagnosis of esophageal carcinoma ranged from 8 to 18 years. Among them, there are ten cases of esophageal cancer at the middle part of esophagus, six cases at the lower part of esophagus, four cases at the upper part of esophagus.All cases were confirmed by both the upper gastrointestinal imaging and fiber gastroscopy. Pathological results is squamous cell carcinoma.

Methods:

Among these 20 cases, left postero-lateral thoracotomy incision was used in six patients with esophageal cancer in the middle but not close to aortic arch and six with lower thoracic segment. The procedure involved surgical exploration of the tumer, whether it can be removed and then abdominal exploration. Include free and ligation of left gastric artery, protecting left gastroepiploic artery and short gastric artery for blood supply of residual stomach, transplanting the remaining stomach with spleen and caudal portion of pancreas into the left thorax and reconstruct the digestive tract using the the remaining stomach. In two patients, Billroth II reconstruction was changed to Roux-Y fashion just because of remnant terminal of duodenum is too short to make esophageal-residual stomach anastomosis.The other cases, four had upper thoracic segment lesions and six patients with esophageal cancer in the middle but close to aortic arch, which were resected and reconstructed by transverse and descending colon transplantation into the neck. Right postero-lateral thoracotomy, upper abdominal and left neck incisions were used.The procedure involved right postero-lateral thoracotomy incision, surgical exploration of the tumer , whether it can be removed; upper abdominal incisions , surgical exploration of abdominal adhesions, the original operation and whether colonic vascular anomalies, careful protecting the colon and relevant left colic artery branches; left neck incisions, tumor resection, making esophageal-colon anastomosis after sternum.

Results:

All cases had successful operation and no serious postoperative complications, no death.16 cases were at follow-up examination and four cases out of touch.1-year survival rate was 16/16, 3-year Survival rate was 10 / 16, 5-year survival rate was 4 / 10 cases.

Discussion:

The incidence of esophageal carcinoma after gastrectomy is relatively low. If the tumor is resectable , surgery is the first choice .The difficulty that faces us is replacement organs to reconstruct digestive tract, the material selected should be long enough and reliable blood supply to ensure no anastomotic leakage. Traditional methods of surgery treatment are to reconstruct the digestive tract using colon and the jejunum with vascular pedicle. Some others use the residual stomach. We believe that all methods are feasible.The key is ① Rigorous

preoperative examination as upper gastrointestinal radiography, gastroscope inspection and CT scan. They are useful to know the surgery way of subtotal gastrectomy and the size of the residual stomach. ②We determined whether residual stomach is long enough to reconstruct the digestive tract with tumor location and height of the patient. ③All patients are with gastrointestinal preparations .In one word, sufficient preoperative preparation, careful operation and intensive postoperative care necessary.

Our experience has shown that the reconstruction of digestive tract using the residual stomach should be preferred when esophageal cancer are located in the middle and lower thoracic segment and the anastomosis will be inferior to the arch of aorta..Lesions were removed through left thoracotomy, spleen and pancreatic tail were dissected and transposed into thorax. The advantages of this method include ① the surgical procedure is simple: one incision and one anastomosis ②short operative time and faster recovery. Whether the residual stomach has reliable blood supply and enough length is the key. Right gastroepiploic artery and right gastric artery were ligated in subtotal gastrectomy. Blood supply of the residual stomach relied on left gastro-epiploic artery, short gastric arteries and left gastric artery.When residual stomach was fully mobilized for anastomosis with the esophagus, short gastric artery and left gastro-epiploic artery were just reserved .Our Experience has proven that these two arteries will be available for the residual stomach and esophageal-residual stomach anastomosis will be not affected. Billroth II reconstruction should be changed to Roux-Y fashion when remnant terminal of duodenum is too short to make esophageal-residual stomach anastomosis. Spleen and caudal portion of pancreas will be fixed in the left thorax, so as to avoid anastomotic tension by gravity, but it is also a related impact for breathing disorders.

The reconstruction of digestive tract using transverse and descending colon should be preferred in patients with carcinoma at the upper part of esophagus or middle part of esophagus but close to aortic arch. Right postero-lateral thoracotomy, upper abdominal and left neck incisions were used. Our experience has shown ① no anastomosis in the chest, little influence of heart and lung, little postoperative complications. ② transverse and descending colon is long enough to alleviate tension of anastomosis. Low anastomotic leak rate ③ gastroesophageal reflux, choking and aspiration pneumonia decrease because of peristalsis of colon.On the other hand, weak points are three incision, the relatively long time and more invasive procedure.

In short, residual stomach and colon can be used for reconstruction of digestive tract, the key lies in the choice of appropriate surgical methods for different patients.

5/1/2010

References:

1. Doki Y, Okada K, Miyata H. Long-term and short-term evaluation of esophageal reconstruction using the colon or the jejunum in esophageal cancer patients after gastrectomy. Dis Esophagus. 2008;21(2):132-8
2. Hashimoto N, Inayama M, Fujishima M.Esophageal cancer after distal gastrectomy. Dis Esophagus.2006;19(5):346-9
3. Dionigi G, Dionigi R, Rovera F.Reconstruction after esophagectomy in patients with partial gastric resection. Case report and review of the literature of the use of remnant stomach. Int Semin Surg Oncol. 2006 Apr 26;3:10
4. Cheng BC, Xia J, Shao K.Surgical treatment for upper or middle esophageal carcinoma occurring after gastrectomy: a study of 52 cases.Dis Esophagus. 2005;18(4):239-45
5. Dabrowski A, Zinkiewicz K, Szumilo J. Unusual clinical course of metachronous melanomas of the upper digestive system. World J Gastroenterol. 2005 Apr 14;11(14):2197-9.
6. Chen YP, Yang JS, Liu DT. Long-term effect on carcinoma of esophagus of distal subtotal gastrectomy. World J Gastroenterol. 2004 Mar 1;10(5):626-9.
7. Chen QQ, Chen YC.Application of jejunum with vascular pedicle in reconstruction of the digestive tract. Di Yi Jun Yi Da Xue Xue Bao. 2004 Feb;24(2):238-9.

Assemblage structure of stream fishes in the Kumaon Himalaya of Uttarakhand State, India

Ram Krishan Negi[1] and Tarana Negi[2]
1Department of Zoology & Environmental Sciences, Gurukula Kangri University, Hardwar U.K. India 249404
2Department of Zoology, Govt. P.G. College, Panchkula (HR)
Email: negi_gkv@rediffmail.com

Abstract: The fish assemblage structure was analyzed in the streams of Kumaon Himalaya of Uttarkhand State, India. Seven sites were sampled by using different fishing gears during Jan, 2007 to December 2008. The physical features like stream habitat, stream classifications, fish assemblage at different sites, habitat preference and riparian vegetations were registered for each site. In the present investigations a total of ten species belonging to three orders and four families were recorded, of which the cyprinides were the most dominant group at all the sites. According to Shannon Weaver diversity index the pool habitat support maximum fish diversity ('H' 0.164-0.292). [Life Science Journal 2010;7(2):69-74]. (ISSN: 1097-8135).

Key words: Classification, cyprinids, fish diversity, substrate, preference

1. Introduction

The highly complex functional and structural elements of running water are largely based on the system-inherent, dynamic genesis and development of those systems. Because of the very intricate interpretations with surrounding environments, running waters are among the most distinctive landscape elements. Especially in alluvial river floodplain systems, the high spatio-temporal heterogeneity and, therefore, the great diversity of complex habitat and ecotones in successional stages, represent key features. The diverse environment support species-rich fish communities that contribute to the overall high biodiversity of rivers/streams ecosystems (Schiemer & Waidbacher, 1992, Ward & Stanford, 1995a).

Importance of habitat is a major concern to fishery biologist. A common use of fish habitat indicates the physical and chemical characteristics of the environment, excluding biological attributed. Habitats for fish is place or for migratory fishes, a set place in which a fish population or fish assemblage can find the physical and chemical features needed for life, such as suitable water quality, migration routes, spawning grounds, feeding sites, resting sites and shelter from enemies and adverse weather. Habitat features have been identified as major determinants in the distribution and abundance of fishes from earlier times (Shelford, 1911) and later individual fish species as well as entire assemblage were studied for the patterns of North America (Baker and Ross, 1981). Fish species diversity is correlated with habitat complexity (Gorman & Karr, 1978; Schlosser, 1982) depth, flow and substrate types. The influence of these habitats attributes on the structure and function of fish assemblage in the streams has been studied in detailed at different latitudes (Mathew and Hill, 1980; Leveque, 1997). Extensive studies on freshwater fishes in India are available, but most of them are concern with taxonomy (Menon, 1992, Jayaram, 1999). Studies on fish assemblage structure and their requirements in Indian streams are lacking, though few initiatives started in the 1980's in south India (Arunachalam *et al*., 1997a), SriLanka streams (Wickramanayake, 1990); Western Himalaya (Johal *et al*., 2002 and Kumaon Himalaya (Negi *et al*., 2007). The present study aims to describe the habitat structure, and its availability to fish assemblage, as well as habitat use and habitat suitability preference in seven streams of Kumaon Himalayas of Uttarakhand State, India.

2. Study area

Kumaon Himalaya lying the latitudes 28^0 44' and 30^0 49' and longitude 78^0 45' and 81^0 1' E is situated at the disjunction of Nepal, Tibet and India in the state of Uttarakhand. A natural water divide separates it from Tibet, the Kali river defines its eastern border with Nepal, High transverse mountain spurs, separate it from Chamoli and Pauri district of Garhwal and the southern limit of the Tarai belt demarcates its southern boundary. Geographically Kumaon has the four longitudinal physiographic subdivisions namely the outer Himalaya with Tarai and Bhabar belt and Shivalik ranges, the lesser Himalayas and the Trans-Himalaya Tethyes domain of Bhotland. Seven study sites were selected for the present study. These sites varied in altitude from 800 msl to 1098 msl and varied geomorphologic characters, substrate and ecological conditions.

3. Material and methods

The parameters like water source, channel materials, dominant habitat type and stream type were taken into consideration for the Kumaon Himalayan streams. The geographic location i.e. longitude, latitude and altitude were determined with the help of Magellan Trailblazer XL GPS system. The habitat type and substrate material were classified after Armantrout (1999). The stream under report were classified following the works of Rosgen (1996).

Stream classification

This classification is based on morphological arrangement of stream characters like entrenchment ratio, width/depth ratio and channel material in the various landforms at level 1 and 2.This is only broad level delineation of stream types. Entrenchment ratio has been considered primary criteria for the present stream classification. Whereas, water shed features, channel features, sediment sources, riparian vegetations and large wood debris were estimated on the spot by stream reach characterization field data sheet. Water temperature, air temperature and water velocity were measure on the spot as per standard methods APHA (1998)

Fish collection

The fishes were caught at each sites with the help of cast net, gill net, drag nets, scoop nets. Samples were carried out for ten times in each habitat on a fixed day every month from Jan. 2007 to December, 2008. The represented specimens were identified upto species level in the laboratory using standard references of Jayaram (1999).

3. Results

Fish diversity

A total of ten species belonging to three orders namely cypriniformes , Mastacembelis ,and perciformes were recorded during the present investigation Table 1. Of these cypriniformes comprises the dominant group represented by 8 species belonging to 7 genera. *Tor putitora*, *Garra gotyla gotyla*, *Barilius bendelisis* were the most abundant fishes in all the study sites. Higher species richness were recorded from Kosi, Saigad and Suyal streams respectively with an altitude range of 1027 to 1398msl and lower values were recorded from the altitude range 860 to 1120msl. This is chiefly because of the severity of anthropogenic activities in the form of extraction of boulders, cobbles from streams habitat in lower altitude leading to decrease in fish assemblage whereas, at higher altitude have greater species richness.

Habitat preference

In total 345 cyprinids fishes were recorded in pool, pool edges, run and edges of riffles. The cascade was least preferred habitat by majority of fishes. The maximum fish diversity was reported in pool habitat H' 0.845 followed by run H' 0.764 and riffle H'0.196 at Kosi stream Table 2. In Saigad stream, it was H' 0.760 in pool, H' 0.590 in run, H' 0.244 in riffle, In Suyal stream it was H' 0.464 in pool, H' 0.461 in run and H' 0.292 in riffle, in Busal stream, it was H'0.423 in pool and H' 0.292 in run, in Garur ganga stream it was H' 0.457 in pool, H' 0.386 in run and H' 0.210 in riffle, in Gagas stream, it was H' 0.581 in pool, H'0.196 in run and H'0.275 in riffle, whereas, it was H' 0.594 in pool, H' 0.454 in run and H' 0.164 in riffle at Gomti stream. In Garur ganga stream, *Tor putitora*, *Barilius bendelisis* and *Schizothorax* preferred deep and shallow pools, while, was found in the shallow pools with low velocity, whereas,*Garra gotyla gotyla* preferred shallow pool with low to medium velocity. In Gomti stream,*Tor putitora* and *Barilius bendelisis* and *Barilius barla* preferred shallow pools with medium velocity.

Fish species richness vs altitude

At level 1, the altitude had been considered as primary criteria for differentiating the streams. High correlation coefficient was observed between altitude r= 0.71. The high altitude site >1000m, had higher FSR (5-10) as compared to lower altitude site<1000m.i.e. Gomti stream which had lower FSR (5). This is because of anthropogenic activities occurring in lower altitude as compared to higher altitude. The relative abundance also inverse relation with altitude. At level 2, the streams were further delineated according to the source of water glacial or spring fed. In the present study streams under report were spring fed and had fish species richness (3-10 and H' 0.778-1.694).

Stream substrate

In Kosi stream, the dominant stream substrate were big boulders, small boulders, and cobbles in Saigad stream, small boulders and cobbles, in the Suyal stream, bed rock, big boulders edge and small boulders were prevalent. In Garur ganga streams, big boulders, bed rock edge and gravel, in the Gagas streams, small stream. Small boulders, cobbles and pebbles, and in Gomti stream, substrate was dominated by big boulders, small boulders and cobbles Table 3. The streams having cobbles as dominant bed materials along with small boulders lead to formation of a more variable types of habitat leading to the greater species richness (5-10).

Stream classification

There was a great variation in channel width almost all selected streams. The minimum cannel width was recorded as (6.3 m) at Busal stream and maximum as (37.53 m) at Gomti stream. Maximum depth was recorded at Suyal (0.76 m) and minimum at Busal stream (0.25 m). The depth width ratio was recorded maximum 63.46 at Kosi stream and minimum 16.93 at Garur ganga stream Table 3. In the present study, entrenchment ratio was considered as primary criteria for the classification of streams. On the basis of entrenchment ratio all the streams has been classified as type 'B' streams with entrenchment ratio range from 1.46- 2.31. The width/depth ratio was very high in the streams of Kosi, Saigad, Gomti, whereas, rest of streams have moderate width/depth ratio.

Stream channel features

The channel features were found to be unstable at Kosi, Saigad, Garur Ganga and Gomti streams, whereas, they were moderately stable in Busal and Gagas streams. The proportion of stream reach morphology type was dominated by riffle, deep pools and runs at Kosi; shallow pools and run at Saigad and

Busal; deep pools, run and riffle at Suyal and riffle , run and cascade at Garur ganga; riffle, run and shallow pools at Gagas; run and riffles at Saryu and riffles and pools at Gomti streams. The local hydrological alterations in the form of channelization of water flow were more prominent in Kosi, Busal, Garur ganga and Saryu streams, leading to the formation of large side pools at different pockets of the streams reaches, which were responsible for sedimentation in the streams. The riparian vegetation was fragmentary with herbs, shrubs and trees at Kosi, Suyal Gagas and Gomti streams. Aquatic vegetation was mainly dominated by attach algae in most of the study sites. All the streams under reports were reported alkaline in nature.

Table 1. Fish species recorded from streams of Kumaun Himalaya of Uttarakhand State, India.

	Kosi	Saigad	Suyal	Busal	Garurganga	Gagas	Gomti
Order:Cypriniformes							
Family:Cyprinidae							
Genus: Tor							
Tor putitora	++	+	+	-	+	+	+
Genus:Barilius							
Barilius bendelisis	++	++	++	++	++	++	++
Barilius barila	+	+	+	-	-	-	+
Genus:Puntius							
Puntius conchonius	+	+	-	-	-	-	-
Genus:Garra							
Garra gotyla gotyla	++	++	++	++	++	++	++
Genus:Chrosochelus							
Chrosochelus latius	+	-	-	-	-	+	-
Genus:Schizothorax							
Schizothorax richardsonii	+	+	+	-	+	+	+
Genus:Nemachelius							
Nemachelius montanus	+	+	+	-	-	+	-
Order:Mastacembeliformes							
Family: Mastacembelidae							
Genus: Mastacembelus Mastacembelus armatus	+	+	+	+	+	+	-
Order: Ophiocephaliformes							
Family:Ophiocephalidae							
Genus: Channa							
Channa punctatus	+	+	-	-	-	-	-

++: Dominant; +Abundant; -: Not recorded

Table 2. Physical characteristic and channel morphology in the streams of Kumaun Hamalaya of Uttrakhand State, India.

Name Of Stream	Stream Width(m)	Stream Depth (m)	Entren-chment ratio	Habitat	Substrate	Longitude	latitude	Altitude	Water velocity	Riparian Vegetation

Kosi	16.5	0.26	2.12	Deep pools, Riffles, Runs	Big boulders	79^{0}30'22.9"E	29^{0}46'55.3"N	1381	0.9	Fragmentary, trees and shrub, Minimum encroachment in stream
Saigad	15.0	0.30	1.6	Shallow pool Runs	Cobbles, Pebbles, Sand	79^{0}36'03.2"E	29^{0}46'51.6"N	1398	0.43	Trees, shrubs, grasses, Moderate encroachment
Suyal	19.5	0.76	1.74	Deep pool, Cascade, Riffles	Dominant bed rock, Large boulders, Cobbles	79^{0}36'44.9"E	29^{0}33'21.5"N	1027	0.22	Shrub dominant, Fragmentary, Minimum encroachment
Busal	6.3	0.25	2.03	Runs, Pools	Cobbles, Pebbles	79^{0}36'59.9"E	29^{0}53'47.0"N	1122	0.39	Trees, shrubs, continuous, moderate encroachment
Garur ganga	8.3	0.49	2.31	Riffles, Cascade, Pool	Big boulders, Bed rock edge, gravels	79^{0}37'01.9"E	29^{0}53'49.2"N	1120	0.70	Shrubs, grasses dominant, Fragmentary
Gagas	7.8	0.36	2.05	Riffles, Runs, Shallow Pools	Cobbles, Small boulders	79^{0}27'28.2"E	29^{0}41'32.9"N	1061	0.51	Tress, shrubs, grasses, Fragmentary Minimum encroachment
Gomti	37.5	0.70	1.46	Runs, Riffles, pools	Big and small boulders	79^{0}46'10.9"E	29^{0}50'11.1"N	860	0.58	Trees, shrubs dominant, grasses, continuous, minimum encroachment

Table 3. Fish species diversity indices (Shannon and Weaver species Diversity) (H'), relative abundance and species richness in the streams of Kumaun Himalaya of Uttarakhand State, India.

Shannon and Weaver	(H')	(H')	(H')		
Streams	Pool	Riffle	Run	Relative Abundance	Species Richness
Kosi	0.845	0.196	0.764	11.62	10
Saigad	0.760	0.244	0.590	12.50	9
Suyal	0.464	0.292	0.461	13.20	7
Busal	0.423	--	0.292	4.91	3
Garur Ganga	0.457	0.210	0.386	8.33	5
Gagas	0.581	0.275	0.196	9.80	5
Gomti	0.594	0.164	0.454	8.62	5

4. Discussions

From the above observations it is clear that water depth and water velocity are the two major factors for the distribution of fish species in the different habitats. Similar observations were made by Gorman and Karr (1978); Arunachalam (2000); Johal *et al*. (2002)and Negi *et al*.(2007). Harvey and Stewart (1991) reported that minnows survives longer in pools. The large numbers of small fishes becomes increasingly restricted to stream margins, because the mid stream reaches are fast or too deep or both (Bains et al., 1988).

Most of the fishes in the small streams are habitat generalists (Horowitz, 1978). Other studies have also indicated a substantial overlap in the habitat utilizations in the cyprinid fishes communities. (Barker and Ross, 1981; Schlosser, 1987a). The studies on the Western Ghats fishes assemblage structure (Arunachalm, 2000) and other parts of the world (Finger, 1982; Schlosser, 1982; Bains *et al*. 1988 and Schlosser 1987a) also reported that the diverse group of small fishes are found to be primarily restricted to habitat that are shallow in depth and slow in current velocity and are concentrated along the stream margin in pools and riffles. Scot and Hall (1997) have stated that fish assemblage as indicator of environmental degradation in Maryland coastal plain streams. The relationship between habitat diversity and fish communities has been analyzed by Gorman and Karr (1978) in temperate area in which they include the diversity of current, depth and substrate, which determines the riverian fish communities. Several studies have supported this generalization for fish communities (Schlosser and Toth, 1984; Aadland, 1993; Mathew *et al.* 1994; Arunachalam, 2000). Physical gradients from unstable shallow to deep, stable pool areas with stream fishes are common in temperate latitudes (Sheldon, 1968. Arunachalam, 2000) reported that non cyprinids such as Balitorids occur mostly in pool edges and cyprinids in big pools with varied habitat heterogeneity. Similar results were observed during the resent investigations having the diverse group of small fish species is restricted primarily to habitat which are shallow in depth and slow in water current velocity, which are the areas along stream margins in rifles and pools. In the Kumaun region of Wester Himalayas, small *Puntius* spp are confined to shallow low flow area and juveniles of big sized *Tor putitora* and *Schizothorax* used the shallow areas with the speed velocity of riffles and riffles-pool transition especially in Suyal stream. Stream assemblages dominated by short lived, rapidly maturing water column fishes generally show greater variability corresponding to environmental fluctuations, such as documented by Grossman et al (1982) and Ross et al (1987).

Acknowledgements: The authors are thankful to University Grants Commission, New Delhi for financial assistance under UGC-SAP NO. F.3-9/2004 (SAP-11).

Corresponding Author:

Dr Ram Krishan Negi

Department of Zoology & Environmental Sciences,

Gurukula Kangri University, Hardwar, UK India 249404

negi_gkv@rediffmail.com

References

1. Aadland LP. Stream habitat type: Their fish assemblages and relationship to flow. North American Journal of Fisheries Management 1993; 13: 790-06.
2. APHA. Standared method for the examination of water and wasteland. 20th edition. Am.Public Health Assoc. Washington D.C. 1998.
3. Armantrout NB. Glossary of aquatic habitat inventory technology. American Fisheries Society. 1999; 150 pp.
4. Arunachalam, M. Assemblage structure of stream fishes in the Western Ghats (India). Hydrobiologia. 2000; 430: 1-31.
5. Arunachalam M, Johnson JA, Sankarnarayanan A Fish diversity in rivers of Northern Karnataka. Int. J. Ecol. Envir. Sci. 1997a; 23: 327-33.
6. Baker JA. Ross ST. Spatial and temporal resource utilization by south eastern cyprinids. Copiea 1981; 178-89.
7. Finger TR. Fish community habitat relations in central New York stream. J. Freshwat. Ecol. 1982; 1: 343-52.
8. Gorman OT, Karr JR. Habitat structure and sream fish communities.Ecology 1978; 59:507-15.
9. Grossman GD, Moyle PB, Whittaker JO Jr. Stochasticity in structural and functional characteristics of an Indian stream fish assemblage a test of community theory. Am. Nat. 1982; 120:423-53.
10. Harvey BC, Stewart AJ. Fish size and habitat depth relationship in a headwater stream. Oecologia 1991; 87:336-342.
11. Horowitz RJ. Temporal variability patterns and the distributional patterns of stream fish. Ecological monogr. 1978; 48:307-21.
12. Jayaram KC. The freshwater fishes of the Indian region. Narendra Publishing House. Delhi 1999; pp 551.
1. 13. Johal MS, Tandon KK, Tyor AK and Rawal YK. 2002. Fish diversity in different habitats in the streams of lower, middle Western Himalayas. Pol .J. Ecol. 50(1):45-56.
13. Leveque C. Biodiversity dynamics and conservation, the freshwater fish tropical Africa. Cambrige University Press, Cambrege 1997; pp 438.
14. Menon AGK. Conservation of freshwater fishes of Peninsular India. Final report submitted to Minist. Envir. Forest. (unpublished) 1992;137pp.
15. Mathew WJ, Hill LG. Habitat partitioning of fish community of a sourthwestern river. Southwest. Nat. 1980; 25:51-66.
16. Methew WJ, Harvey BC, Power ME. Spatial and temporal pattern in the fish assemblages of individual pools in a mid western stream (USA). Envir. Biol. Fishes 1994; 39:381-97.

17. Negi RK, Joshi BD, Negi Tarana, Chand P. A study on stream morphology of some selected streams hill streams of district Nainital with special reference to its biotic communities. Proceedings of National Seminar on Limnology at Jiapur, India. 2007;

18. Rosgen D. Applied river morphology. Wild land Hydrology, Colorado, U.S.A. (Reprint edition) 1996

19. Ross ST, Baker JA, Clark KE. Microhabitat partitioning of south eastern streams fishes: temporal and spatial predictability. In: Methew WJ Heins WJ (ed) Community and Evolution Ecology of North American stream fishes. University of Oklahoma 1987; 42-51.

20. Schiemer F, Waidacher H. Strategies of conservation of a Danubian fish fauna. In: Boon, P.J.P. Carlow & G.E. Petts ed. River conservation and management. John Wiley & Son. 1992 ; 363-82.

21. Schlosser IJ. Fish community structure and function along two habitat gradients in headwater stream Ecol. Monogr. 1982; 52: 395-14.

22. Sheldon AL. Species diversity and longitudinal succession in stream fishes.Ecology1968; 9:193-98

23. Shelford VE. Ecological succession: stream fishes and the methods of physiographic analysis. Bio.Bull. 1911; 21: 9-35.

24. Schlosser IJ, Toth LA. Niche relationships and population ecology of raibow (Etheostoma caeruleum) and fantil (E. flabellare) darters in a temporally variable environment. Oikos 1984; 42:229-38.

25. Scot MC, Hall LW jr. Fish assemblages as indicators of environmental degradation in Maryland coastal plain streams. Trans. Am. Fish Soc. 1997; 126:349-60.

26. Shannon CE, Weaver W. The Mathematical Theory of Communication. Urbana 243III. University of Illinois Press 1949.

27. Ward JB, Stanford JA. Ecological: connectivity in alluvial rivers ecosystem and its distribution by flow regulation. Regul.Riv.Res. Manage. 1995b; 11: 105-19.

28. Ward JB, Stanford JA. The serial discontinuity concept: Extending the models of flood lai rivers. Regul. Riv. Res. Manage., 1995a; 10:159-68.

29. Wikramanake ED. Ecomorphology and biogeography of a tropical stream fish assemblage: evolution of assemblage structure. Ecology 1990; 1756-64.

4/8/2010

The Gag Specific T lymphocyte Response of Chinese HIV-1 B/C Infectors at different stages

Peichang Yang[1], Hongwei Liu[2], Yuan Yuan[2], Chunhua liu[2], Xiaojin Wang[3*], Zhe Wang[2]

[1]The Nursing School of Zhengzhou University, Zhengzhou，Henan，450052. China,[2]Center for AIDS/STD Control and Prevention, Henan Center for Disease Control and Prevention，Zhengzhou 450016，China,[3]The First Affiliated Hospital of Zhengzhou University, Zhengzhou，Henan，450052. China. ypch@zzu.edu.cn

Abstract: *Background* Gag is very important structural protein of human immunodeficiency virus type 1 (HIV-1) and could be detected in early infection. Specific T lymphocyte immune response was regarded as essential in controlling the production and infection. HIV-1 subtype B/C epidemic is speeding in China but limited data is available on the T cell responses covering Gag in the HIV-1 subtype B/C infectors at different stages. *Materials and Methods.*10 antiretroviral treatment（ART） naïve HIV-1 recombinant subtype B/C infectors with infected time in 1 year, 25 ART-naive infectors with infected time more than 3 years and 10 HIV-1-seronegative healthy individuals were enrolled. HIV-1-specific T lymphocyte responses were analyzed by an IFN-γ Elispot assay against 123 overlapping peptides spanning HIV-1 Gag protein in the present study. *Results* Gag-specific T lymphocyte responses of interferon-gamma secretion were identified in 8(80％) Chinese HIV-1 recombinant subtype B/C infectors with infected time in 1 year, the specific T lymphocytes are mainly targeted at five peptides: GAG7895 in Gag p17, GAG7912, GAG7951 in p24, GAG7979 in p7and GAG7992 in p6. Responses were identified in 17(68％) infectors with infected time more than 3 years, the specific T lymphocytes are mainly targeted at seven peptides: GAG7896 in Gag p17and GAG7911, GAG7912, GAG7917, GAG7923, GAG7924 and GAG7945 in p24. There was obviously positive correlation (P=0.0318，r^2 =0.269) between the magnitude of IFN-γ secretion T lymphocyte responses and plasma viremia in infectors infected time more than 3 years. The magnitude of response in infectors infected in 1 year was significantly higher than that in infectors with infected time more than 3 years (P=0.021). None of the seronegative healthy individuals gave the positive responses. *Conclusions* HIV-1 recombinant subtype B/C Infectors at different stages of diseases recognize different region of Gag. [Life Science Journal 2010;7(2):75-79]. (ISSN: 1097-8135).

Keywords: Human Immunodeficiency Virus (HIV)；Gag; Specific T lymphocyte Response；Elispot；IFN-γ

1 Introduction

Gag is very important structural protein of human immunodeficiency virus type 1 (HIV-1).The Gag specific T lymphocyte against HIV-1 could be detected in early infection[1]. Thus, the characterization of Gag specific T lymphocyte immune responses was regarded as essential in controlling the production and infection of HIV-1[2]. Molecular epidemiological studies in China have shown that the HIV-1 subtype B/C epidemic is speeding, but limited data is available on the T cell responses covering Gag at the single peptide level in the HIV-1 subtype B/C infection at different stages. The aim of this study was to use the overlapping peptides spinning the Gag to determine the scope and specificity of specific T lymphocyte immunity in Chinese HIV-1 subtype B/C infectors at different stages.

2 Materials and Methods

2.1 Materials

FITC-CD3 Ab,PE-CD4 Ab,APC-CD8 Ab and PerCP-CD45 Ab(Immunotech,USA),viral load reagents(Shenzhen, China), Peptides were obtained from the National Institute of Health AIDS Research and Reference Reagent Program (Cat # 8117 ， 7872-7994, USA). Ficoll(Sigma,USA),RPMI 1640, fetal calf serum,HEPES buffer(GIBCO,USA), Human IFN-γ ELISPOT kit (U-CyTech, Netherlands),flow cytometry (Beckman-Coulter,USA),fluorescence real time PCR (Roche,USA), Elispot plate reader (Bio-Sys,Germany). SigmaPlot 5.0 (SPSS,USA)

2.2 Study subjects

Ten antiretroviral treatment（ART） naïve HIV-1 recombinant subtype B/C infectors with infected time in 1 year, 25 ART-naive infectors with infected time more than 3 years and 10 HIV-1-seronegative healthy individuals were enrolled from Xinjiang, China. All individuals in this study were infected by HIV-1 B/C recombinant, as determined by gag, nef, and pol sequencing. Relevant clinical and demographic data of the study subjects are summarized in Table 1. There was significant correlation between the number of CD4 T cell and plasma viral load (p=0.00230 r2=0.251). The study was approved by the respective institutional review boards and all subjects gave written informed consent.

TABLE 1. Clinical and demographical information about the study subjectsa

Infected time	Statistics	Age (year)	Plasma viral load (RNA copies/ml) a	CD4 count (Per mm3) a	CD8 count (Per mm3) a
<1year	Mean	30	374083	467	1406
	Median	30	274900	475	1359
	Range	21～38	<LDL～1300000	252～715	730～2464
>3year	Mean	32	308127	324	1060
	Median	32	10510	321	967
	Range	17～44	<LDL～2415000	86～603	381～2619

a Measured at time of HIV-1-specific T-cell analysis, there were six infectors whose Plasma viral load less than lowest detection level.

2.3 Determination of CD4 cell count

The CD4 cell count from EDTA anticoagulated whole blood was performed by using FITC-conjugated CD3 antibody, PE-conjugated CD4 antibody, PC5-conjugated CD45 antibody and a Beckman-Coulter elite flow cytometry equipped with argon ion laser (488 nm) according to the manufacturer's instructions.

2.4 Determination of HIV-1 viral load

Plasma viral loads were detected by fluorescence real time PCR according to the manufacturer's instruction, the detection limit of PG assay is 100 HIV-1 RNA copies per ml.

2.5 Preparation of peripheral blood mononuclear cell

Peripheral blood mononuclear cells (PBMCs) were prepared from whole blood by density-gradient centrifugation on Ficoll-Hypaque. After washing twice with Hank's solution, the pellet was resuspended in R10 medium (RPMI 1640 that contained 10% fetal bovine serum, 100 U/ml penicillin, 100 μg /ml streptomycin, and 2 mmol L-glutamine/L) and the final concentration of PBMC was adjusted to 1.0×106 cells/ml.

2.6 Design of peptide matrix

Peptides consisted of a total of 123 overlapping peptides that spanned the HIV-1 genes encoding the Gag. All 15-mers overlapped by 11 amino acids. The sequences of the peptides were based on the HIV-1 clade B consensus sequence. All peptides were included in one-peptide matrix systems which included 23 peptide pools, respectively, at two different axes. Each peptide was represented in two different peptide pools, allowing for the identification of the respective peptide by responses in the two corresponding pools. This is exemplified for the identification of the GAG7937 peptide in Table 2 (e.g., Pool Y6 =peptides GAG7932 to GAG7943, aggregately 12 peptides; Pool X6= GAG7877, GAG7889, GAG7901, GAG7913, GAG7925, GAG7937, GAG7949, GAG7961, GAG7973 and GAG7985, aggregately 10 peptides). The final concentration of each peptide within a peptide pool was 50 μg/ml.

TABLE 2. Example of peptide matrix setup for Gag

	X1	X2	X3	X4	X5	**X6**	X7	X8	X9	X10	X11	X12
Y1	GAG7872	GAG7873	GAG7874	GAG7875	GAG7876	**GAG7877**	GAG7878	GAG7879	GAG7880	GAG7881	GAG7882	GAG7883
Y2	GAG7884	GAG7885	GAG7886	GAG7887	GAG7888	**GAG7889**	GAG7890	GAG7891	GAG7892	GAG7893	GAG7894	GAG7895
Y3	GAG7896	GAG7897	GAG7898	GAG7899	GAG7900	**GAG7901**	GAG7902	GAG7903	GAG7904	GAG7905	GAG7906	GAG7907
Y4	GAG7908	GAG7909	GAG7910	GAG7911	GAG7912	**GAG7913**	GAG7914	GAG7915	GAG7916	GAG7917	GAG7918	GAG7919
Y5	GAG7920	GAG7921	GAG7922	GAG7923	GAG7924	**GAG7925**	GAG7926	GAG7927	GAG7928	GAG7929	GAG7930	GAG7931
Y6	**GAG7932**	**GAG7933**	**GAG7934**	**GAG7935**	**GAG7936**	**GAG7937**	**GAG7938**	**GAG7939**	**GAG7940**	**GAG7941**	**GAG7942**	**GAG7943**
Y7	GAG7944	GAG7945	GAG7946	GAG7947	GAG7948	**GAG7949**	GAG7950	GAG7951	GAG7952	GAG7953	GAG7954	GAG7955
Y8	GAG7956	GAG7957	GAG7958	GAG7959	GAG7960	**GAG7961**	GAG7962	GAG7963	GAG7964	GAG7965	GAG7966	GAG7967
Y9	GAG7968	GAG7969	GAG7970	GAG7971	GAG7972	**GAG7973**	GAG7974	GAG7975	GAG7976	GAG7977	GAG7978	GAG7979
Y10	GAG7980	GAG7981	GAG7982	GAG7983	GAG7984	**GAG7985**	GAG7986	GAG7987	GAG7988	GAG7989	GAG7990	GAG7991
Y11	GAG7992	GAG7993	GAG7994									

a Example, shown in bold: a positive response to peptide Gag7937 would be reflected in positive responses in pools X6 and Y6

2.7 Characterization of HIV-1 specific T cell responses by Elispot assay

HIV-1 specific T lymphocyte responses were quantified by Elispot assay. Elispot assay was performed according to the manual of Human IFN-γ ELISPOT kit. Briefly, fresh PBMC were plated onto 96-well plates that had been precoated with 0.5 g of anti-IFN- γ monoclonal antibody; PBMC were added at a concentration of 100 000 cells per well in a volume of 100 μl of R10 medium (RPMI 1640, 10% fetal calf serum, 10 mmol/L HEPES buffer) with antibiotics (50 U of penicillin-streptomycin/ml). The final concentration of the peptides in the well was 5 μg/ml. Plates were incubated overnight at 37°C, 5% CO2, and developed. Wells containing PBMC and R10 medium were used as negative controls. Wells containing PBMC and phorbol 12-myristate 13-acetate (PMA) and inomysin served as positive controls. Duplicate experimental wells and quadruple control wells were used. The numbers of spots per well were counted using an automated Elispot plate reader, and the number of

specific T cells was calculated by subtracting the negative control values. A response was considered positive when the mean spot forming cell for the experimental wells was at least three times the mean SFC for the negative control wells and the mean SFC/106 cells in the experimental wells had to be more than 50 SFC/106 PBMC.

2.8 Statistical analysis

Statistical analysis and graphical presentation were done by SigmaPlot 5.0. Results are given as mean ± standard deviation (SD) or medians with ranges. Mann-Whitney Rank Sum test was used to test for significant differences between the magnitude of response of infectors at different stages, Spearman rank correlations were used to assess the relationships between responses and viral load or CD4 count.

3 Results

3.1 Gag specific T lymphocyte responses of Chinese HIV-1 recombinant subtype B/C infectors at different stages

Using the above-described peptide matrix approach, we screened a total of 35 HIV-1-infected individuals and 10 HIV-1-seronegative healthy individuals for Gag specific T lymphocyte responses in order to comprehensively assess the total breadth and magnitude of virus-specific responses on the single peptide level. None of HIV-1-seronegative healthy individuals was detected response. 25 (71.43%) subtype B/C HIV-1-infected individuals responded to one or more of the 123 peptides used in this study. The mean of magnitude of response was 2913 SFC/106 PBMC (median: 1762, range: 81~14032). The mean of breadth of response was 19.2 peptides/infector (median: 12, range: 2~71). Figure 1 shows the distribution of the number of positive peptide across the Gag for the infectors at different stages. There were 8 (80%) infectors with infected time in 1 year responsed. five most frequently recognized peptides were found. GAG7912 and GAG7951 lie in p24; GAG7895 lie in p17; GAG7979 lie in p7 and GAG7992 lie in p6 (Figure 1A). There were 17 (68%) infectors with infected time more than 3 years responsed. seven most frequently recognized peptides were found. GAG7896 lie in p17; six peptides: GAG7911, GAG7912, GAG7917, GAG7923, GAG7924 and GAG7945 lie in p24 (Figure 1B). The amino acid sequence, position, recognized rate and the mean, median, range of magnitude of response was showed in Table 3.

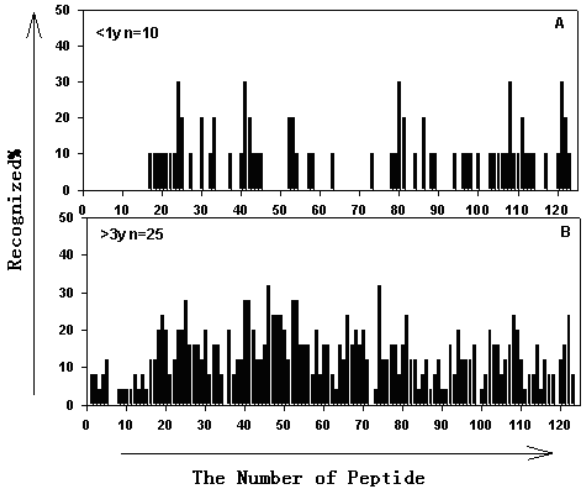

FIG. 1. Peptide recognition across the Gag of infectors at different stages. The 123 individual overlapping peptides are represented on the x-axis, and the corresponding percentage of study subjects with a response to the individual peptide are represented on the y-axis. The horizontal bar indicates the corresponding regions for the individual peptides.

TABLE 3. Most frequently recognized peptides in HIV-1 B/C recombinants infectors at different stages

Peptide	Amino acid position	Sequence	Recognized%		Magnitude(SFC/106PBMC) Mean(Median:Min~Max最大值)	
			<1year	>3year	<1year	>3year
GAG7895	Gag 93-107 = p17 93 -> 107	EVKDTKEALEKIEEE	30		340（345:210～465）	
GAG7896	Gag 97-111 = p17 97 -> 111	TKEALEKIEEEQNKS		28		139（61:45～572）
GAG7911	Gag 157-171 = p24 25 -> 39	KVVEEKAFSPEVIPM		28		164（78:33～626）
GAG7912	Gag 161-175 = p24 29 -> 43	EKAFSPEVIPMFSAL	30	28	373（373:343～403）	162（83:47～632）
GAG7917	Gag 181-195 = p24 49 -> 63	PQDLNTMLNTVGGHQ		32		166（109:15～623）
GAG7923	Gag 205-219 = p24 73 -> 87	INEEAAEWDRLHPVH		28		176（133:50～405）
GAG7924	Gag 209-223 = p24 77 -> 91	AAEWDRLHPVHAGPI		28		179（113:60～387）
GAG7945	Gag 293-307 = p24 161 -> 175	FRDYVDRFYKTLRAE		32		68（42:18～207）
GAG7951	Gag 317-331= p24 185 -> 199	MTETLLVQNANPDCK	30		253（306:61～391）	
GAG7979	Gag 429-443 = p7 52 -> p1 11	RQANFLGKIWPSHKG	30		348（375:134～537）	
GAG7992	Gag 481-495= p6 33 -> 47	KELYPLASLRSLFGN	30		248（266:63～415）	

3.2 The Difference between Gag specific T lymphocyte responses of Infectors at different Stages

For infectors with infected time in 1 year，the mean of magnitude of response was 2846 SFC/106 PBMC (median:3231, range:273~5627), the mean of breadth of response was 9.6 peptides/infector (median:9 , range:5~18); For infectors with infected time more than 3 years，the mean of magnitude of response was 2944 SFC/106 PBMC (median:1471, range:81~14032), the mean of breadth of response was 23.7 peptides/infector (median:16 , range:2~71); The magnitude of response of infectors with infected time in 1 year was obviously higher (P =0.021) than that of infectors with infected time more than 3 years. There was no difference (P =0.076) between breadths of these two group infectors.

3.3 The relationship between HIV-1-specific T-cell responses and plasma viremia or the number of CD4 count of Infectors at different Stages

For infectors with infected time in 1 year，there was no significant correlation between magnitude (P=0.885，r2 =0.002) or breadth (P=0.460，r2 =0.086)of specific T lymphocyte responses and plasma viral loads. No significant correlation between magnitude (P =0.160，r2 =0.275) or breadth (P =0.120，r2 =0.315)of specific T lymphocyte responses and CD4 counts; For infectors with infected time more than 3 years，there was a significant correlation between magnitude (Fig. 3. P=0.0318，r2 =0.269) of specific T lymphocyte responses and plasma viral loads, but no significant correlation between breadth (P =0.981，r2 =0.000) and response No significant correlation between magnitude (P =0.173，r2 =0.118) or breadth (P =0.974，r2 =0.000)of responses and CD4 counts.

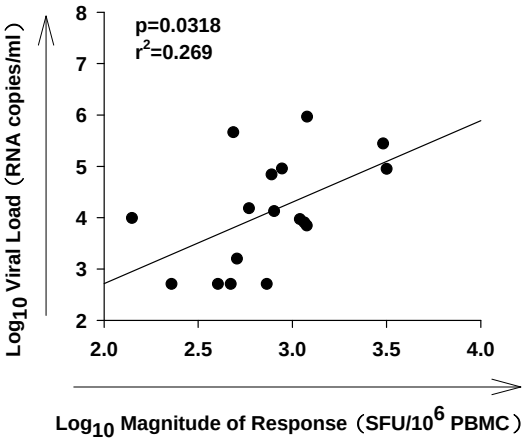

FIG. 2. Correlations between log10 magnitude of Gag specific T lymphocyte response and log10 plasma viral loads of with infected time more than 3 years

4 Conclusion

Gag encodes an important 55kD structure protein of HIV which could be dissociated to p17, p24, p7 and p6. Our results showed that infectors with infected time in 1 year responded five most frequently recognized peptides: GAG7912 and GAG7951 lie in p24; GAG7895 lie in p17; GAG7979 lie in p7 and GAG7992 lie in p6; infectors with infected time more than 3 years responded seven most frequently recognized peptides were found. GAG7896 lie in p17; six peptides: GAG7911, GAG7912, GAG7917, GAG7923, GAG7924 and GAG7945 lie in p24. In these peptides, GAG7911 and GAG7912, GAG7923 and GAG7924 are adjacent to each other. These two adjacent peptide might contain one epitope because the peptides we used were all 15-mers overlapped by 11 amino acids and the length of the epitope could be presented by MHC-I molecular is 8~11 amino acid. Our results also showed that the infectors recognized different region of Gag at different stages. This might be caused of variation of virus under immune pressure. It suggests that the mainly recognized region should be paying more attention for vaccine design and ore research on infectors of early stages should be conducted.

Our results showed that the magnitude of response of infectors with infected time in 1 year was obviously higher than that of infectors with infected time more than 3 years. Past research has found that the functional profile of HIV-specific CD8 T cells in progressors was limited. Their cell functions, such as degranulation, IFN-gamma, MIP-1beta, TNF-alpha, and IL-2 were impaired compared to that of nonprogressors [3].These functions could be restored partially by cultured with IL-2. Recent study also shown that the expression of granzyme B and interferon-γ of CD8+ T cells in HIV infection is dissociated[4]. The difference between magnitudes of response of infectors at different stages might coursed by decreased CD4 T cells or impaired functions of CD8 T lymphocytes.

The emergence and preservation of specific T lymphocyte are fundamental in the host defense against HIV-1 infection [5, 6]. But it remains controversial on the correlation between viral load and HIV-1 specific T cell responses, different studies of HIV-1 infected individuals have shown that there is an positive [7], negative[8] or no correlation[9]. This might be partly due to the different stages of infection or which parameters were measured. Our study showed a significant correlation between the magnitude of specific T lymphocyte response to HIV-1 Gag and the viral load infectors with infected time more than 3 years. These observations support the hypothesis that IFN-γ production of HIV-1-specific T lymphocyte is not main mechanism of control of viral replication and these effector cell expansions and contractions are driven by changes in antigen load [10]. The functional impairment of CD8 T lymphocyte responses in late-stage infection could not be reflected by gamma interferon-based screening techniques[11]. Future studies, such as the investigation of mechanism of control of viral replication and the “quality” of HIV-1-specific T cell responses[12, 13] are therefore needed to identify the correlates of immune mediated control of HIV-1 replication.

References

1. Ndongala ML, Peretz Y, Boulet S, Doroudchi M, Yassine-Diab B, Boulassel MR, et al. HIV Gag p24 specific responses secreting IFN-gamma and/or IL-2 in treatment-naive individuals in acute infection early disease (AIED) are associated with low viral load. Clin Immunol 2009.
2. Serwanga J, Shafer LA, Pimego E, Auma B, Watera C, Rowland S, et al. Host HLA B*allele-associated multi-clade Gag T-cell recognition correlates with slow HIV-1 disease progression in antiretroviral therapy-naive Ugandans. PLoS ONE 2009,4:e4188.
3. Oxenius A, Price DA, Easterbrook PJ, O'Callaghan CA, Kelleher AD, Whelan JA, et al. Early highly active antiretroviral therapy for acute

HIV-1 infection preserves immune function of CD8+ and CD4+ T lymphocytes. Proc Natl Acad Sci U S A 2000,97:3382-3387.
4. Kleen TO, Asaad R, Landry SJ, Boehm BO, Tary-Lehmann M. Tc1 effector diversity shows dissociated expression of granzyme B and interferon-gamma in HIV infection. Aids 2004,18:383-392.
5. Ueno T, Motozono C, Dohki S, Mwimanzi P, Rauch S, Fackler OT, et al. CTL-mediated selective pressure influences dynamic evolution and pathogenic functions of HIV-1 Nef. J Immunol 2008,180:1107-1116.
6. Wang YE, Li B, Carlson JM, Streeck H, Gladden AD, Goodman R, et al. Protective HLA Class I Alleles Restricting Acute-Phase CD8+ T Cell Responses are Associated with Viral Escape Mutations Located in Highly Conserved Regions of HIV-1. J Virol 2008.
7. Northfield JW, Loo CP, Barbour JD, Spotts G, Hecht FM, Klenerman P, et al. Human immunodeficiency virus type 1 (HIV-1)-specific CD8+ T(EMRA) cells in early infection are linked to control of HIV-1 viremia and predict the subsequent viral load set point. J Virol 2007,81:5759-5765.
8. Novitsky V, Gilbert P, Peter T, McLane MF, Gaolekwe S, Rybak N, et al. Association between virus-specific T-cell responses and plasma viral load in human immunodeficiency virus type 1 subtype C infection. J Virol 2003,77:882-890.
9. Bartovska Z, Beran O, Rozsypal H, Holub M. HIV-1-specific CD8(+) T cells do not correlate with viral load in HIV-1-positive patients. Acta Virol 2007,51:59-61.
10. Alter G, Tsoukas CM, Rouleau D, Cote P, Routy JP, Sekaly RP, Bernard NF. Assessment of longitudinal changes in HIV-specific effector activity in subjects undergoing untreated primary HIV infection. Aids 2004,18:1979-1989.
11. Draenert R, Verrill CL, Tang Y, Allen TM, Wurcel AG, Boczanowski M, et al. Persistent recognition of autologous virus by high-avidity CD8 T cells in chronic, progressive human immunodeficiency virus type 1 infection. J Virol 2004,78:630-641.
12. Addo MM, Draenert R, Rathod A, Verrill CL, Davis BT, Gandhi RT, et al. Fully differentiated HIV-1 specific CD8+ T effector cells are more frequently detectable in controlled than in progressive HIV-1 infection. PLoS ONE 2007,2:e321.
13. Jiang Y, Karita E, Castor D, Jolly PE. Characterization of CD8+ T lymphocytes in chronic HIV-1 subtype A infection in Rwandan women. Cell Mol Biol (Noisy-le-grand) 2005,51 Suppl:OL737-743.

10/26/2009

Pharmacokinetic comparison of orally disintegrating, β-cyclodextrin inclusion complex and conventional tablets of nicardipine in rats

Bin Du*, Xiaotian Li, Qiuying Yu, Youmei A, Chengqun Chen
Pharmacy School，Zhengzhou University，China

Abstract: The goal of this study was to compare the pharmacokinetics of nicardipine hydrochloride orally disintegrating tablets and β-cyclodextrin inclusion complex with its conventional tablets. Forty-five rats were divided into three groups evaluating the effect of dosage forms on the pharmacokinetics of nicardipine hydrochloride. Blood samples were taken at predefined sampling points 0–24h after medication, and the plasma concentrations of nicardipine hydrochloride orally disintegrating tablets, β-cyclodextrin inclusion complex and its conventional tablets were determined by high-performance liquid chromatography. The orally disintegrating tablets increased in C_{max}, AUC and $t_{\beta 1/2}$ were observed, t_{max} occurred at 1.0 and 2.0h with orally disintegrating tablets and conventional tablets. The orally disintegrating tablets exhibited a longer elimination half-life ($t_{1/2\,\beta}$ 5.5h) compared with its conventional tablets ($t_{1/2\,\beta}$ 1.4 h). The mean dose corrected area under the plasma concentration-time curve extrapolated to infinity AUC (0−∞) of orally disintegrating tablets was 5.60 times greater than its conventional tablets. This research showed that formulation of nicardipine hydrochloride orally disintegrating tablets and β-cyclodextrins inclusion complex resulted in increase of bioavailability and prolong its activity time. [Life Science Journal 2010;7(2):80-84]. (ISSN: 1097-8135).

Keywords*:* Nicardipine hydrochloride; orally disintegrating; Pharmacokinetics; HPLC

Abbreviations：
C---concentration
t---time
NC--- Nicardipine hydrochloride
CDs ---Cyclodextrins
HPMC---hydroxypropyl methyl cellulose
L-HPC---low-substituted hydroxypropyl cellulose
CMC-Na---sodium carboxymethyl cellulose
PVPP --- poly (vinylpolypyrrolidone)
MCC--- microcrystalline cellulose
DSC---differential scanning calorimetry
FTIR --- fourier transformation-infraredHPLC
QC---quality control
HPLC---heigh perform liquid chromatography

1 Introduction

Nicardipine hydrochloride (NC), a calcium channel-blocking agent, is an effective drug in the management of mild to moderate hypertension, angina pectoris and cerebral disease (Pomponio et al. 2004; Catarina et al. 2002). However, the drug bioavailability is very limited (15 – 40 %) to short elimination half-life (about 1 h), and like other dihydropyridine derivatives, its standard formulation undergoes rapid absorption and extensive biotransformation in the liver, which often results in significant fluctuations in plasma concentrations (Catarina et al. 2002; Dollo et al. 1999).

To attain a prolonged therapeutic effect and a reduced incidence of side effects, sustained/controlled release formulations of NC have been developed to maintain a suitable plasma level for a long period of time, with minimal frequency of daily administration. NC microspheres using acrylic polymers (Zyazici et al. 1999), and NC microcapsules with ethylcellulose as a coating material have been prepared for this purpose (Catarina and Fernandesa 2003). Cyclodextrins (CDs), cyclic oligosaccharides with a hydrophobic central cavity that provides a microenvironment for appropriate sized non-polar molecules, are also strong candidates for achieving drug controlled release at the desired level. These carriers have been widely applied as multi-functional (Catarina et al. 2002). Pharmaceutical excipients due to their remarkable molecular complex property with many drugs modifying their physical, chemical and biological properties (Catarina et al. 2002; Uekama et al. 1998). The structure of nicardipine hydrochloride is showed in Figure 1. Then we used hydroxypropyl methyl cellulose (HPMC), low-substituted hydroxypropyl cellulose (L-HPC), sodium carboxymethyl cellulose (CMC-Na), poly (vinylpolypyrrolidone) (PVPP), microcrystalline cellulose (MCC) to prepare the orally disintegrating tablets not only to prolong its interaction time but improve stability and disintegrating time.

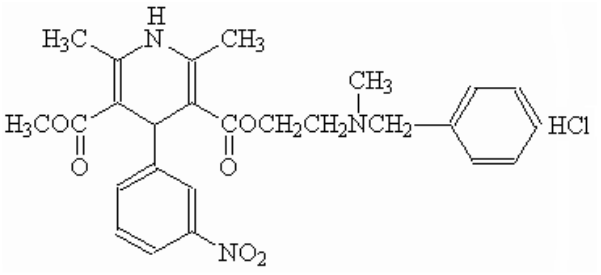

Figure 1. Chemical structure of nicardipine hydrochloride

2 Materials and Methods

2.1 Materials

Nicardipine hydrochloride (99.99%, purity) was a gift from Fusen Pharmaceutical Factory (Henan,China). Nicardipine hydrochloride orally disintegrating tablets, β-cyclodextrins inclusion complex and conventional tablets were prepared at our laboratory. HPMC, PVPP, L-HPC, CMC-Na, MCC were purchased from Shanghai Concord Tech Reagent Company (Shanghai, China). SD rats were purchased from the Center of Experimental Animals in Henan (Zhengzhou, China). Methanol of HPLC grade was purchased from Tianjin Concord Tech Reagent Company (Tianjin, China). All

the other reagents were of analytical grade.

2.2 Production of β-cyclodextrins inclusion complex

The preparation of NC-β-CD solidbinary systems was performed by different techniques (Kneading, Evaporation, Ultrasonic-Evaporation, Freeze-drying). We used differential scanning calorimetry (DSC) and fourier transformation-infrared (FTIR) spectroscopy to ensure the information of this chemical complex. In the end, the ultrasonic-evaporation (50℃, 3h, 100W) was chosen to produce the inclusion complex, the NC: β-CD (1:2) molar ratio based on the previous solubility studies (Sugimoto et al. 2001).

2.3 Preparation of nicardipine orally disintegrating tablets

Orthogonal test was used to confirm the optimum prescription, and according to the standard of Chinese Pharmacopoeia (2005) to product the orally disintegrating tablets and conventional tablets. The optimum prescriptions of single tablet is nicardipine hydrochloride β-cyclodextrins inclusion complex 60 mg, HPMC 7.5 mg, L-HPC 5.0 mg, MCC 30 mg, PVPP 12 mg, Magnesium stearate 0.15 mg, added to 35 mg mannitol .

2.4 Instrument conditions of HPLC

LC 2010A series (Shadows, Janpan) was used in the present work. Chromatographic separation was performed on a Diamonsil TM C_{18} column (250mm × 4.6mm I.D., 5 μm, Shadows, Janpan) at ambient temperature. The mobile phase consisting of a mixture of methanol and 0.01mol/L potassium dihydrogen phosphate buffer solution (90:10, v/v) was delivered at a flow rate of 1.0 ml/min. The injection volume was 20 μl and the detection wavelength was 237 nm.

2.5 Preparation of calibration standards and quality control samples

Stock solutions (1 mg/ml) of nicardipine hydrochloride and diethylstilbestrol (internal standard) were individually prepared in methanol. The stock solution of nicardipine hydrochloride was further diluted with methanol to give a series of standard solutions with concentration of 0.040, 0.18, 0.72, 2.5, 10, 40, 80, 320 μg/ml. Working solution of diethylstilbestrol was freshly prepared by diluting stock solution with methanol to give a concentration of 10 μg/ml.

Calibration standards of nicardipine hydrochloride were prepared by spiking appropriate amount of the standard solutions of nicardipine hydrochloride in blank plasma. Quality control (QC) samples were prepared at concentrations of 0.1, 40, 300μg/ml of nicardipine hydrochloride using the blank plasma.

2.6 Sample preparation

0.5 ml aliquot of each plasma sample was transferred to a 1.5 ml centrifuge tube, then centrifuged and added 10μg/ml of diethylstilbestrol. The supernatant was separated and 600μl of methanol were added, and shaken well, the contents were mixed by vortexing for 1 min and centrifuged for 10 min to separate the phases and evaporated under a stream of nitrogen at room temperature (Eiling et al. 2006). The residue was reconstituted with 200 μl of mobile phase and 20μl was injected into the HPLC column.

2.7 Method validation

Validation runs were conducted on six separate days. Each validation run consisted of a set of calibration standards at three concentrations over the concentration range and QC samples at three concentrations (0.1, 40, 300 μg/ml, n = 5 at each concentration) (Eiling 2006a; Dawes 2006b etc.). The results from QC samples were used to evaluate the accuracy and precision of the method developed. The analysis concentrations in plasma samples were determined by BAPP3.0 (supplied by China Pharmaceutical University)of the observed peak area ratios of the analysis and internal standard from the best-fit calibration curve. During routine analysis, each analytical run included a set of calibration standards, a set of QC samples in duplicate and plasma samples were determined.

The selectivity of the method was investigated by comparing chromatograms of blank plasma, standard plasma sample spiked with nicardipine hydrochloride (10μg /ml) and diethylstilbestrol (10μg/ml) and plasma sample after an oral dose of nicardipine hydrochloride orally disintegrating tablets and β-cyclodextrins inclusion complex and conventional tablets. An additional test was performed to demonstrate if there was any interference from the plasma matrix (Zhang et al. 2003). The test was performed as follows: the standard solutions of nicardipine hydrochloride at 2.5, 10, 40μg/ml were added in blank plasma after extraction and determined by the present HPLC method. Standard solutions of nicardipine hydrochloride at 0.1, 40, 300μg/ml were directly determined without extraction. Based on the percentage of peak area ratio of the analysis added in plasma after extraction was relative to that of the analyte without extraction, RE (%) was calculated to evaluate the accuracy of the determination without interferences from the matrix (Zhang et al. 2003).

The linearity of each calibration curve was determined by plotting the peak area ratio (y) of the analysis to internal standard versus the nominal concentration (x) of the analysis. The calibration curves were obtained by weighted ($1/x2$) linear regression analysis (Eiling et al. 2006).

The extraction recoveries of nicardipine were determined at 0.1, 40, 300μg/ml by comparing the responses from plasma samples spiked before extraction with the corresponding standard solutions without extraction.

2.8 Application of the method

The HPLC method was successfully applied in the pharmacokinetic studies of nicardipine hydrochloride orally disintegrating tablets, β-cyclodextrins inclusion complex and conventional tablets in 45 female SD rats of 200±20g in weight. The rats were randomly divided into three groups with fifteen rats which were divided into five of each group. The rats were fasted 12h before the test. 6, 12, 24mg/kg low-middle-high three doses of

nicardipine hydrochloride orally disintegrating tablets, β-cyclodextrins inclusion complex and conventional tablets were tested in this study. The rats in the three groups were given single dose of low-middle-high three doses with 9ml of warm water. Within 24 h after oral administration of the tablets, the rats had a standard diet while water intake was free . Blood samples (0.5 ml) were obtained immediately pre-dose and 5,10, 20, 30min, 1, 2, 4, 6, 8, 10, 12, 24h post-dose, which were collected in tubes previously treated with heparin and plasma was separated by centrifugation and kept frozen at −20℃ until analysis. Plasma concentrations of nicardipine were determined by the present HPLC method.

3 Results and Discussion

3.1 Method development

Liquid–liquid extraction was used for the sample preparation. This simple procedure produced a clean chromatogram for blank plasma sample and yielded satisfactory recoveries of the analytes from the plasma. In this work, 10% potassium dihydrogen phosphate buffer solution (0.01mol/l) were added in the process of sample preparation to adjust the medium to about pH 5.5 and thus to free the drug bases from their hydrochlorides for the following extraction by organic solvent. In this study, methanol and 0.01mol/L potassium dihydrogen ghosphate buffer solution (90:10, v/v) were used for extraction.

A Diamonsil TM C18 column (250mm × 4.6mm I.D., 5μm) was used. Other chromatographic conditions, especially the composition of mobile phase, were tested to achieve good resolution and symmetric peak shapes of analytes as well as short run time. Internal standard plays an important role in biopharmaceutical analysis and is often required to have similar physical and chemical properties with the analyte such as solubility and acid–base properties (p*K*a) (Eiling et al. 2006). On the basis of the above requirements, diethylstilbestrol was found to be suitable for the present work and finally used as the internal standard.

After liquid–liquid extraction, both analytes are present in drug base forms. For the analysis of basic drugs by HPLC methods, it was found that a mixture of methanol and 0.01mol/l potassium dihydrogen phosphate buffer solution (90:10, v/v) could achieve our purpose and was finally adopted as the mobile phase for the chromatographic separation. The retention times were 5.3 min for nicardipine and 3.0 min for diethylstilbestrol. The run time was less than 7min.

3.2 Selectivity

The results of selectivity demonstrated a clean chromatogram from blank plasma sample after sample preparation by liquid–liquid extraction (Figure 2) and the absence of endogenous interferences from the plasma matrix and the satisfying selectivity of the present method for the determination of nicardipine hydrochloride in rats plasma.

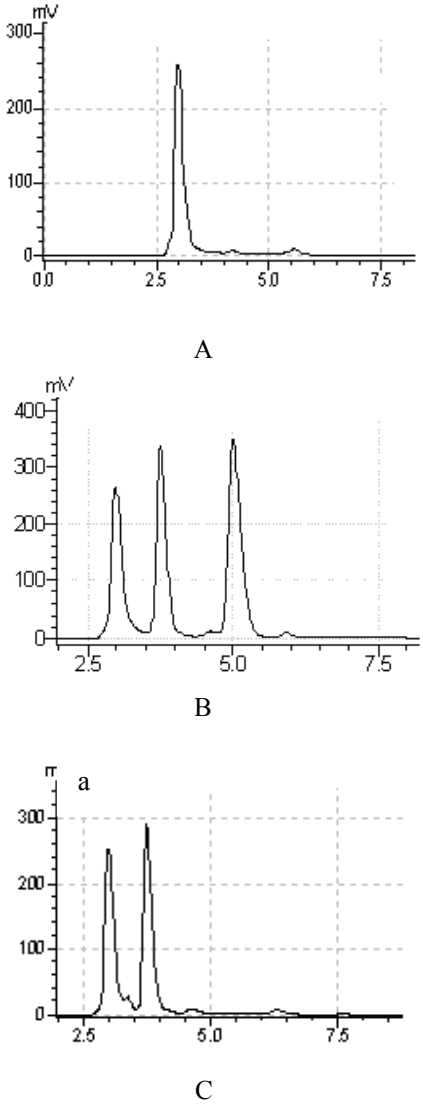

Figure 2. The chromatogram of separation: A. blank plasma, B. plasma sample added diethylstilbestrol (a-diethylstilbestrol; b-nicardipine hydrochloride), C. plasma sample

3.3 Linearity

To evaluate the linearity of the HPLC method, plasma calibration curves were determined in triplicate on six seperate days. Representative regression equation for the calibration curve was y = 0.7567x + 0.6555, r = 0.9998, for nicardipine hydrochloride. Good linearity was observed over the concentration range of 0.040-320 μg/ml.

3.4 Precision

The precision of the method were evaluated based on the data from QC plasma samples at three concentrations (0.1, 40, 300 μg/ml) in five validation runs. The intra-day and inter-day precision were expressed as the relative standard deviation (R.S.D.). As shown in Table 1, for each QC level of nicardipine hydrochloride, the intra-day and inter-day mean precisions (R.S.D.) were 0.45 and 7.69 %, indicating acceptable precision of the present HPLC method for the determination of nicardipine hydrochloride in rat plasma.

Table 1. The precision for the determination of nicardipine in rat plasma

Origin（μg/ml）	Intra-precision		Inter-precision	
	Found（μg/ml）	RSD（%）	Found（μg/ml）	RSD（%）
0.1	0.094	0. 78	0.11	5. 79
40	41.3	0.36	44.72	8.52
300	290	0.21	295	8.76

3.5 Extraction recovery and accuracy

The extration recovery of nicardipine hydrochloride from rat plasma was determined by comparing concentration from plasma samples spiked with the adding standard solutions concentration. The accuracy of nicardipine hydrochloride from rat plasma were determined by comparing peak areas from plasma samples spiked before extraction with the corresponding standard solutions without extraction. The results showed in table 2 at concentrations of 0.1, 40, 300 μg/ml of nicardipine hydrochloridel.

Table 2. Extraction recovery and accuracy for the determination of nicardipine in rat plasma

Origin (μg/ml)	Extraction-recovery		Accuracy		
	Found（μg/ml）	Recovery（%）	Normal- area	Sample-area	Accuracy（%）
0.1	0.094	94.0	6157	5497	89.3
40	41.3	103.3	2007621	1817562	90.5
300	298	99.3	18471000	16595000	89.8

3.6 Pharmacokinetics of nicardipine orally disintegrating tablets in rats

The present HPLC method achieved satisfactory results for the determination of nicardipine hydrochloride in rat plasma and was successfully applied in the pharmacokinetic study of nicardipine hydrochloride orally disintegrating Tablets following oral administration to rats. The result of the pharmacokinetics of orally disintegrating Tablets, conventional tablets, β-cyclodextrins inclusion complex shown in Table 3 and Figure 3.

Table 3. Pharmacokinetic parameters of orally disintegrating tablets, conventional tablet, β-cyclodextrins inclusion complex（mean±SD，n = 6）

Pharmacokinetic parameters	conventional tablet	β-cyclodextrins inclusion complex	orally disintegrating tablets
$AUC_{0-\infty}$ (μg h /ml)	123.15 ± 31.00	269.02 ± 67.00	689.10 ± 147.00
C_{max} (μg /ml)	41. 47 ± 13.11	44.38 ± 12.79	151.17 ± 31.06
T_{max} (h)	2 ± 0.12	1 ± 0.00	1 ± 0.00
$t_{½\beta}$ (h)	1.4 ± 0.01	4.1 ± 0.02	5.5 ± 0.04

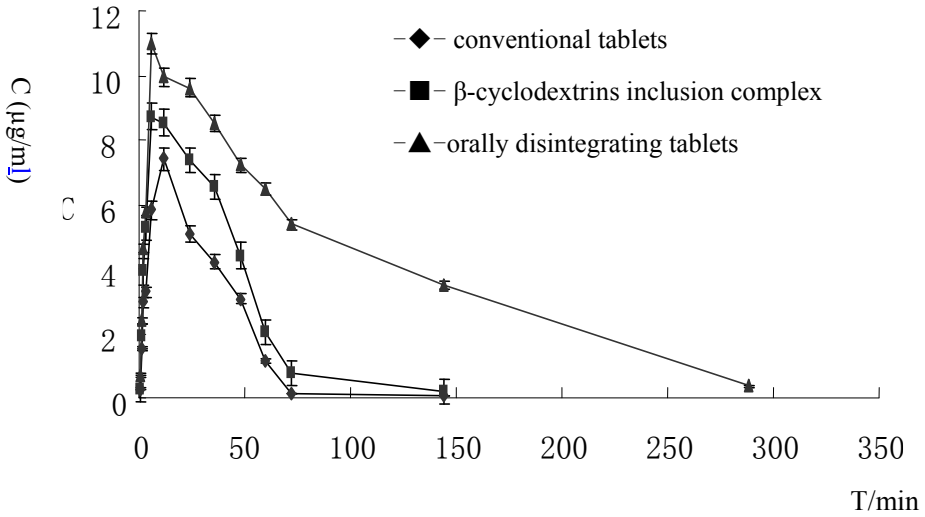

Figure 3. Concentration–time profiles of nicardipine hydrochloride orally disintegrating tablets, β-cyclodextrins inclusion complex and conventional tablets after oral administration of in rat plasma（mean±SD，n = 6）

The orally disintegrating tablets increased in C_{max}, AUC and $t_{1/2\beta}$were observed, t_{max} occurred at 1.0 and 2.0h with orally disintegrating tablets and conventional tablets. The orally disintegrating tablets exhibited a

longer elimination half-life ($t_{1/2\,\beta}$ 5.5h) compared with its conventional tablets

($t_{1/2\,\beta}$ 1.4h). The mean dose corrected area under the plasma concentration-time curve extrapolated to infinity AUC (0−∞) of orally disintegrating tablets was 5.60 times greater than its conventional tablets. The β-cyclodextrin inclusion complex were statistically significantly increased compared to the conventional tablets. This showed that formulation of nicardipine hydrochloride orally disintegrating tablets and β-cyclodextrins inclusion complex resulted in increase of bioavailability and prolong its activity time.

The pharmacokinetic results provide the proof of concept: nicardipine hydrochloride formulated as a medicated orally disintegrating tablets results in a statistically significant increase in its bioavailability as the results of this study. The main results from this study are orally disintegrating tablets and β-cyclodextrins inclusion complex formulation increased in the bioavailability compared to conventionall tablet, expressed as dose-corrected AUC (0−∞).

Acknowledgment

This study was supported by a grant (08) from Department of Science and Technology, Henan Province,China.

References

1. Pomponio R, Gotti R, Fiori J. Photostability studies on nicardipine–cyclodextrin complexes by capillary electrophoresis. J Pharm.and Biomed Anal 2004; 35:267–275.
2. Catarina M, Fernandes J, Veiga B. Physicochemical characterization and in vitro dissolution behavior of nicardipine–cyclodextrins inclusion compounds. Eur J Pharm Sci 2002;15:79–88.
3. Dollo G, Corre P, Chollet M, Chevanne F. Improvement in solubility and dissolution rate of 1,2-dithiole-3-thiones upon complexation with β-cyclodextrin and its hydroxypropyl and sulfobutylether-7 derivatives. J Pharm Sci 1999; 88: 889–895.
4. Zyazici O, Sevgi F, Ertan G. Micrometric studies on dissolution characteristics of famotidine by inclusion in β-cyclodextrin-nicardipine hydrochloride microcapsules. Int J Pharm 1996; 138: 25–35.
5. Catarina M, Fernandesa. Hydrophilic and hydrophobic cyclodextrins in a new sustaine dreleaseoral formulation of nicardipine: invitro evaluation and bioavailability studies in rabbits. J Control Release 2003; 88:127–134.
6. Uekama K, Hirayama F, Irie T. Cyclodextrin drug carrier system.Chem Rec 1998; 98: 2045–2076.
7. Meiling Q, Peng W, Xin J. Liquid chromatography–mass spectrometry method for the determination of nicardipine in human plasma. J Chromatogr B 2006; 830: 81–85.
8. Dawes C. Absorption of urea through the oral mucosa and estimation of the percentage of secreted whole saliva inadvertently swallowed during saliva collection. Arch Orallly Biology 2006; 51:111–116.
9. Zhang YF, Chen XY, Zhong DF, Dong YM Pharmacokinetics of loratadine and its active metabolite descarboethoxy loratadine in healthy Chinese subjects. Acta Pharm Sci 2003; 24: 715–718.
1. 10. Sugimoto M, Matsubara K, Koida Y. The preparation of rapidly disintegrating tablets in the mouth Pharm Dev Technol 2001; 4: 487–493.

5/1/2010

Reliability of Wireless Body Area Networks used for Ambulatory Monitoring and Health Care

Ali Peiravi[1], Maria Farahi[2]
Department of Electrical Engineering, School of Engineerinf, Ferdowsi University of Mashhad
Mashhad IRAN. [1]Ali_peiravi@yahoo.com, [2] mari.252@gmail.com

Abstract: Ambulatory monitoring and health care using wireless sensor networks is an active area of applied research. The general network topology used for wireless body area networks is the star topology with the sensor nodes sending their data to a central processing node for data fusion. Reliability of these networks is very important since they deal with human life. Reported applications have had performance and reliability problems. In this paper, several reported applications of wireless body area networks are reviewed and the reliability of a sample WBAN is computed. [Life Science Journal 2010;7(2):85-91]. (ISSN: 1097-8135).

Keywords: Reliability, wireless body area network, ambulatory monitoring, MEMS sensors

Introduction

Measurement of human position, balance, posture, orientation and body status is not only of interest to the medical scientists but also of importance in the entertainment field for computer generated especial effects. The complexities of motion analysis and the various parameters involved in the estimation or measurement of body position and orientation usually require the use of a complex set of wireless sensor nodes in the form of a wireless body area network and including accelerometers, gyroscopes, magnetometers, etc. plus the application of data fusion. In some applications, estimation may require the inclusion of some form of a Kalman filter or a particle filter.

Data fusion may be defined as the use of techniques to combine data from multiple sources and gather that information in order to achieve inferences that are more efficient and potentially more accurate than if they were achieved by means of a single source. There are various fusion processes that are usually described as low, intermediate or high level that depend on the processing stage at which data fusion takes place (Mandic et al. 2005).

In low level data fusion several sources of raw data are combined to produce new raw data that is expected to be more useful than the inputs. In intermediate level data fusion that may also be called feature level fusion, various features are combined into a feature map that may then be used by further processing. High level data fusion usually refers to a situation where decisions coming from several experts are fused together. These include voting methods, statistical methods, fuzzy logic, etc.

Another potential application of data fusion is in capturing motion. Such areas as interactive game and learning, animation, film special effects, health-care and navigation may be named. Human motion capture techniques using multiple high resolution cameras in especial studios are highly costly and complex. With the recent developments in MEMS technology, micro inertial sensors-on-hip (MMocap), low cost real-time human motion capture systems have become possible.

Earlier works

An early application of ambulatory measurements was reported by Tanka et al. (1994) for long term monitoring of posture. They argued that human postures such as standing, sitting, lying, walking, etc. may be estimated from the angles corresponding to gravitational direction in three portions of the body, namely the chest, the thigh and the legs which may be measured using tri-axial accelerometers as shown in Fig. 1.

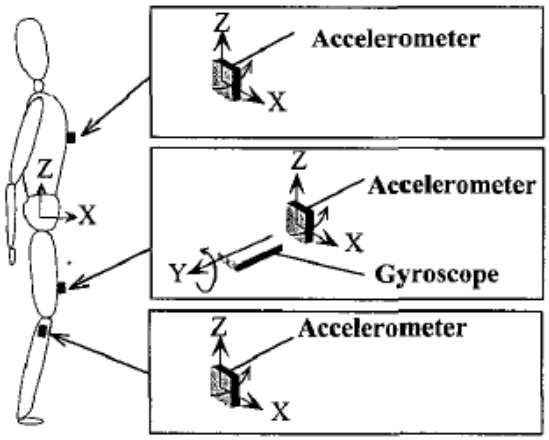

Fig 1 – Accelerometers and gyroscope for measuring body posture and walking speed adopted from Motoi et al. (2003).

The angles in question may be obtained from the low frequency signals of these accelerometers. Later on, Motoi et al. (2003) suggested the addition of a gyroscope on the thigh for measuring walking speed whereby the angular change in the saggital plane is obtained by integrating the gyroscope's signal during walking. They concluded that fairly good results with a reasonable degree of accuracy may be obtained for walking speeds of less than 0.6m/s.

What has caused major progress in this area in recent years is mainly due to the developments in wireless sensor networks, nanoelectronics, MEMS technology and advances in data fusion. Solaiman et al. (1999) presented a monosensor/multiple source data fusion system for the detection of the esophagus in

ultrasound images where the authors describe an approach in which various features extracted from the image are first combined using fuzzy processing and fuzzy reasoning methods. Models of the underlying physical image formation process were also used for feature extraction.

Sensors

Recent technological advances in sensors, low-power integrated circuits, and wireless communications have enabled the design of low-cost, miniature, lightweight, intelligent physiological sensor platforms that can be seamlessly integrated into a wireless body area network.

Accelerometry may be used as sensors for monitoring human movements. They have been used to monitor a range of different movements, including gait, sit-to-stand transfers, postural sway, falls, and various forms of physical activity. The accelerations generated during human movement vary across the body and depend on the activity being performed. Their magnitude usually increases from the head to the ankle with the largest value in the vertical direction. Running produces the greatest magnitude of acceleration in the vertical direction of 8.1–12.0g at the ankle, up to 5.0g at the low back and up to 4.0g at the head. Accelerations up to 8.1g at the angle are produced during walking down stairs. Other activities such as trampoline jumping, walking up stairs, level walking and cycling produce acceleration up to 7.0g at the ankle during trampolining, 7.4g walking up stairs and 2.9–3.7g during level walking. The upper body accelerations in the vertical direction have been found to range from -0.3 to 0.8g during walking, whereas horizontal accelerations range from -0.3 to 0.4g at the low back and from −0.2 to 0.2g at the head.

Mathie et al. (2004) reviewed the use of accelerometer-based systems in each of these areas and present an integrated approach in which a single, waist-mounted accelerometry system is used to monitor a range of different parameters of human movement in an unsupervised setting.

Nyan et al. (2004) presented a comparison of experimental results for sensors mounted on different locations on the human body and different sensitivity in the usage of MEMS accelerometers based on the eigenvector-based signal identification algorithm for multi-dimensional signal identification related to ambulatory daily activities. They used ADXL105 single axis accelerometers and a Kistler 8392B capacitive silicon micromachined 3-D accelerometer. The outputs of the accelerometers were sampled at 256HZ and then filtered using a 50Hz cutoff low pass digital filter. Their main goal was to extract features from the signals in order to identify daily human activities.

Information management for critical care monitoring is a very difficult task and medical staff are often overwhelmed by the amount of data provided by the increased number of specific monitoring devices and instrumentation, and the lack of an effective automated system. Arrhythmia detection produces a large amount of undesirable alarms. Hern´andez et al. (1999) presented a multisensor/multisource data fusion scheme to improve atrial (AA) and ventricular activity (VA) detection in critical care environments. They integrated complementary data from hemodynamic processes or from the esophageal ECG (EECG) with the usual electrocardiogram (ECG) signals. They proposed a general structure based on a distributed detection scheme applicable to both VA and AA detection. VA detection makes use of the ECG and pressure signal, while AA detection is based on combining ECG and EECG.

Wireless body area networks (WBANs) promise ambulatory health monitoring for extended periods of time and near real-time updates of patients' medical records through the Internet or intranet. Jovanov et al. (2006) presented a WBAN as shown in Fig. 2 utilizing a common off-the-shelf wireless sensor platform with a ZigBee-compliant radio interface and an ultra low-power microcontroller. The standard platform interfaces to custom sensor boards that are equipped with accelerometers for motion monitoring and a bioamplifier for electrocardiogram or electromyogram monitoring. They used TinyOS operating system to develop the software modules for on-board processing, communication, and network synchronization.

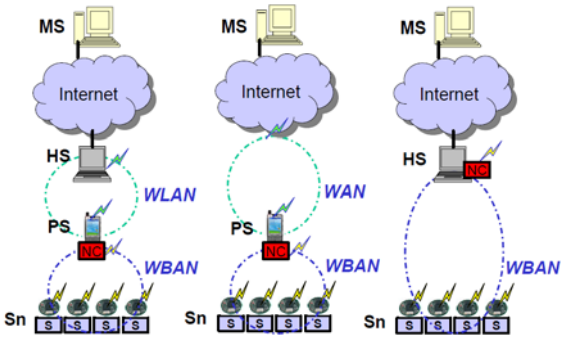

Fig. 2 - The Wireless Body Area Network (WBAN) for ambulatory monitoring adopted from Jovanov et al. (2006)

Dong et al. (2007) presented a physical activity monitoring system in body sensor networks using data fusion for providing real time body status information and identifying body activities. The data collected from several accelerometer sensors placed on different parts of the body were fused to identify and track physical activity. They used Kalman filter, hidden Markov model, and biaxial accelerometers. When the accelerometers are placed on the thigh, the flexion angle of the thigh would be the angle between the accelerometer and the direction of gravity as shown by θ in Fig. 3. Thus the swing velocity or the angular velocity would be $v = \frac{d\theta}{dt}$

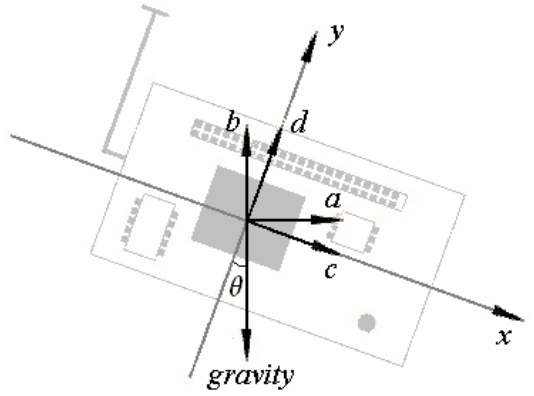

Fig. 3 – The variables involved in the accelerometer adopted from Dong et al. (2007)

They applied this system to monitoring and identifying daily activities in laboratory and comparatively intensive activities in a gym room with the performance evaluation done based on video. They used data fusion at a higher level by setting up an activity description table where the parameters involved in deciding what activity each body part is involved in are tabulated. For example, for the thigh, they have included flexion angle, dynamic energy, periodicity of 0.5-2Hz and cycling hidden markov model state are listed. Comparative results indicate that body status of daily activities can be estimated with good accuracy in real time, and can be measured with a high degree of accuracy with a short system latency using a Kalman filter, discrete fourier transform and hidden markov model.

Iso-Ketola et al. (2008) proposed a wearable measurement system called HipGuard for patients recovering from a hip replacement operation. HipGuard, should be used at home during the recovery period of 8 to 12 weeks after surgery. It measures the posture and monitors the load put on the operated leg using seven wireless posture sensor nodes for measuring the orientation of the hip and the legs, and a wireless load sensor node for measuring the load put on the operated leg. An audio signal or a haptic vibration is used to inform the patient in case the position of the operated hip or the load put on the operated hip approaches previously set limits.

Small size and low power consumption are the main requirements in these systems. The orientation measurements are done in the posture sensor nodes using accelerometers, magnetic sensors

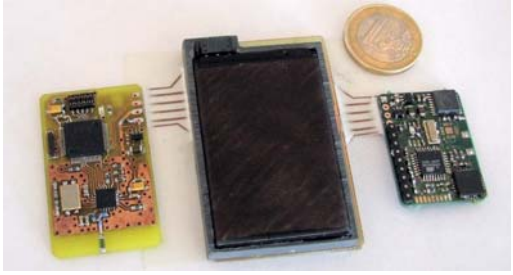

and gyroscopes as shown in Fig. 4.

Fig. 4 - The electronic circuits used in the posture sensor node adopted from Iso-Ketola et al. (2008)

The load sensor nodes are capacitive with a self restoring collapsible insulator material placed in the insole of the patient's shoe on the operated side. Since it is difficult to measure the whole force that is directed to the foot, measurements from two selected areas under the heel and the ball of the foot are fused together to obtain an estimate. The only drawback of this system is that the sensors are not integrated with the patient's body and have a degree of error and the measurements do not yield the exact position of the hip bone and the thigh bone since the movement of the muscles and joints between the skin and the skeleton produce some inaccuracy. A sampling rate of 40Hz is used in the wireless sensor network to obtain data from the posture sensor nodes to calculate the posture of the hip with each sensor node calculating its horizontal and vertical angle. Thus, there is no need to transmit the individual values of the three axes of the accelerometers and the two axes of the magnetometer to the control unit.

Zhiqiang et al. (2009) presented a motion estimation algorithm by hierarchical fusion of sensor data and constraints of human dynamic model for human upper limb motion capture. In this study, a particle filter is used to fuse 3D accelerometer and 3D microgyroscope sensor data to estimate upper limb motion recursively. Orientations of upper limb segments are presented in quaternion, which is computationally effective and able to avoid singularity problem. Since drift is an important problem in motion estimation with inertial sensors, the geometrical constraints in elbow joint are modeled and fused to the particle filter process to compensate drift and improve the estimation accuracy.

Magnetometer signals from sensors are usually affected by the presence of ferromagnetic materials or other magnetic fields since these magnetic materials disturb the local earth magnetic field and thus affect the orientation estimation. This usually poses a problem in ambulatory applications. Roetenberg et al. (2005) presented the design of a complementary Kalman filter to estimate orientation of human body segments by fusing gyroscope, accelerometer, and magnetometer signals from miniature sensors. The gyroscope bias error, orientation error, and magnetic disturbance error are all estimated in the Kalman filter. They tested the Kalman filter under both quasi-static and dynamic conditions with ferromagnetic materials close to the sensor module. The quasi-static experiments implied static positions and rotations around the three axes. In the dynamic experiments, three-dimensional rotations were performed near a metal tool case. The comparison of orientation estimated by the filter with that obtained with an optical reference system called Vicon showed accurate and drift-free orientation estimates. The average static error reported was 1.4° (standard deviation 0.4) in the magnetically disturbed experiments. The dynamic error reported was 2.6° root means square.

Dejnabadi et al. (2006) proposed a new method of estimating lower limbs orientations using a combination of accelerometers and gyroscopes. Their

model was based on estimating the accelerations of ankle and knee joints by placing virtual sensors at the centers of rotation. In their technique, human locomotion and biomechanical constraints were taken into consideration. They used data fusion and fused the data of gyroscopes and accelerometers to obtain stable and drift-free estimates of segment orientation. Their method was validated by measuring lower limb motions of eight subjects, walking at three different speeds, and comparing the results with a reference motion measurement system. The results they presented were very close to those of the reference system presenting very small errors (Shank: rms=1.0, Thigh: rms=1.6°) and excellent correlation coefficients (Shank: r=0.999, Thigh: r=0.998). Their ambulatory system is portable, easily mountable, and can be used for long term monitoring.

Roetenberg et al. (2007) presented the design and testing of a portable magnetic system combined with miniature inertial sensors for ambulatory 6 degrees of freedom human motion tracking. In their study, the magnetic system consisted of three orthogonal coils as the source fixed to the body and 3-D magnetic sensors that were fixed to the remote body segments in order to measure the fields generated by the source.

Performance and Reliability of WBAN

In recent years, interests in the application of Wireless Body Area Network (WBAN) have grown considerably. A WBAN can be used to develop a patient monitoring system which offers flexibility and mobility to patients. However, there are serious performance and reliability issues in WBANs that must be addressed. The network topology that is generally used in wireless sensor networks for such ambulatory studies is of the star configuration as shown in Fig. 5. This is because nodes usually are sensor nodes and do not need to communicate with each other. Therefore, the star topology is used and each sensor node communicates with the central node using a hub. This raises reliability questions as the hub or the central node may fail leading to total system failure. Even the communication links may perform poorly or fail . Since data fusion is used in almost all applications, even the failure of any of the sensors or the communication links would result in system failure.

Ylisaukko-oja et al. (2004) presented the implementation and practical use of an unobtrusive five-point acceleration sensing wireless body area network (WBAN) with mobile device data logging capabilities shown in Fig. 5. They used TDMA based MAC protocol and RS232 for serial communications with external devices. They reported good communications performance in laboratory conditions but weaker field test performance. Their tests indicated significant losses in communication. Under laboratory conditions, they lost the remote slots from 0.31% to 3.09% in various parts of the test while in the field tests, they lost central data up to 3.84% and lost remote slots from 13.66% to 52.51%. This indicates a high degree of reliability problems especially in communications.

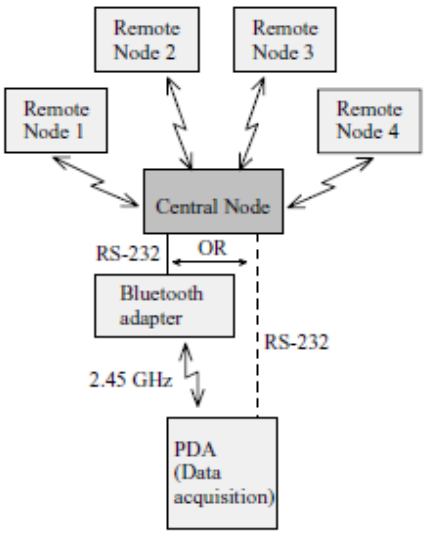

Fig 5 – The general network topology used in WBAN adopted from Ylisaukko-oja et al. (2004)

Various other approaches have been proposed for performance evaluation of WBAN systems. For example, Hamel et al. (2008) investigated the performance issues in wearable wireless body area sensor networks by considering various wireless technologies and platforms. They developed a Zigbee-based WBAN system with custom sensor platforms and evaluated its performance both in the laboratory and at home. They concluded that the use of a typical setup with four wireless sensor nodes with eight sensor inputs per node sampled at 100Hz offers the most reliable radio communication performance and reliability.

Use of a WBAN allows the flexibility of setting up a remote monitoring system via either the internet or an intranet. The main advantage of WBAN is the automatic real-time collection of signals that are needed in medical treatment and healthcare. One may even go further and extend the range of services provided to remote locations using either the internet or satellite communications. Li et al. (2008) presented an experimental system comprised of a wireless body area network (WBAN) and satellite communication links to enable remote medical treatment and healthcare services. They implemented the WBAN using ultra-wideband technology and adopted multi-hop mechanism to achieve a reliable connection. By introducing satellite communication links as shown in Fig. 6 it is possible to use WBAN's to perform remote health monitoring and provide remote instructions for emergency medical care in case of emergencies in isolated areas. Multi-hop mechanism of WBAN is shown to work well and the relative delay of WBAN data delivery via satellite links is strongly dependent on the satellite link capacity.

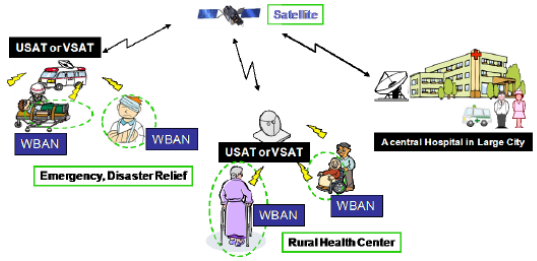

Fig 6 - WBAN used in connection with satellite communications to provide remote health care monitoring and advice adopted from Li et al. (2008).

Performance of the data fusion in such applications may also be studied. For example, Similä et al. (2006) evaluated the performance of a wireless acceleration sensor network such as shown in Fig 5 in balance estimation. The test has been carried out in eight patients and seven healthy controls. The patients group had larger values in lateral amplitudes of the sensor displacement and smaller values in vertical displacement amplitudes of the sensor. The step time variations for the patients were larger than those for the controls. They used fuzzy logic and clustering classifiers and obtained promising results suggesting that a person with balance deficits can be recognized with this system. They used the SOM toolbox for clustering and the leave-one-out method to obtain membership functions for their fuzzy logic analysis.

Khan et al. (2008) studied the performance of an IEEE802.15.4/Zigbee MAC based WBAN operating in different patient monitoring environments using an OPNET based simulation model. Their results indicated that patient monitoring using WBAN over the internet could be performed from remote locations with a reasonable delay if the WBAN is not directly connected to the main hospital network via a service node, and that the multihop network should be used instead of a fixed network to optimize the transmission time.

Reliability of such networks is highly important since they deal with humans and lives may be endangered in case of failures. The estimates of failure rate and mean time to failure for the components that are typically used in WBAN systems for ambulatory monitoring are listed in Table 1 plus an indication of the source of data.

Table 1 – Estimation of failure rate and mean time to failure for common components used in WBAN

Component	$\lambda(FPMH$	MTTF (Hours)	Data Source
Accelerometer	20.3327	49181	NPRD-95
Gyroscope	45.7778	21844	NPRD-95
Magnetometer	20	50000	Honeywell
PDA (Data Acquisition Unit	200	5000	Newland PT980 Series RS232/USB
Bluetooth Adapter	1	1000000	Sena Parani Bluetooth adapter

The reliability of the common star type topology of WBAN systems may be computed based on the fact that the sensor nodes are usually all needed in the data fusion, and that all the components must work for the WBAN system to work. Therefore, the reliability of a system composed of n components would easily be estimated by computing the overall failure rate of the system as shown in (1):

$$\lambda_{WBAN} = \sum_{i=1}^{n} \lambda_i \quad (1)$$

Then the reliability of the WBAN system would be as shown in (2) assuming that the system is in its useful life period and obeying the exponential lifetime probability distribution.

$$R_{WBAN} = e^{-\lambda_{WBAN} t} \quad (2)$$

Then we can easily compute the system reliability. For example, the total failure rate for the WBAN system shown in Fig 5 adopted from Ylisaukko-oja et al. (2004) will be as indicated in Table 2 assuming that three of the sensor nodes consist of accelerometers and one is a gyroscope.

Table 2 - Estimation of the total failure rate of the WBAN shown in Fig 5.

Component	No. of components	$\lambda(FPMH)$	Total Failure Rate
Accelerometer	3	20.3327	60.9981
Gyroscope	1	45.7778	45.7778
PDA (Data Acquisition Unit	1	200	200
Bluetooth Adapter	1	1	1
Central Node	1	1	1
Total Estimated Failure Rate		$\lambda_{WBAN} = \sum_{i=1}^{n} \lambda_i =$ 308.7759	

Single failures in such systems lead to total system malfunctioning or failure. Going from star topology to a higher degree of connectivity by adopting a loop network would not solve this reliability issue with single node failure since still all the nodes have to communicate with the central processing node via a hub the failure of which would lead to total system failure. Therefore, other approaches should be pursued.

In addition to single mode failures, there is a possibility of multiple mode failures and multiple failures that makes it even harder to address the reliability concerns. Wang et al. (2010) have addressed the reliability modeling of wireless body area networks with the aim of increasing the reliability in the presence of multi-type failures, while saving energy. They classified the nodes into types with regard to their capabilities on relaying and sensing and modeled their behavior in the presence of failures such as energy

exhaustion and/or malicious attacks using a semi-markov process.

Conclusion

Although a lot of progress has been reported in the application of WBAN, a lot more work should be done in improving the performance and reliability of wireless body area networks used for health monitoring and care. Topology, protocols, mix of sensors and their redundancy plus more advanced means of data or decision fusion and feature extraction are needed to make better and more reliable ambulatory monitoring and health care systems.

Corresponding Author:
Dr. Ali Peiravi
Department of Electrical Engineering
Ferdowsi University of Mashhad
MAshhad IRAN
P.O. Box 91775-1111
E-mail: ali_peiravi@yahoo.com

References

1. Dejnabadi, H.; Jolles, B.M.; Casanova, E.; Fua, P.; Aminian, K., "Estimation and visualization of sagittal kinematics of lower limbs orientation using body-fixed sensors," Biomedical Engineering, IEEE Transactions on , Vol.53, No.7, pp.1385-1393, July 2006.
2. Dong, L., Wu, J., Chen, X., "Real-time physical activity monitoring by data fusion in body sensor networks," FUSION 2007 - 10th International Conference on Information Fusion, 9-12 July 2007, pp.1-7.s
3. Hamel, M., Fontaine, R., Boissy, P., "In-home telerehabilitation for geriatric patients", IEEE Engineering in Medicine and Biology Magazine, July/August 2008, pp. 29-37.
4. Hernandez, A.I.; Carrault, G.; Mora, F.; Thoraval, L.; Passariello, G.; Schleich, J. M., "Multisensor fusion for atrial and ventricular activity detection in coronary care monitoring," IEEE Transactions on Biomedical Engineering, Vol. 46, No. 10, pp.1188-1190, Oct. 1990.
5. Iso-Ketola, P.; Karinsalo, T.; Vanhala, J., "HipGuard: A wearable measurement system for patients recovering from a hip operation", Proceedings of the 2nd International Conference on Pervasive Computing Technologies for Healthcare 2008, PervasiveHealth 2008, pp.196-199.
6. Jovanov, E.; Milenkovic, A.; Otto, C.; De Groen, P.; Johnson, B.; Warren, S.; Taibi, G., "A WBAN system for ambulatory monitoring of physical activity and health status: applications and challenges," 27th Annual International Conference of the Engineering in Medicine and Biology Society, 2005. IEEE-EMBS 2005. pp.3810-3813, 17-18 Jan. 2006.
7. Khan, Jamil Y.; Yuce, Mehmet R.; Karami, Farbood, "Performance evaluation of a Wireless Body Area sensor network for remote patient monitoring," 30th Annual International Conference of the IEEE Engineering in Medicine and Biology Society, 2008, EMBS 2008., pp.1266-1269, 20-25 Aug. 2008.
8. Li, Huan-Bang; Takahashi, T.; Toyoda, M.; Katayama, N.; Mori, Y.; Kohno, R., "An experimental system enabling WBAN data delivery via satellite communication links," IEEE International Symposium on Wireless Communication Systems - ISWCS '08, pp.354-358, 21-24 Oct. 2008.
9. Mandic, Danilo P. et al. "Data fusion for modern engineering applications: an overview," Artificial Neural Networks: Formal Models and Their Applications - ICANN 2005, 15th International Conference, Warsaw, Poland, September 11-15, 2005, Proceedings, Part II 2005.
10. Mathie, M. J. ; Coster, A. C.; Lovell, N. H.; Celler, B. G., "Accelerometry: providing an integrated, practical method for long-term, ambulatory monitoring of human movement" Physiological measurement, Vol. 25, No. 2, April 2004, pp.R1-R20.
11. Motoi, K.; Tanaka, S.; Nogawa, M.; Yamakoshi, K., "Evaluation of a new sensor system for ambulatory monitoring of human posture and walking speed using accelerometers and gyroscope," SICE 2003 Annual Conference , Vol.2, pp. 1232-1235, 4-6 Aug. 2003, Fukui, Japan.
12. Nyan, Myo Naing; Tay, Francis Eng Hock; Koh, Teck Hong; Sitoh, Yih Yiow; Tan, Kwong Luck "Location and sensitivity comparison of MEMS accelerometers in signal identification for ambulatory monitoring," Proceedings of the 54th Electronic Components and Technology Conference, , 1-4 June 2004, Vol.1, pp. 956-960.
13. Roetenberg, D.; Luinge, H. J.; Baten, C. T. M.; Veltink, P. H., "Compensation of magnetic disturbances improves inertial and magnetic sensing of human body segment orientation," IEEE Transactions on Neural Systems and Rehabilitation Engineering, Vol.13, No.3, pp.395-405, Sept. 2005.
14. Roetenberg, D.; Slycke, P.J.; Veltink, P.H., "Ambulatory Position and Orientation Tracking Fusing Magnetic and Inertial Sensing," Biomedical Engineering, IEEE Transactions on , vol.54, no.5, pp.883-890, May 2007.
15. Roetenberg, D.; Baton, Chris, T. M.; Veltink, P.H., "Estimating body segment orientation by applying inertial and magnetic sensing near ferromagnetic materials," IEEE Trans. on Neural Systems and Rehabilitation Engineering, Vol. 15, No. 3, Sept.2007, pp. 469-471.
16. Similä, H.; Kaartinen, J.; Lindholm, M.; Saarinen, A.; Mahjneh, I., "Human balance etimation using a Wireless 3D acceleration sensor network,"Proceedings of the 28th EMBS Annual International Conference, New York, USA, August 30-Sept 3, 2006, pp.1493-1496.
17. Solaiman, B.; Debon, R.; Pipelier, F.; Cauvin, J. -M.; Roux, C., "Information fusion: Application to data and model fusion for ultrasound image

segmentation," IEEE Transactions on Biomedical Engineering, Vol. 46, No. 10, Oct. 1999, pp.1171-1175.
18. Tanaka1, S.; Yamakoshi, K.;Rolfe, P., "New portable instrument for long-term ambulatory monitoring of posture change using miniature electro-magnetic inclinometers," Medical and Biological Engineering and Computing, Vol. 32, No. 3, May 1994, pp.357-360.
19. Wang, S., IEEE, Park, J. T., "Modeling and analysis of multi-type failures in wireless body area networks with semi-markov model," to appear in IEEE Communications Letters, 2010.
20. Ylisaukko-oja, A.; Vildjiounaite, E.; Mantyjarvi, J., "Five-point acceleration sensing wireless body area network - design and practical experiences," Eighth International Symposium on Wearable Computers, 2004. ISWC 2004, Vol.1, pp. 184-185, 31 Oct.-3 Nov. 2004.
21. Zhiqiang, Z.; Zhipei, H.; Jiankang, W., "Hierarchical information fusion for human upper limb motion capture," 12th International Conference on Information Fusion, FUSION 2009, pp.1704-1711.

.

5/5/2010

Sports injury and the role of medical diagnostic devices

Szu-Ming Wu[1], Kuo-Chen Wu[2,] Hsiang-Chi Wu[3,4*], Ching-Hui Yeh[4]
1 Department of Mechanical Engineering, Cheng Shiu University,2 Department of Computer Science, National Chung Hsing University,3 Department of Kinesiology, Health, and Leisure Studies, National University of Kaohsiung,4 Department of Family Medicine, Tzuo-Ying Armed Forces General Hospital
*Corresponding Author: Hsiang-Chi Wu, E-mail: wu533833@gmail.com

Abstract: Objectives: Sport participation always carries the risk of injury. The aim of this paper is to investigate the incidence of sports injury, the role of medical diagnostic devices and concepts of sports injury prevention. Various medical diagnostic devices are not always helpful without any damage. The conclusion of this study gives viewpoints of clinical medicine and biomedical engineering on sports injury. Highlighting the importance of sports injury with regard to incidence rates and risk factor is also the main goal of the study [1]. Results: The study population includes patients and their family members from the outpatient department of Tzuo-Ying Armed Forces General Hospital in Kaohsiung City, Taiwan. The data demonstrates the most common sites of injuries are ankles (34.4%). Regarding the knowledge of sports injury prevention, 38.3 % believe that sports protective devices using can decrease risk of injury and 51.5 % think that enough warm-up exercise will make exercise course smoothly. Regarding actions taken by persons after the occurrence of a sports injury, more than half (54.7%) of them attempt to treat the condition themselves at the initial stage, and only 33.6% look for medical attention immediately .It warns policy makers that the high rate of people ignore the sports injury and taking no thoughts about sports injury may result in more costs of the medical service at the later stage. Conclusions: The results show that increasing population levels of the knowledge about sports injury prevention and providing realistic medical diagnostic devices are important. [Life Science Journal 2010;7(2):92-95]. (ISSN: 1097-8135).

Keywords sports injury; medical diagnostic device; X-ray radiation

1. Introduction

Sport participation always carries the risk of injury. The aim of this paper is to investigate the incidence of sports injury, the role of medical diagnostic devices and concepts of sports injury prevention. Various medical diagnostic devices are not always helpful without any damage.

The cross-section study aims to evaluate the prevalence of sports injury in general population. The incidence probability of sports injury depends on the physical condition, sports safety equipment, skill levels, the knowledge of injury prevention and etc [2]. The study results may show some ideas for the directions of promoting sports injury prevention ability of general population, preventive medicine and the efficiencies and facilities of medical diagnostic medical devices in the future [3].

2. Materials and methods

The study is a cross-sectional designed by the application of questionnaire in sample survey about sport –related injuries between Mar 2009 and June 2009 for people and their family members visiting Tzuo-Ying Armed Forces General Hospital. There is only one questionnaire used in the study. The questionnaire includes information about persons participated in the study as follows: age, gender, height , weight, frequency of taking exercise, education level, medical and injury history , coping strategies attitudes in injuries, and knowledge about sports injury [4][5]. The research team consults the orthopedic specialists in order to develop expert validity and content validity of the questionnaire.

Structured questionnaires are sent to patients and their family members at the waiting room . A total of 136 questionnaires are returned, a valid questionnaire response rate is 47%. Because of the characteristics of armed forces general hospital service, most cases of our study are soldiers in active service. Descriptive statistics and inferential statistics are performed using Student's t tests and Chi-square analysis. Spearman correlation is used to determine the relationships between different parameters. SPSS version 12.0 (SPSS Inc, Chicago, IL, USA) is used to analyze the data.

3. Results

From the 136 questionnaires sent out, there is a valid questionnaire response rate of 47%. There seems to be no significant difference in age, height, body weight, BMI (body mass index), education level, history and frequency of exercise between people participated in the study. There is a deemed homogeneous sample for participants who belong to the same subculture or have similar characteristics. A total of 64 persons participate voluntarily in this study (57 males and 7 females). During the survey, most people have experiences of sport injury in the past. The common sites of injuries are ankles (34.4%), thigh (25.0%), and knees (12.5%) in the study. A muscle strain is a common problem among many individuals who are physically active (59.4 %). A sprain is an injury to a ligament caused by excessive stretching and also it happens when there's an injury to the tendon or muscle (26.6%) (Fig.1).

Sports injuries are common especially in economical and competitive sports such as ball exercise, swimming and running. 45.3% have experiences of sport injuries associated with playing ball games. 28.1% sustain a foot injury when running [6] (Fig.2). Regarding the knowledge of sports injury prevention, 38.3 % believe that using sport protective devices during exercise can decrease risk of injury and 51.5 % think that enough warm-up exercise will make exercise course smoothly.

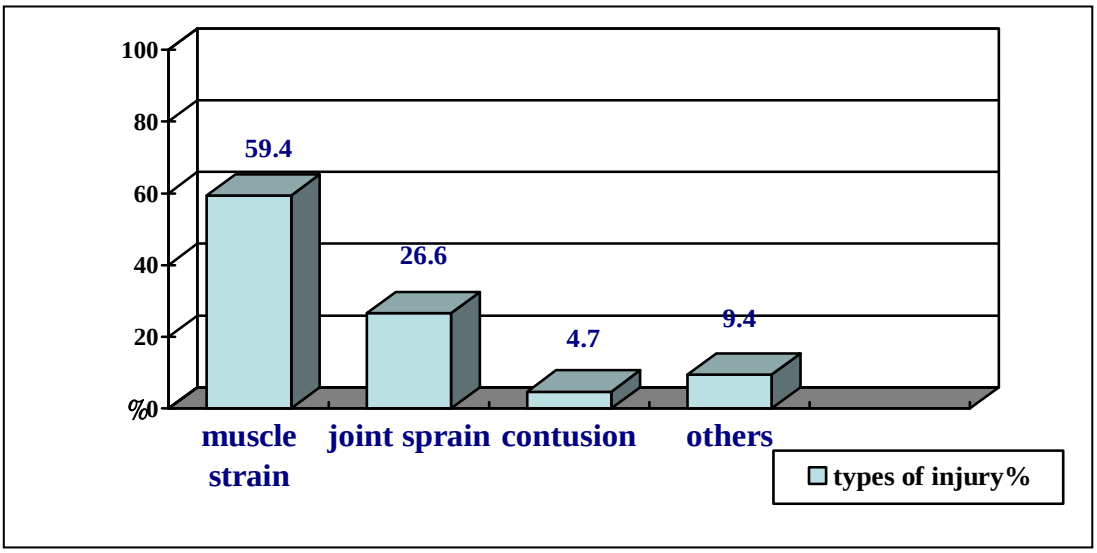

Figure1. Different types of sporty injury: The common sites of injuries are ankles (34.4%), thigh (25.0%), and knees (12.5%) in the study.

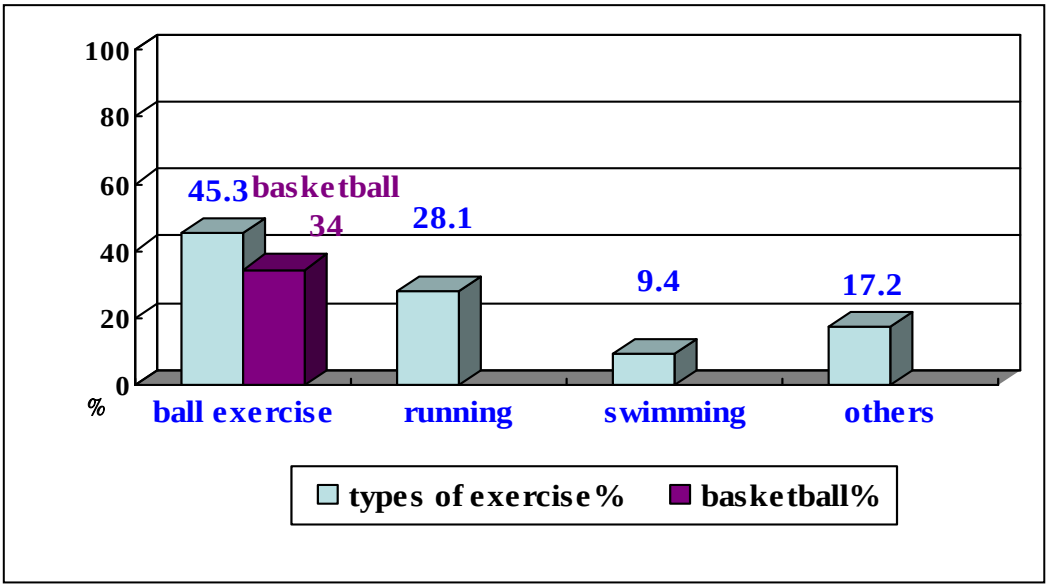

Figure 2. Sports - related injuries at different categories.

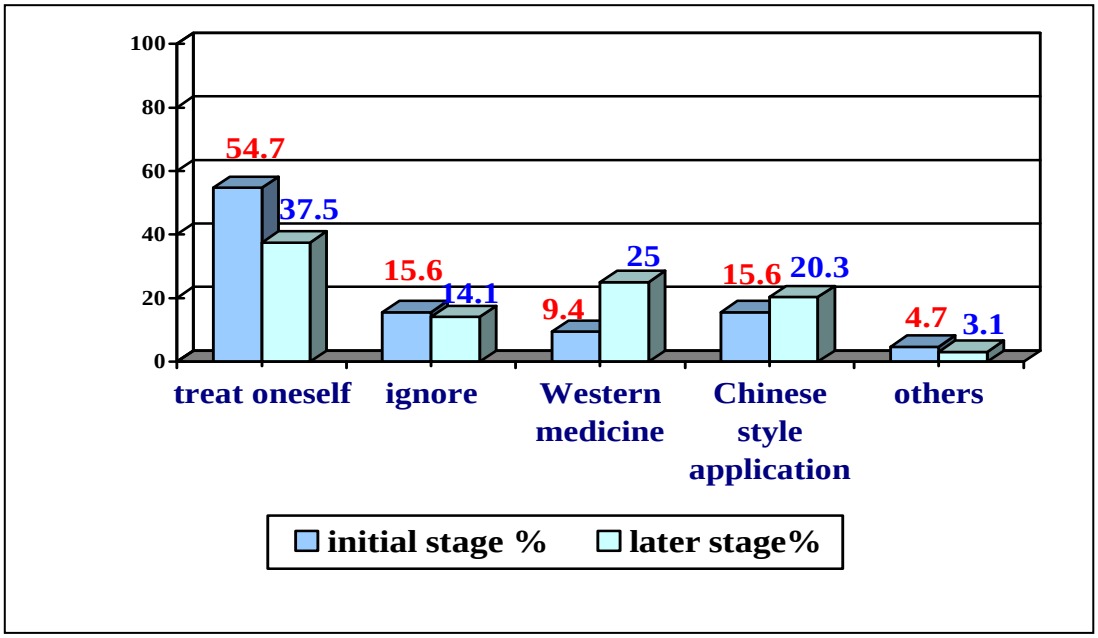

Figure 3. Different coping strategies in sports injury injuries

Regarding actions taken by persons after the occurrence of sports injury, 54.7% of them attempt to treat the condition themselves at the initial stage, and only 33.6% look for medical attention immediately at the initial stage.15.6 % and 20.3% select Chinese style application at the initial stage and later stage. Chinese style application includes the herb patch, massage, cupping, acupuncture therapy and other associated alternative medicine treatments. Post the occurrence of acute sport injury, 40.6% have no idea that RICE principles of rest, ice, compression, and elevation are the first steps in sports injury treatment. It warns policy makers that more than half of people attempt to treat the condition themselves at the initial stage ,and high rate of people taking no thoughts about sports injury may result in more cost of the medical service .(Fig.3) .

4. The role of medical diagnostic devices

Joints are more prone to injury when the muscles and ligaments that support them are weak, especially after damages. Diagnostic imaging plays a key role in the evaluation of patients with illness. Specialists may use of the proper equipment to diagnose injuries such as x-rays , computed tomography (CT), and magnetic resonance imaging (MRI) by clinical symptoms of patients [7].

MRI examinations are widely utilized for soft tissues such as joints (ligaments), spinal cord, blood vessels, and etc. Computed tomography (CT) is practical and functional in assessing the condition of the tissues in avulsion injury. MRI and CT scans cost $1000 to $2500 per examination in USA or other countries where most people can not afford it without healthy insurance. X-ray films should be regarded as the first-line diagnostic imaging technique of musculoskeletal diseases for its convenience, function, and cheaper cost.

X-rays exposure can be dangerous and cause mental stress to pregnant women. The recommendations for fetal dose should be limited to 5 millisieverts (mSv) or 500 mrem [8], even not all exposures can be harmful [9]. At fetal doses above this level, the decision should be based upon the individual circumstances.

5. Discussion

X-radiation is a form of electromagnetic radiation. X-rays have a wavelength in the range of 10 to 0.01 nanometers. X-rayfilms are specially hepful in the detection of pathology of the skeletal system, but are also useful for detecting some disease processes in soft tissue.The average radiation dose of a person in USA is about 3 mSv of exposure per year from artificial causes or natural sources as followings: radioactive materials, cosmic radiation from outer space and iatrogenic event and etc.

Post receiving once radiation scan, the radiation dose of chest X ray is about 0.05-0.1 mSv and higher dose with 10 mSv in whole body scanning using Computed Tomography [11][12].

The doses of natural background vary throughout different geographic environments. An exposure of greater than 20 mSv is considered higher than acceptable range, while greater than 3 mSv to 20 mSv is considered relatively safe.

There are several limitations that need to be addressed regarding the present study. The first limitation concerns the characteristics of the study sample. In the sample people, most of them (92%) are under the age of thirty-five years. Young people who are active in many types of competitive sports and the characteristic about age of the study sample leads a high estimate for the incidence of sports injury. Small sample size is another study limitation. Other possible limitations of this study are sampling method and

geographic location.

6. Conclusion

The study puts efforts and concern on the research and techniques in medical engineering and related sciences in addition to researches in clinical medicine. At the same time supporting specialists with up-to-date medical instruments and systems are crucial and vital. Preventive medicine plays a more important role than the care medicine, rehabilitation and so-called best medical diagnostic devices.

Acknowledgment

I would like to express my deep and sincere gratitude to my family. Last but not least, my heartfelt appreciation is also presented to my dearest and most precious love gone away: forever partner, Pi-Pi Wu.

References:

1. M.Stevenson, P. Hamer, C. Finch, B. Elliot, M-jo Kresnow.(2000).Sport, age, and sex specific incidence of sports injuries in Western Australia: Br J Sports Med.,34(3):188–94.
2. Estell J, Shenstone B, Barnsley L.(1995). Frequency of injuries in different age groups in an elite rugby league club. Aust J Sci Med Sport, 27 (4):95–7.
3. A Comprehensive Study of Sports Injuries in the U.S.,conducted by American Sports Data.2003:271. (www.americansportsdata.com).
4. Chen,S.-K., Lu, Y.-M., Lin. Y.-C., Wu.W.-L., & Lue.Y.-J. (2008).The Self-Efficacy of Sports Injury Prevention for the National Athletes, FJPT;33 (4):219-227.
5. Chen, S.-K., Cheng, Y.-M., Huang, P.-J., Chou, P.-H., Lin, Y.-C., & Hong, Y.-J. (2005). Investigation of Management Models in Elite Athlete Injuries. The Kaohsiung Journal of Medical Sciences, 21(5), 220-227.
6. Menz, H. B., & Morris, M. E. (2006). Clinical determinants of plantar force and pressures during walking in older people. Gait & Posture, 24(2), 229-236.
7. Bussieres AE, Ammendolia C, Peterson C, Taylor JAM.(2006) Ionizing radiation exposure – more good than harm? The preponderance of evidence does not support abandoning current standards and regulations. J Can Chiropr Assoc, 50(2):103–106.
8. Oakley PA, Harrison DD, Harrison DE, Haas JW. (2005) On “phantom risks” associated with diagnostic radiation: evidence in support of revising radiography standards and regulations in chiropractic. J Can Chiropr Assoc;49 (4):264–269.
9. Wagner LK, Lester RG, Saldana LR,(1997) Exposure of the pregnant patient to diagnostic radiations: A guide to medical management,(2nd ed.). Madison WI: Medical Physics Publishing.
10. S.B. Thacker, D.F. Stroup and C.M. Branche et al. (1999), The prevention of ankle sprains in sports: a systematic review of the literature, Am J Sports Med**,** 27:753.
11. Fazel R, Krumholz HM, Wang Y, Ross JS, Chen J, &Ting HH et al.(2009) Exposure to low-dose ionizing radiation from medical imaging procedures, New England Journal of Medicine,361:849-857
12. Health Risks from Exposure to Low Levels of Ionizing Radiation: BEIR VII Phase 2 (2006) (ISBN 030909156X) Committee to Assess Health Risks from Exposure to Low Levels of Ionizing Radiation, National Research Council.

3/1/2010